NAT'L INST. OF STAND & TECH
A11106 173437
NIST PUBLICATIONS
REFERENCE

Ceramics Division

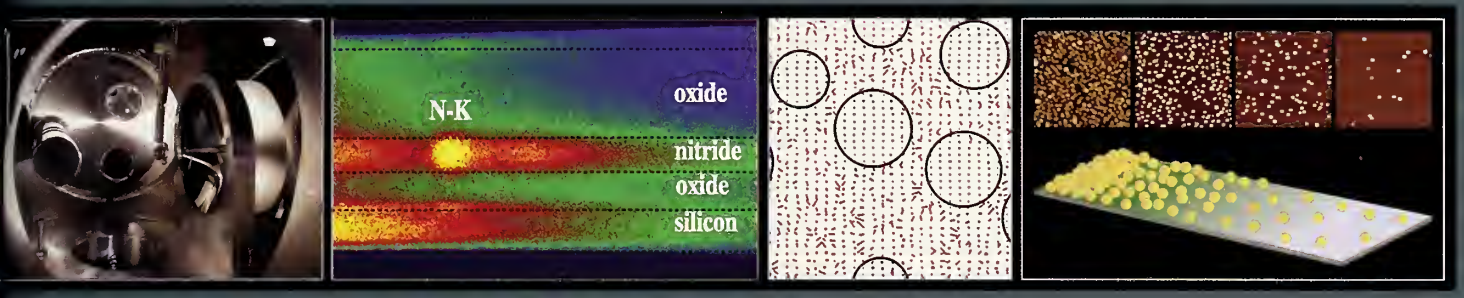

Materials Science and Engineering Laboratory

FY 2002 Programs and Accomplishments

NIST
National Institute of Standards and Technology
Technology Administration
ment of
4
2002

QC
100
.U56
#6904
2002

On the Cover:

Cover images from right to left:

Atomic force microscope images of gold nanoparticles adsorbed on a silica-covered substrate, above a cartoon of the gold nanoparticles with continuous number density gradient. From "Measuring Monolayer Templates for Fabricating Nanoparticle Assemblies of Number Density Gradients," page 6.

Local electric fields in a model for the relaxor ferroelectric PbSc1/2Nb1/2O3 (PSN). Experiments suggest that relaxor ferroelectrics contain chemically ordered regions in a disordered matrix and that such inhomogeneities may be responsible for the relaxor behavior. Computations show that chemically-ordered regions in PSN (circles) have much lower local fields than the disordered matrix. The large circles are approximately 5 nm in diameter. From "Phase Equilibria and Properties of Dielectric Ceramics," page 25.

Two-dimensional (2D) electron energy loss spectra (EELS) from a silicon oxide-nitride-oxide (ONO) stack, in which the horizontal dimension corresponds to energy loss, and the vertical represents a spatial coordinate; that is, each 2D spectrum represents a collection of EELS spectra spatially-resolved across the interfaces. From "Nanoscale Structural/Compositional Characterization of Ultra-Thin Films," page 4.

Focusing multilayer mirror inside the NEXAFS chamber where the monolayer, templates of gold nanoparticles were measured, page 6.

[back cover]
Contour plot of the maximum principle stress field created from two head-disk collisions between an asperity (represented by a semi sphere in the figure) and the substrate. From "High-Speed Contact at Head-Disk Interface in a Magnetic Hard Disk Drive: Experiment and Modeling," page 9.

National Institute of Standards and Technology
Arden L. Bement, Jr.
Director

Technology Administration
Phillip J. Bond
Undersecretary of
Commerce for Technology

U.S. Department of Commerce
Donald L. Evans
Secretary

Materials Science and Engineering Laboratory

FY 2002 Programs and Accomplishments

Ceramics Division

Gabrielle G. Long, Acting Chief

NISTIR 6904

September 2002

Certain commercial entities, equipment, or materials may be identified in this document in order to describe an experimental procedure or concept adequately. Such identification is not intended to imply recommendation or endorsement by the National Institute of Standards and Technology, nor is it intended to imply that the entities, materials, or equipment are necessarily the best available for the purpose.

Table of Contents

Executive Summary 1

Technical Highlights 3

Nanoscale Structural/Compositional Characterization of Ultra-Thin Films 4

Measuring Monolayer Templates for Fabricating Nanoparticle Assemblies of Number Density Gradients 6

High-Speed Contact at the Head-Disk Interface in a Magnetic Disk Hard Drive: Experiment and Modeling 8

Elastic Moduli Data for Polycrystalline Oxide Ceramics 10

Infrared Reflectance Spectrum of $CaTiO_3$ Calculated from First Principles 12

Mechanical Reliability and Lifetime Prediction for Brittle Materials 14

Materials Structure Characterization 16

Synchrotron Beam Line Operation and Development 17

Small-Angle Scattering Characterization of Materials 18

Nano-Structure of Grain Boundaries in Vitreous Bonded Ceramics 19

Powder Diffraction Standards 20

Powder Measurements 21

Materials for Micro- and Optoelectronics 22

Optical and Structural Characterization of Optoelectronic Semiconductors 23

Nanotribology 24

Phase Equilibria and Properties of Dielectric Ceramics 25

Phase Diagrams in High Temperature Superconductors 26

Combinatorial Methods 27

Combinatorial Tools for Oxide Thin Films 28

Materials Property Measurements 29
Failure Modes in Biomechanical Layer Structures 30
Mechanical Property Measurements 31
Microstructural Design 32

Data Evaluation and Delivery 33
Ceramic Phase Equilibria Database 34
Crystallographic Databases for Non-Organic Materials 35
Materials Property Data and Data Delivery 36

Advanced Manufacturing Methods 37
Processing of Low Temperature Co-Fired Ceramics 38
Contact Damage 39

Ceramics Division Databases and Standards 41

Ceramics Division FY02 Annual Report Publication List 43

Ceramics Division 49

Research Staff 50

Organizational Charts 55

Executive Summary

It has been a noteworthy year for the Ceramics Division. Our Division Chief, Stephen Freiman, was elevated to the post of Deputy Director of the Material Science and Engineering Laboratory. We wish him every success in that office, and we express our gratitude to him for his 10 years of service leading this Division.

In a year when there were serious budgetary issues that had to be addressed, the Division staff responded with considerable professionalism and perseverance, leading to a number of noteworthy accomplishments. We made significant advances in the development of unique techniques for use in chemical analysis of nanomaterials as well as in the development of practical functional tests for nanoscale devices.

The *NIST Recommended Practice Guide: Mechanical Reliability and Life Prediction for Brittle Materials*, completed this year, is a compendium of 30 years of research and experience into a single, systematic document. *Elastic Moduli Data for Polycrystalline Ceramics (NISTIR 6853)*, also completed this year, includes moduli for 53 polycrystalline ceramics, as well as analytic model fits. The data, and the analytical results in particular, are expected to be extraordinarily valuable for product design and in-service simulations. The Division also completed a large number of Databases and Standards, which are now given a separate listing in this Report. We expect to continue to expand our efforts in this important area.

The scientific results that emanate from the Division are another measure of success. Serving as Acting Division Chief, I welcome the opportunity to lead our research efforts, to place new emphasis on our Strategic Focus Areas, and to continue the Division's efforts toward providing better services to our customers. Division scientists conduct a broad range of research, from optical and structural characterization of microelectronic and optoelectronic materials, to nanotribology, phase diagrams for high temperature superconductors, phase equilibria and properties of dielectric ceramics, microstructure modeling and microstructure characterization, and mechanical properties measurements. Division scientists also operate and utilize leading edge materials science facilities at synchrotron x-ray sources, in support of our programs. These unique facilities are open to all qualified researchers from industry, universities and government laboratories for advanced materials characterization. Looking toward the future, we expect to place an increasing emphasis on the NIST Strategic Focus Areas in nanotechnology and healthcare, and highlights in this Report already include significant achievements in those areas.

Division scientists have been able to characterize the structure and composition of the nanometer scale silicon oxide-nitride-oxide layers, which are of high current interest as possible charge storage structures in non-volatile memory devices. This research is an important contribution to the Program in Microelectronics at NIST. In another nanotechnology area, nanoparticle assemblies have been attached by means of monolayer templates onto silicon substrates where the entire process was comprehensively characterized. As a result of this research, nanoparticles can now be placed into chemically and structurally well-defined environments on silicon substrates.

Other Highlights in this Report include both experimental and theoretical investigations. Studies were made of high-speed contact at the head-disk interface in a magnetic disk hard drive, and exciting new first principles calculations were made of properties from atomic scale structure of microwave dielectrics.

In addition to these selected Highlights, we report numerous other significant accomplishments in our projects under the 9 Programs in the Materials Science and Engineering Laboratory. These brief reports provide a fairly comprehensive synopsis of the breadth and depth of research conducted in our Division. I hope that you enjoy reading about these activities.

Gabrielle G. Long
Chief, Ceramics Division (Acting)

Technical Highlights

The Technical Highlights section of this Report comprises six examples of the exciting outputs of the Ceramics Division. They are:

- Nanoscale Structural/Compositional Characterization of Ultra-Thin Films
- Measuring Monolayer Templates for Fabricating Nanoparticle Assemblies of Number Density Gradients
- High Speed Contact at the Head-Disk Interface in a Magnetic Disk Hard Drive: Experiment and Modeling
- Elastic Moduli Data for Polycrystalline Oxide Ceramics
- Infrared Reflectance Spectrum of $CaTiO_3$ Calculated from First Principles
- Mechanical Reliability and Lifetime Prediction for Brittle Materials

Nanoscale Structural/Compositional Characterization of Ultra-Thin Films

Many modern device structures are critically dependent on the properties of ultra-thin layers approaching 1 nm in thickness. Examples of such layers include interfaces and reaction layers and gate dielectrics in CMOS devices. As a result, comprehensive understanding of the structure (amorphous or crystalline) and the chemistry (composition, chemical bonding, etc.) of these ultra-thin films is one of the most important aspects of successful device engineering. The present work demonstrates the application of high-resolution transmission electron microscopy combined with spatially resolved electron energy-loss spectroscopy to the analysis of (i) silicon oxide-nitride-oxide heterostructures and (ii) zirconium oxide ultra-thin films on silicon.

Silicon oxynitrides are leading candidates to replace pure thermally grown SiO_2 as gate dielectrics because they suppress boron penetration from the poly-Si gate, enhance reliability, and reduce hot-carrier-induced degradation. At the same time, silicon oxide-nitride-oxide multilayers (ONO stacks) attract considerable interest as possible charge storage structures in non-volatile memory devices. The critical structural and compositional parameters that affect electrical performance of ONO-based devices include the physical density of the amorphous oxide/nitride layers and the depth distributions of both oxygen and nitrogen atoms. However, few systematic studies that analyze the effect of processing conditions on these parameters in stacked ONO structures have been reported.

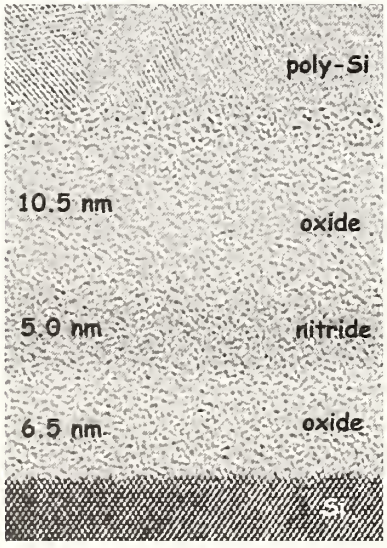

Figure 1: Typical high-resolution TEM image of an ONO stack.

In this study, we applied spatially-resolved electron-energy loss spectroscopy (EELS) in a transmission electron microscope (TEM) to analyze elemental distributions in differently processed ONO stacks (Figure 1) while physical densities of individual layers were measured using x-ray reflectometry. The results of structural/compositional analysis were correlated with the electrical performance of ONO-based flash-memories.

The ONO stacks for this study (Figure 1) were provided by Tower Semiconductor Ltd. Typical profiles of O-K and N-K characteristic intensity distributions, obtained using an imaging filter in a fixed-probe TEM, are shown in Figure 2. The O-K intensity decreases to the noise level in the middle of the nitride layer. The nitrogen signal disappears in the oxide layers, but produces small peaks both at the Si/SiO_2 and poly-Si/SiO_2 interfaces. The presence of nitrogen at the Si/SiO_2 interface in the oxy-nitride films has been reported previously, based on similar EELS measurements, and was attributed to nitrogen segregation during film processing. Such nitrogen segregation could explain the improved electrical breakdown strength of the bottom oxide observed after nitride deposition. However, we found that the amount of nitrogen at both interfaces

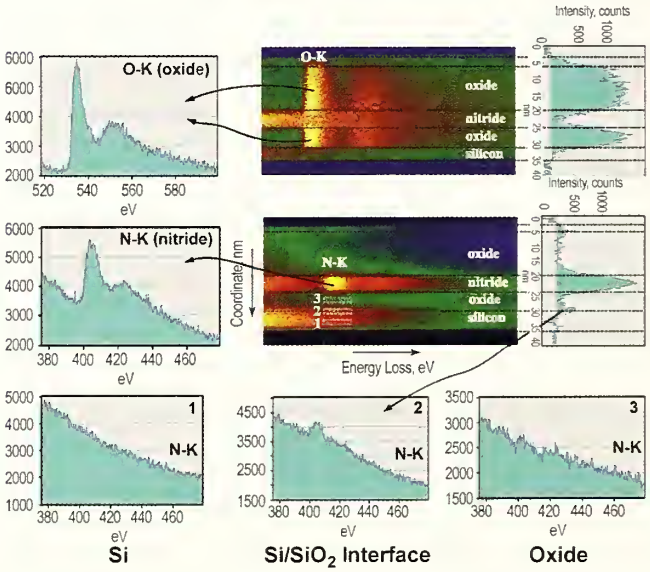

Figure 2: O-K and N-K spectrum-lines. The interfaces in the HRTEM image were set parallel to the energy-dispersion direction of the spectrometer. Each 2D spectrum has two dimensions: horizontal, corresponding to energy loss, and vertical, representing a spatial coordinate; that is, each 2D spectrum represents a collection of EELS spectra spatially-resolved across the interfaces. The individual spectra are shown on the left. The spectrum-lines were processed to remove background, and the intensities under each edge were integrated over an energy window of 2 eV. The profiles of integrated intensity distributions as a function of spatial coordinate are shown on the right.

increased with increasing irradiation time for the analyzed area, which suggested that the nitrogen distribution might be affected by the electron beam.

The effect of the electron beam on the nitrogen segregation was further tested using EELS spectrum-imaging in a dedicated scanning TEM (STEM). In these experiments, spectrum-images provided a collection of spatially-resolved (along the interface) line-scans across the ONO stack; the line-scans were separated in time by about 2.5 s. The first line-scan yielded no significant nitrogen signal at either the Si/SiO_2 or the poly-Si/SiO_2 interfaces. However, the next line-scan revealed a small, but detectable, nitrogen signal at the Si/SiO_2 interface, while the nitrogen signal from the nitride layer was reduced (Figure 3); the magnitude of this effect decreased with decreasing radiation dose. These results suggest radiation-induced nitrogen segregation to both the Si/SiO_2 and poly-Si/SiO_2 interfaces.

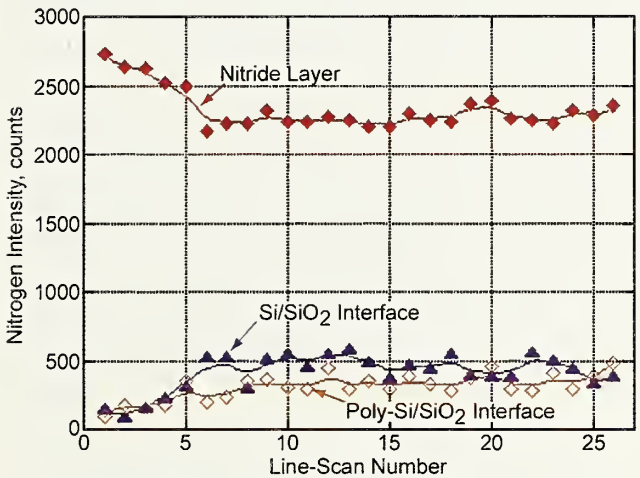

Figure 3: *Integrated nitrogen intensity as a function of line-scan number in the EELS spectrum-image acquired in the dedicated STEM. The nitrogen signal at both Si/SiO_2 and poly-Si/SiO_2 interfaces increases significantly with increasing scan number. A corresponding decrease in the nitrogen signal from the nitride layer is consistent with the beam-induced nitrogen diffusion/segregation.*

The implications of the beam-induced nitrogen segregation in the ONO stacks are several. First, similar artifacts could be present in other spectroscopic techniques that involve high-energy probes, such as secondary ion-mass spectroscopy (SIMS); therefore, the SIMS data on nitrogen segregation in ONO reported in the literature may need to be revisited. Second, reasons other than nitrogen segregation can be responsible for the improved dielectric properties of the bottom oxide observed after nitride deposition in the present ONO stacks. Additionally, our results indicate that electron-beam-induced damage can be a serious obstacle to EELS analysis at nanoscale resolution. More studies of radiation-induced damage in industrially relevant materials are needed to identify potential artifacts.

In another example, we applied TEM/EELS to the analysis of ZrO_2 ultra-thin films on silicon. Metal oxides, such as ZrO_2, are key candidates for gate dielectrics to replace SiO_2 and SiO_xN_y in CMOS transistor technology. Despite a large effort invested in the characterization of ultra-thin ZrO_2 films, many issues related to the effect of processing conditions on both morphology and thermal stability of ZrO_2 films on silicon remain the subject of a continuing debate. The present work is part of a systematic study of these effects in gate dielectrics, which is conducted in collaboration with the UCLA. The ZrO_2 films for this study were deposited using a state-of-the-art atomic layer CVD (ALCVD) system and subjected to annealing in different atmospheres. The high-resolution TEM images of 2.5 nm ZrO_2 films deposited on the HF-treated silicon surface are presented in Figure 4. The as deposited film is largely crystalline and exhibits a rough morphology; the latter was attributed to a discontinuous nucleation of the ZrO_2 film on the HF-treated Si surface. (A much smoother morphology was observed for films deposited on thermally grown 1 nm SiO_2 layer.) The film includes an interfacial layer having a thickness of about 1 nm. Spatially resolved EELS spectra indicate a lack of any significant Zr content in this layer, suggesting a silicon oxide rather than a silicate phase. Although the presence of a small amount of Zr in the layer still could not be ruled out, the near-edge structure of both the Si-$L_{2,3}$ and O-K edges for this interfacial layer were also consistent with a silicon oxide.

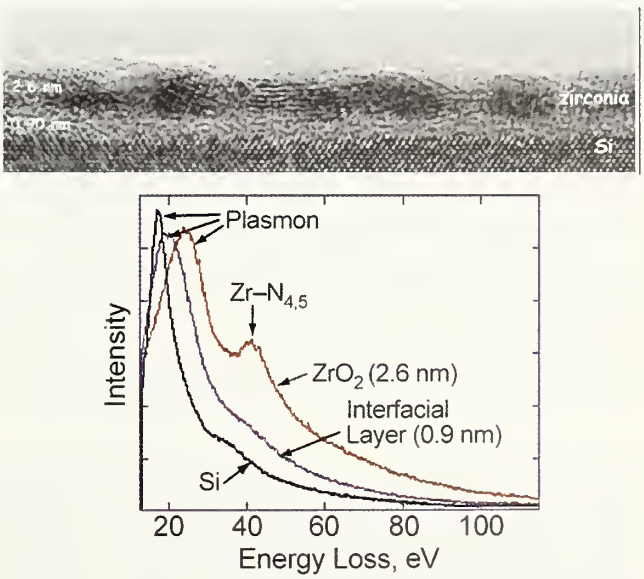

Figure 4: *Upper: HRTEM image of a ZrO_2 film deposited on HF-treated silicon at 460°C. Lower: Spatially-resolved EELS spectra from the same area.*

For More Information on this Topic

Contact: I. Levin

Measuring Monolayer Templates for Fabricating Nanoparticle Assemblies of Number Density Gradients

Nanoparticle-based structures are envisioned to play an important role in futuristic devices such as single-electron tunneling-based computer chips, high-density information storage devices, and other commercially important applications such as sensors and high-efficiency solar cells. In order to position nanocomponents onto functional devices, it is vital to develop methods for placing them into chemically and structurally well-defined environments. Near edge x-ray absorption fine structure spectroscopy was utilized to measure monolayer templates for fabricating gold nanoparticles with continuous number density gradients on flat silica-covered substrates.

Nanoparticle number density gradients are fabricated by following a pre-designed chemical template formed by a monolayer of organosilane "sticky" groups. The ability to manipulate the underlying template allows us to prepare gradient structures of nanoparticles with varying surface characteristics. For surface–property optimization, it is useful to fabricate samples with a continuously varying number density of immobilized particles along the surface. Such a nanoparticle gradient surface serves as a combinatorial platform for surface adsorption selectivity. In this way, large numbers of structures can be combined on a single substrate and used for high-throughput processing. It might, for example, save time for chemists testing clusters of nanoparticles for use in catalysis. Clusters made of a different number or size nanoparticle could be put on a single surface, and this surface could be tested once in a chemical reaction, instead of having to run each cluster separately through the reaction. The material could also be used as a sensor to detect species that have specific affinities for nanoparticles or as a filter to select particles of given sizes.

The gold nanoparticle surface was created by forming a one-dimensional molecular gradient template of amino groups on the substrate and then attaching the gold nanoparticles to the amino groups by immersing the substrate in a colloidal gold solution. The amino group gradient was produced by vapor diffusion of dihydrate and (3-aminopropyl) triethoxysilane (APTES) in paraffin oil (PO). Atomic force microscopy (AFM) demonstrated that the number density of the nanoparticles (diameter of 16.7 ± 1.8 nm) varied continuously as a function of position on the substrate from 500 mm^{-2} to zero mm^{-2} over a distance of 45 mm. Near-edge x-ray absorption fine-structure studies (NEXAFS) confirmed that the nanoparticle number density gradient was closely correlated with the concentration gradient of amino groups anchored to the substrate. As a result of this research, the number density of nanoparticles within the gradient and the length of the gradient can now be tuned by controlling the initial amino group gradient.

Figure 1 shows AFM images taken at various positions along the longer side of the substrate (x-direction) prepared by first allowing APTES molecules to diffuse for 5 min and then immersing the APTES coated substrate in gold colloid for 24 h. A gradient in number density of gold nanoparticles is clearly evident as one scans farther away from the end of the substrate that was closer to the APTES diffusion source (x=0). The particle number density changes continuously from approximately 500 mm^{-2} near the end of the substrate (closer to the diffusing source) to zero (the other end of the substrate). (See Figure 2.)

The template molecular density and the gradient length were tailored by adjusting the APTES diffusion time. Figure 2 shows the number density profile of nanoparticles along the gradient (x-direction) for two samples with APTES diffusions times of 3 min (•) and 5 min (■). It can be clearly seen that as the APTES diffusion time increases, the number of the adsorbed gold particles increases and the nanoparticles adsorb over longer distances on the substrate.

Partial electron yield (PEY) NEXAFS was utilized to measure the template concentration of the grafted

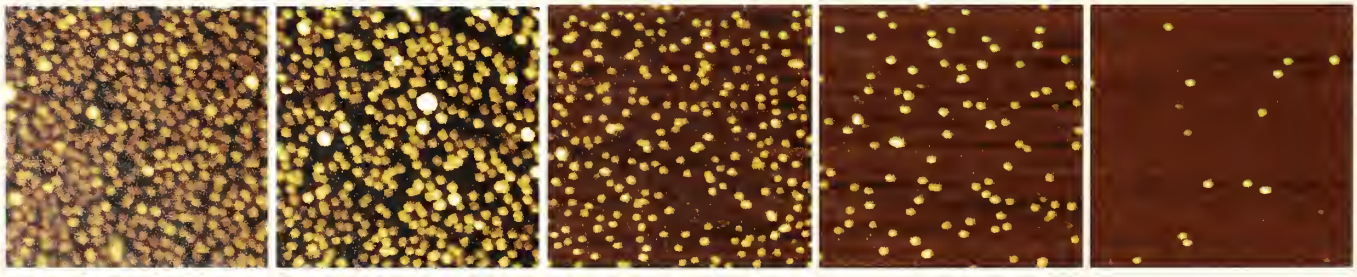

Figure 1: *AFM images of gold particles adsorbed along a substrate prepared by evaporating an APTES/PO mixture for 5 min followed by immersion in colloid gold solution for 24 h (edge of each image = 1 mm).*

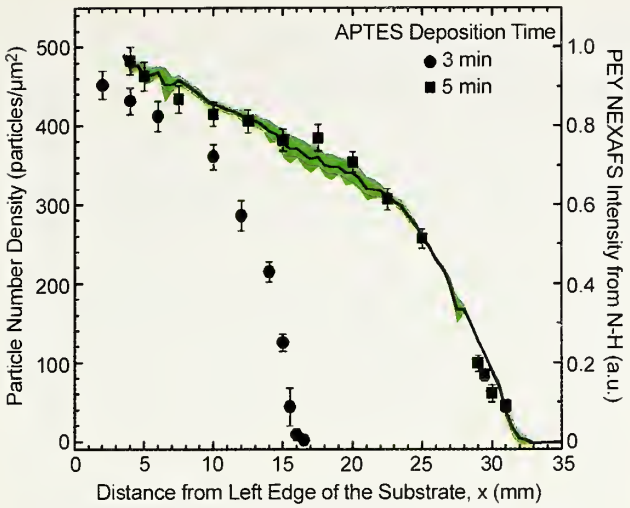
APTES Deposition Time
● 3 min
■ 5 min
Particle Number Density (particles/μm²)
PEY NEXAFS Intensity from N-H (a.u.)
Distance from Left Edge of the Substrate, x (mm)

Figure 2: *Particle number density profile (left axis) for two gradients prepared by evaporating APTES/PO mixtures for 3 (●) and 5 min (■). The data points represent an average from 3 transverse scans along the gradient taken at the center of the sample (y = 0 mm, y = –3 mm, and y = +3 mm). The line represents the PEY NEXAFS profile (right axis) of N-H bonds from an APTES gradient prepared by evaporating APTES/PO mixture for 5 min. The area around the PEY NEXAFS line denotes the measurement uncertainty (based on 9 line scans along the gradient taken between –3 mm and +3 mm from the center of the sample).*

APTES molecules after nanoparticle deposition. By comparing the results of the NEXAFS and AFM measurements, the relationship between the spatial variation of the particle density and the APTES concentration along the gradient was established. NEXAFS involves the resonant soft x-ray excitation of a K or L shell electron to an unoccupied low-lying antibonding molecular orbital of σ symmetry, σ^*, or π symmetry, π^*. The initial-state K shell excitation gives NEXAFS its element specificity, while the final-state unoccupied molecular orbitals provide NEXAFS with its bonding or chemical selectivity. A measurement of the intensity of PEY NEXAFS spectral features thus allows the identification of chemical bonds and determination of their relative population density within the sample. This facilitates the determination of the template APTES concentration profile after particle adsorption by collecting PEY NEXAFS line scans at a fixed photon excitation energy corresponding to the N-H bond (≈406.0 eV) along the x-direction of the sample. An average from several PEY NEXAFS scans (measured between –3 mm and +3 mm from the center of the sample) for the sample prepared by first evaporating APTES for 5 min and then immersing the substrate into a colloidal gold solution for 24 h is depicted in Figure 1. There is excellent agreement between the gold particle density profile determined from AFM measurements and the PEY NEXAFS N-H bond intensity profile for the APTES monolayer on the substrate. This bolsters our assertion that gold particle gradient is indeed formed on the underlying template $-NH_2$ gradient.

The vapor diffusion technique can be utilized to prepare other interesting nanoparticle architectures. In Figure 3, we show a "double gradient" nanoparticle architecture created by diffusing APTES molecules simultaneously from both ends of the substrate, thus producing a valley in nanoparticle concentration. This architecture also shows excellent agreement between the particle gradient and the underlying APTES template.

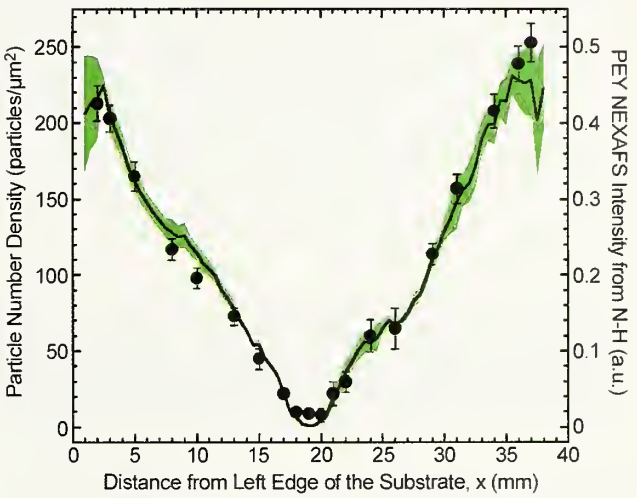

Figure 3: *Particle number density (left axis) and NEXAFS PEY (right axis) profile for a "double gradient" prepared by evaporating APTES/PO mixture for 3 min from both ends of the substrate followed by immersion in colloid gold solution for 24 h. The data points represent an average from 3 transverse scans along the gradient taken at the center of the sample (y = 0 mm, y = –3 mm, and y = +3 mm). The area around the PEY NEXAFS line denotes the measurement uncertainty (based on 7 line scans along the gradient taken between –3 mm and +3 mm from the center of the sample).*

For More Information on this Topic

Contact: D.A. Fischer (Ceramics); J. Genzer (NCSU)

R.R. Bhat, D.A. Fischer, and J. Genzer, *Langmuir* **18** (2002), pp. 5640–5643. "Fabricating planar nanoparticle assemblies with number density gradients."

Press release, July 18, 2002, Brookhaven National Laboratory, "Scientists Create New Material With Varying Densities of Gold Nanoparticles."

High-Speed Contact at the Head-Disk Interface in a Magnetic Hard Disk Drive: Experiment and Modeling

As magnetic data storage technology moves towards higher areal density with lower flying heights and higher rotational speeds, the propensity of random contacts at the head-disk interface is bound to increase. The tribological performance of the head-disk interface will have significant impact on the performance and durability of the hard disk drive. A high-speed impact test method has been developed for evaluating nanometer-thick lubricant film/carbon overcoat materials on hard-disk surfaces, and a three-dimensional finite element model has been constructed to calculate the stress concentrations and the effect of material parameters on the resulting deformation. The availability of an experimental technique and a model enables effective screening of different material chemistries and lubricant combinations to improve the level of protection for hard disk technology.

Development of newer generations of hard disk drives with higher data storage capacity poses many technological challenges. The magnetic disk drive consists of a multilayer disk that stores the data and an air-bearing slider that contains a magnetic head for reading and writing. As the areal density of data storage increases towards 155 Gb/cm^2, the physical spacing between the head and disk surfaces needs to be reduced from (10 to 15) nm to 3.5 nm. The rotational speed needs to increase to 15,000 rpm (45 m/s) from 7200 rpm. The combination of the low flight height and high speed makes occasional contacts inevitable due to disk waviness, spindle wobble, and disk surface roughness. Sometimes catastrophic collisions (avalanche) result in the loss of data.

Besides improving the spindle and surface roughness, new overcoats and lubricants are being investigated to improve the protection of the disk against such high-speed collisions. Actual durability field trials to evaluate new materials under such conditions are time-consuming and expensive as well as statistics-based. Thus, there is an urgent need to develop an accelerated test methodology to evaluate materials under controlled conditions.

The experimental research includes development of a one-pass, high-speed impact test instrumentation and test method to evaluate materials on a hard disk surface. The basic concept is to artificially create a ridge (500 to 2000) nm high with a 0.002° to 0.01° angle of incline) on the disk surface by controlled scratching at the substrate side of the disk to create a ridge on the top surface with its multilayers intact. A 3 mm diameter ruby ball collides with the ridge under 7200 rpm rotational speed. The impact force is measured with an acoustic emission (AE) sensor and the deformation volume is obtained with an atomic force microscope (AFM).

For the experiments reported here, the height of the ridge is 2000 nm and the angle of incline is 0.003°. There is considerable difficulty in alignment, z-height control, and force calibration. Figure 1 shows a typical electrical signal from the AE sensor during an impact. The intensity of the signal is converted to force which is about one newton or less. The calibration of the AE signal is carried out using both the ball-drop method and pencil–lead break method. A modified ball drop method was developed to improve the accuracy of the calibration. Figure 2 shows the setup: one ball drops onto another ball to create the signal. The bottom ball is pressed into the disk and the area of contact is measured with an optical microscope.

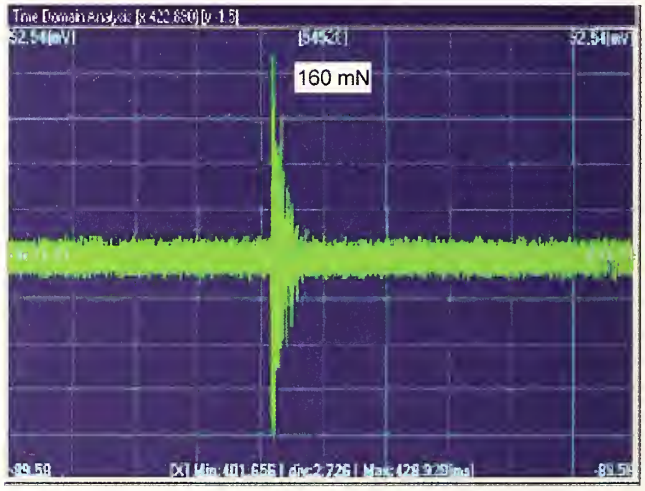

Figure 1: *Acoustic emission signal from an impact event.*

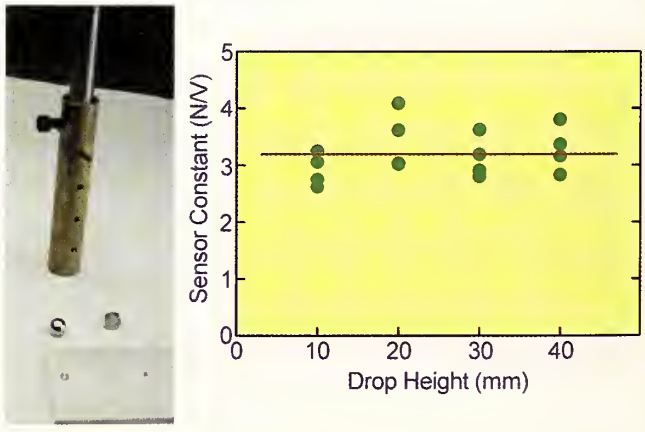

Figure 2: *Ball-dropping apparatus (left) and data (right) for the force calibration.*

By dropping one ball on top of a second ball positioned at the pre-formed deformation zone, the signal transmits through the known contact area between the ball and the disk. The acoustic signal from the collision is recorded with the sensor placed on the other side of the disk. The resulting calibration curve indicates a sensor constant of (3.2 ± 0.4) N/V under these experimental conditions.

A series of impact tests was conducted on disk samples with different monolayer (1 nm) coatings. The transmitted force measured for a blank disk is (0.92 ± 0.23) N. For perfluoro-polyether (PFPE), the transmitted force is (0.61 ± 0.04) N and for PFPE + 5% phosphazine, the transmitted force is (0.31 ± 0.07) N. This ranking corresponds with industrial field experience in terms of robustness of lubricant coatings.

The computational component of this research investigates the dynamic problem of a high-speed spherical asperity impacting on a flat surface of a hard disk at a shallow angle. The objective is to ascertain the result of such an impact and to investigate the complex interactions of multilayer materials such as a hard disk. We seek to obtain the values of contact duration, contact zone size, time history solutions of stress field (including residual stress), damage/plastic yield zone, contact area, and contact force for a given set of attributes including the layered structure of the disk. Due to the time-dependent nature and the difficulty of the problem (such as the geometric complexity, the materials' nonlinear, nonuniform and path-dependent properties, and inertial effects), analytical closed form solutions are not possible. A numerical method using finite element simulation was used. It should be emphasized that this approach is continuum in nature as implied by the conventional finite element theory. However, as the thicknesses of the layers are reduced to a few nanometers, the effect of surface mechanical stresses present at the free surface and interfaces becomes significant and, thus, cannot be ignored.

Using the guidelines described above, we constructed a 3*D* finite element model. The model includes only the top half of the disk due to the shallowness of the impact. The slider is modeled by a two-mass system linked by a spring simulating a nanoasperity on the head surface.

For a given layered structure and geometry, asperity size, and impact velocity, the model is capable of predicting sliding contact events, including contact duration, zone size, forces, penetration depth, underlying plastic zone, and energy transfer. The simulations use realistic values from current disk design: asperity size = 30 nm in radius, impact speed = 10 m/s, and (5, 30 and 50) nm thicknesses for the overcoat, media layer and substrate, respectively. The results are given below.

Figure 3 is a contour plot of the maximum principle stress field created by two collisions. Each collision occurs on a time scale of approximately 10 ns. The *in-situ* stress field under the asperity demonstrates compression ahead and tension behind the penetration. The plastic deformation zone created in the substrate as a result of two collisions between the asperity and substrate is shown in Figure 4. When the asperity has left the disk surface after a collision, there exists a well-defined zone of residual stress, indicating that elastic recovery causes stress redistribution. The stress field distribution is influenced by the different mechanical properties of the individual layers as noted in Figure 3.

The simulation also gives an indication of the energy partition as a result of collision under an adiabatic assumption. Results suggest that under a short duration, relatively light normal load, the momentum transfer due to velocity change results in a substantial temperature rise at the interface. The energy attributable to frictional dissipation is about 40 fJ per impact for a given friction coefficient of 0.3. The energy from plastic deformation is only about 7 fJ when a portion of the kinetic energy from the moving slide is transferred onto the disk. It is clear that the dominant mechanism of energy consumption is due to heat generated from friction, an outcome consistent with experimental observations.

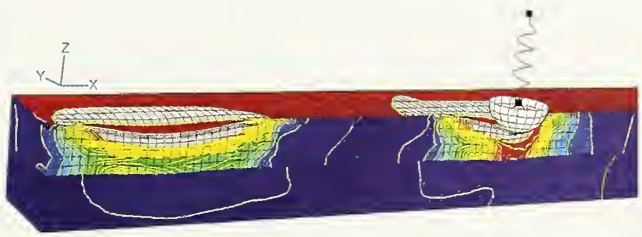

Figure 3: *Contour plat of the maximum principle stress field created from two collisions between an asperity (represented by a semi sphere in the figure) and substrate.*

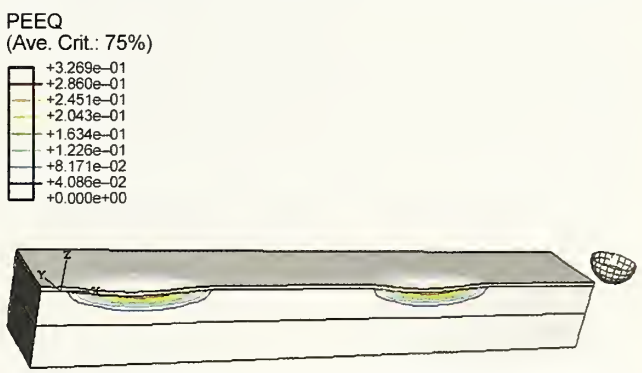

Figure 4: *Plastic zones developed underneath the collision sites. Also shown are the deformed craters on the top surface.*

For More Information on this Topic

Contact: M. Bai, T.J. Chuang, S.M. Hsu, Z.C. Ying

"Simulation of a Single Asperity Impact at Head-Disk Interface," Chuang, T.-J., and Hsu, S.M., ASME/STLE Proceedings on the Frontiers of Magnetic Hard Disk Drive Tribology and Technology, Cancun, Mexico; also submitted to ASME *Trans. Journal of Tribology.*

Elastic Moduli Data for Polycrystalline Oxide Ceramics

A critical consideration in the development and application of advanced materials is the variation of the material properties with respect to the internal microstructural characteristics of the material and the environmentally controlled external parameters such as temperature. Elasticity is especially important to all engineering applications in which the material components experience mechanical stresses. As part of our effort to provide evaluated data for advanced ceramics, we have conducted a detailed review of the variation of the elastic moduli of polycrystalline oxide ceramics with respect to porosity and temperature. A compilation of data for 53 oxide ceramics was constructed, and the data were analyzed in the context of a suitable model expressing the simultaneous dependence on porosity and temperature analytically.

Elastic moduli data were compiled for 53 specifications of polycrystalline oxide ceramics resulting in a collection of nearly 4000 property values extracted from publicly-accessible technical literature. Data presented originally as graphs were digitized so that the entire compilation was given in the form of tabulated numeric values. For each material specification having sufficient data, an analytic model was fit to the data. The results for the analytic model may be especially valuable for product design applications and real time, in service simulations in which varying temperatures require the use of continuously variable elastic properties.

All solid materials can deform from their original unstressed sizes and shapes when subjected to external forces or internal thermal stresses. This propensity of materials to deform under exerted forces is critically important in the design of any mechanical component whose operation depends on its ability to sustain loads or to maintain dimensions within specified tolerances. For advanced ceramics, the particular condition known as elastic deformation is, perhaps, the most important property required for designs in which the material must perform its useful functions while sustaining thermal or mechanical stresses.

Quantitative results describing the observed relationship between the magnitude of the applied force and the amount of deformation were presented as early as the 1660s by the English scientist, philosopher, and inventor, Robert Hooke [1]. In contrast, the development of the class of materials now broadly known as advanced ceramics began only as recently as the middle of the twentieth century. The first substantial review of the elastic properties of advanced ceramics appears to have been the work of S.M. Lang in 1960 [2]. That collection presented the bulk density and dynamic moduli, at room temperature, determined for 20 different materials consisting of oxides, carbides, borides, cermets, and intermetallic compounds. Over approximately the following three decades, O.L. Anderson, et al. produced a series of papers [3–5] regarding the elastic properties of polycrystalline ceramics and minerals of importance to geophysics. More recently, R.W. Rice undertook a series of reviews of the physical properties of ceramics [6–8] with the particular interest of gaining insight into the manner in which physical properties are influenced by porosity. Beginning in the late 1980s, the discovery of high temperature superconductivity led to a whole new class of advanced ceramics for which property data began to appear rapidly. Early reports of the mechanical properties of these materials (principally oxide ceramics) were reviewed by R.G. Munro [9]. These diverse collections were consolidated and expanded in the present work.

Advanced ceramics (*a.k.a.*, fine ceramics and engineering ceramics) are primarily polycrystalline materials containing randomly oriented crystalline grains and intervening void spaces. When a stress is transmitted to a grain, the response of the grain is determined, in part, by the mechanical reaction of the neighboring grains. The presence of a neighboring void space, however, allows a grain to yield more readily (less stiffly) than when that same space is occupied by another material grain. Consequently, void spaces cause the material to be less rigid, as illustrated in Figure 1. In this example, a porosity of about 10% causes the elastic modulus to be diminished from its maximum value by nearly 30%.

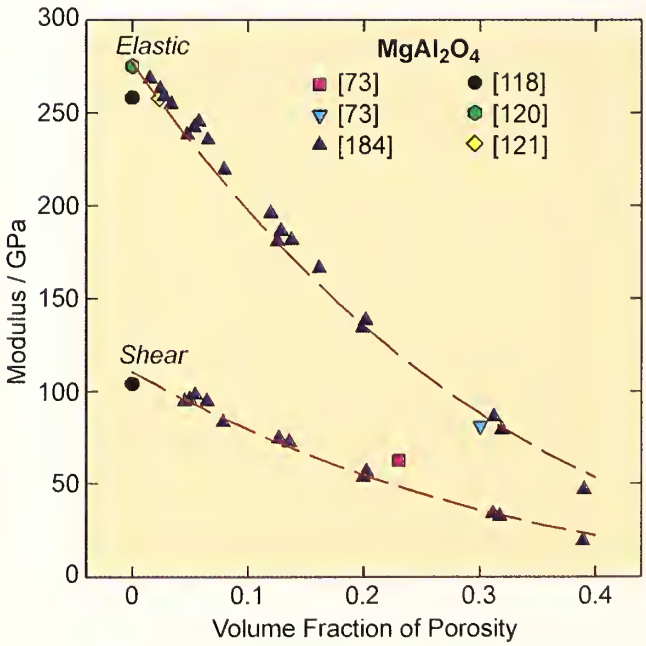

Figure 1: *The elastic and shear moduli of $MgAl_2O_4$ at 23°C decrease rapidly as the volume fraction of porosity increases. [Numbers in brackets are references in NISTIR 6853.]*

The porosity dependence of the elastic properties of solids has been the subject of extensive investigation for decades. Many models have been proposed to represent the general trend of elastic moduli with porosity. Analytical models have been of considerable interest because of their potential use as smoothing and interpolation functions and because of their capacity to provide highly effective descriptions of the mean trends of the moduli with porosity. Two theoretical studies, one on the elastic modulus [10] and one on the bulk modulus [11], gave closed form analytical models exhibiting the same functional form, M, for the dependence on the volume fraction of porosity, ϕ; specifically, $M \sim (1-\phi)^m$, with m as a parameter. That functional form was used to model the porosity dependence in the present work and was found to provide an accurate representation over the complete range of the observed porosity values.

The temperature dependence of the elastic moduli for most ceramics is relatively simple. Empirically, the moduli generally decrease monotonically with increasing temperature. At very low temperature, the slope of the modulus with respect to temperature must approach zero. On the basis of lattice dynamics, Born and Huang [12] estimated that the elastic constants should vary as T^4 at low temperature. To describe the behavior extending from low to high temperature, Wachtman, et al. [13] suggested empirically a temperature dependence of the form $-T\exp(-T_0/T)$ where T_0 is an adjustable parameter. However, above room temperature, the moduli generally decrease linearly with increasing temperature, as illustrated in Figure 2. Since the present work principally was concerned with moduli at elevated temperature, it was found to be sufficient to consider only a linear dependence on temperature.

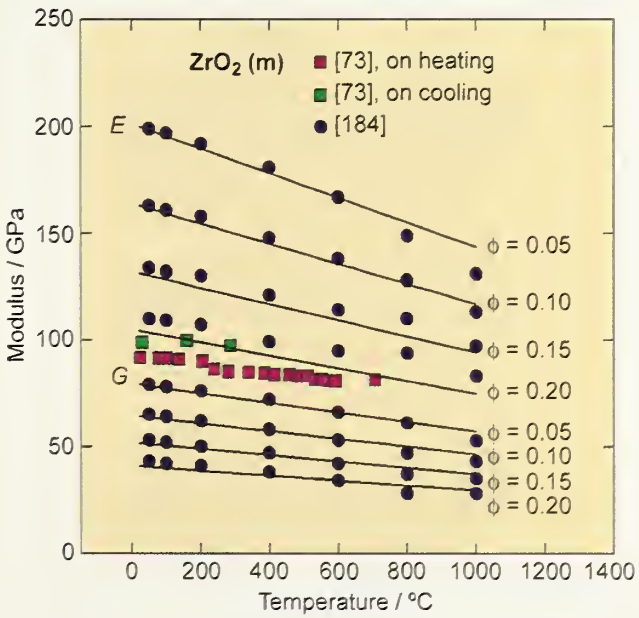

Figure 2: The elastic modulus, E, and shear modulus, G, of monoclinic zirconium oxide decrease linearly with increasing temperature. [Numbers in brackets are references in NISTIR 6853.]

In addition to the dependence on temperature and porosity, it must be noted that the elastic responses of crystals may vary in different directions. For a polycrystalline ceramic, however, the randomness of the orientations of the grains renders the material approximately isotropic with respect to its bulk properties. Consequently, only two of the possible elastic moduli are required to specify the elastic properties completely. The model describing simultaneously the dependence on porosity and temperature, therefore, is given by means of a pair of expressions:

$$E = E_0(1-aT)(1-\phi)^n \qquad (1)$$

and

$$B = B_0(1-bT)(1-\phi)^m \qquad (2)$$

where E is the elastic modulus and B is the bulk modulus.

For each material specification in the compilation, the model parameters E_0, a, n, B_0, b, and m were determined whenever the data set was sufficient to perform a least squares fit of the model to the data.

Cited References

1. R. Hooke, De Potentia Restitutiva, London, (1678).
2. S.M. Lang, *Properties of High-Temperature Ceramics and Cermets, Elasticity and Density at Room Temperature*, Monograph 6, National Bureau of Standards, (1960).
3. O.L. Anderson, *Phys. Acoust.*, **3B**, pp. 43–95, (1965).
4. O.L. Anderson, E. Schreiber, and R.C. Liebermann, *Revs. Geophys.*, **6**, pp. 491–524, (1968).
5. O.L. Anderson, D. Isaak, and H. Oda, *Revs. Geophys.*, **30**, pp. 57–90, (1992).
6. R.W. Rice, *Mat. Sci. Eng.*, **A112**, pp. 215–224, (1989).
7. R.W. Rice, *Key Eng. Mat.*, **115**, pp. 1–20, (1995).
8. R.W. Rice, *J. Mat. Sci.*, **31**, pp. 102–118, (1996).
9. R.G. Munro, in *Handbook of Superconductivity*, edited by C.P. Poole, Academic Press, New York, pp. 570, pp. 625, (1999).
10. A.S. Wagh, R.B. Poeppel, and J.P. Singh, *J. Mat. Sci.*, **26**, pp. 3862–3868, (1991).
11. R.G. Munro, *J. Am. Ceram. Soc.*, **84**, pp. 1190–1192, (2001).
12. M. Born and K. Huang, *Dynamical Theory of Crystal Lattices*, Oxford University, New York, (1954).
13. J.B. Wachtman, Jr., W.E. Tefft, D.G. Lam, Jr., and C.S. Apstein, *Phys. Rev.*, **122**, pp. 1754–1759, (1961).

For More Information on this Topic

Contact: R. Munro

Elastic Moduli Data for Polycrystalline Oxide Ceramics, R.G. Munro, *NISTIR 6853*, National Institute of Standards and Technology, (June 2002).

Infrared Reflectance Spectrum of $CaTiO_3$ Calculated from First Principles

An important route to progress in wireless communications is the development of microwave dielectrics with improved properties and lower costs. Understanding the structure–property relationships of these technologically important materials will lead to the rational design of new materials with desired properties. Infrared reflectivity is an important tool for characterizing such materials because the IR reflectance spectrum is closely related both to the dielectric properties and to the atomic scale structure. Materials for microwave dielectrics, such as those based on $CaTiO_3$, have complicated crystal structures and thus complicated infrared spectra. This work shows that the IR reflectance spectrum of $CaTiO_3$ can be computed from first principles density functional theory, and can be interpreted in terms of the structure and chemistry of $CaTiO_3$.

Microwave dielectrics are used as resonators and filters in applications such as wireless communications. Microwave dielectric materials must have: (1) high dielectric constant ε', (2) low dielectric loss, and (3) temperature stability. $BaZn_{1/3}Ta_{2/3}O_3$ (BZT), currently in use, has excellent properties but contains the expensive metal tantalum. The development of lower-cost, next generation, devices will require a replacement for BZT.

Fundamental knowledge of structure–chemistry–property relationships in dielectric materials will help achieve this goal. Current empirical knowledge of structure–property relationships in dielectrics is insufficient for the rational design of new materials. First-principles (FP) calculations complement experiment and are ideally suited for studying the physics of dielectric materials because they allow the origin of their physical properties to be studied on an ion-by-ion basis.

$CaTiO_3$ (CT) (Figure 1) is an important material for microwave dielectrics because it has very high dielectric constant ε' (approximately 180 at room temperature) and a positive temperature coefficient. By combining CT in solid solutions with materials with negative temperature coefficients, a large variety of potentially useful, zero temperature coefficient, materials can be obtained.

The dielectric constant of a material as a function of frequency ν is given by

$$\varepsilon(\nu) = \varepsilon_{elec} + \Sigma_\mu S_\mu \nu_\mu^2/(\nu_\mu^2 - \nu^2 + i\gamma_\mu\nu), \quad (1)$$

where ε_{elec} is the electronic contribution to ε, the sum is over phonon modes μ, S_μ are the phonon oscillator strengths, ν_μ their frequencies, and γ_μ their damping coefficients. The oscillator strength of phonon μ, in turn, is proportional to $Z^*_\mu{}^2/\nu_\mu^2$, where Z^*_μ is the phonon's effective charge. Note that the number of phonon modes in Eq. (1) is determined from the crystal structure (25 in the case of CT), while Z^*_μ and ν_μ are determined by the crystal chemistry.

The dielectric constant as a function of frequency can be measured in many ways. Infrared reflectivity is a very useful, though indirect, method. Infrared reflectivity measurements are commonly fit using equation (1) to determine the phonon parameters. This becomes difficult, however, for a system as complicated as CT.

Alternatively, one can use FP methods to *compute* the phonon and dielectric properties, and thus the IR reflectance spectrum. Advances in FP methods have made it possible to compute Z^*_μ and ν_μ of a crystal, given as input only the experimental unit cell and atomic positions. The ability to correctly compute Z^*_μ is a relatively recent development and has led to the discovery that large Z^*_μ are common in perovskites, which enhances their dielectric constants.

Because of the technological importance of CT, and its strongly temperature-dependent ε', collaborators at the Czech Academy of Sciences used IR reflectivity to explore the temperature dependence of ε' in terms of the temperature dependence of the phonon properties.

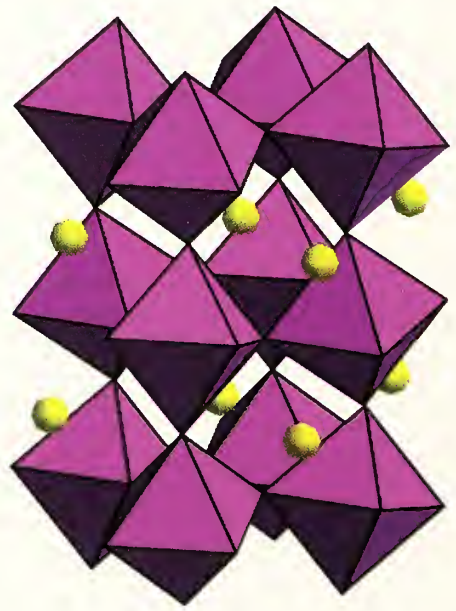

Figure 1: Perovskite-type structure of $CaTiO_3$. Ti ions are at the centers of oxygen octahedra, which are joined at their corners. Ca ions (yellow) occupy special positions between the octahedra.

The experimental IR reflectance spectrum at T = 6 K is shown in Figure 2. The IR reflectance spectrum that we calculated from FP is shown for comparison. (Although calculation of the damping parameters from FP is not yet practical, simply setting all γ_μ to the same value of 5 cm^{-1} leads to good agreement with experiment in this case.)

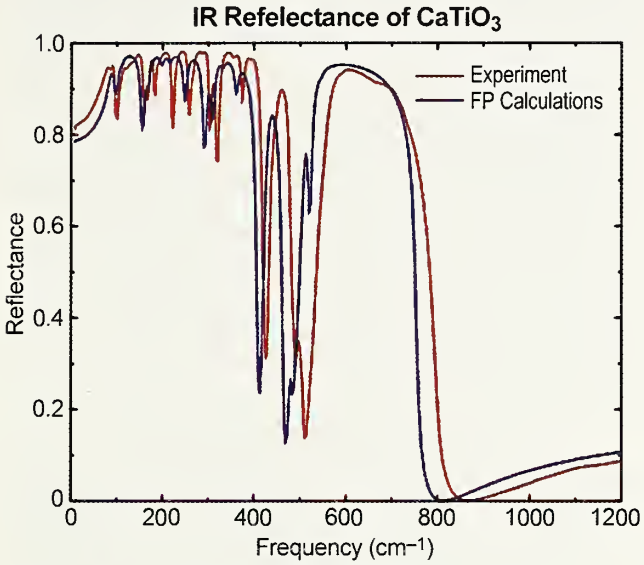

Figure 2: *Comparison of the experimental infrared reflectance spectrum of $CaTiO_3$ with that computed from first principles. (Experimental results courtesy of V. Zelezny.)*

Except for a systematic shift of the FP results toward slightly lower frequencies, the agreement between the two spectra is excellent. The results clearly demonstrate that FP calculations are able to compute IR reflectance spectra for perovskite-type oxides such as CT.

Given the accuracy of the FP calculations, it becomes possible to interpret the IR spectrum in terms of crystal structure and chemistry in unprecedented detail. In fact, a number of unexpected results were found. Many of these concern the importance of the tilting of the oxygen octahedra. If the oxygen octahedra were not tilted, only 3 phonon triplets would contribute to the dielectric function of CT, instead of the 25 modes for CT with octahedral tilting. Previous interpretations of the IR reflectance spectrum of CT were based on fitting the results to a 3 phonon model. However, the FP results show that it is impossible to correctly fit the experimental results with only 3 phonons, because the oscillator strengths of some of the modes that arise due to octahedral tilting are *larger* than those associated with the ideal perovskite structure. The three sets of phonons associated with the ideal perovskite structure have frequencies of approximately 80 cm^{-1}, 220 cm^{-1}, and 550 cm^{-1}, respectively. However, the modes near 160 cm^{-1} that arise due to octahdedral tilting have higher oscillator strength than those near 220 cm^{-1} and are more dominant in the spectrum.

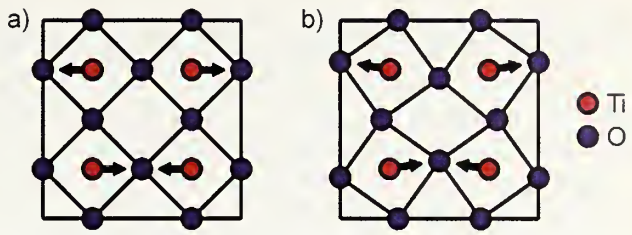

Figure 3: *A phonon mode which is (a) nonpolar in the perovskite structure with untilted octahedra becomes (b) polar upon octahedral tilting.*

One of the most significant features in the spectrum is the deep dip in reflectivity near 400 cm^{-1}. This feature arises due to the octahedral tilting as shown in Figure 3. In one of the normal modes of vibration of a perovskite, the atoms that are in the centers of oxygen octahedra (Ti for CT) vibrate out of phase with each other (Figure 3(a)). When the octahedra are tilted (Figure 3(b)), the same normal mode now has a net in-phase motion of Ti ions along one direction. In-phase motion of charged ions leads to a nonzero mode effective charge Z^*_μ and thus a contribution to the dielectric constant and IR reflectance spectrum.

An issue particularly relevant to industry is the temperature dependence of dielectric constants. Here, too, FP calculations have led to insight into the connection between the structure of CT and its rapidly decreasing dielectric constant as a function of temperature. FP calculations show that the large dielectric constant of CT is dominated by the contributions of the low-frequency phonons, which have both high Z^*_μ and low ν_μ. The large Z^* of these modes is due to the nature of the vibration. The Ti vibrate against the oxygen octahedra, while the Ca vibrate in-phase with the Ti. Experimentally, one finds that ε' decreases as temperature increases because the frequencies of the lowest-frequency phonons increase. The structure of CT also changes as the temperature increases. In particular, the oxygen octahedra tilting angles decrease. FP calculations on the phonon frequencies as a function of octahedral tilting show that the frequencies increase as octahedral tilting decreases, in agreement with experiment. The increase in phonon frequency can be explained by the shortening of Ti-O bonds as tilting decreases and the sensitivity of Ti-O force constants to bond length.

For More Information on this Topic

Contact: E. Cockayne

V. Zelezny, E. Cockayne, J. Petzelt, M.F. Limanov, D. Usvyat, V.V. Lemanov, and A.A. Volkov, "Temperature Dependence of Infrared-Active Phonons in $CaTiO_3$: A Combined Spectroscopic and First Principles Study," submitted to *Physical Review B*.

Mechanical Reliability and Lifetime Prediction for Brittle Materials

The need to design structures containing brittle material extends from aeronautical components to integrated circuitry. Because the mechanical failure of brittle materials is typically both catastrophic and difficult to predict, it is necessary for engineers to know how to build in adequate safety margins and how to predict realistic lifetimes. In response to this need, we have written a Recommended Practice Guide for brittle material lifetime prediction as a tool for designers and engineers. We provide descriptions of the tests required for lifetime prediction, a discussion of why the tests are required and how they fit together, and an extensive list of references for further study.

Mechanical failure of brittle materials is usually catastrophic and almost always occurs without warning. Consequently, designers are often hesitant to design components with brittle materials despite advantages regarding strength, weight, and/or resistance to harsh thermal and chemical environments. To address concerns associated with brittle failure, techniques to determine reliability of components fabricated from brittle materials (*e.g.*, ceramics and glasses) have been extensively developed over the last thirty years. In this context, reliability is defined as the probability that a component, or system, will perform its intended function for a specified period of time. *NIST Recommended Practice Guide: Mechanical Reliability and Life Prediction for Brittle Materials* (NIST SP 960-9) was written to gather conclusions from three decades of research into a single, systematic document for use by design engineers.

The two main principles influencing reliability of brittle materials are the statistical nature of component strength and its time-dependent, environmentally-enhanced degradation under stress. The statistical aspect of strength derives from the fact that the strength is limited by the distribution of the most severe defects in the components (*i.e.*, the strength-determining flaws). Because flaws are generated both by processing and by in-service use and handling, the initial strength of a set of components is described by a statistical distribution rather than by a fixed value. The time-dependent aspect of strength arises because, in most brittle materials, defects grow under the combined effects of stress and environmental attack. These concepts have led to a lifetime prediction formalism that incorporates strength and crack growth as a function of stress. Predicted reliability, or lifetime, is only meaningful, however, when coupled with a confidence estimate. Therefore, the final step in the lifetime prediction process must be a statistical analysis of the experimental results.

As described above, the lifetime prediction approach represents the currently accepted procedures involved in the various steps of reliability assessment of homogeneous, brittle materials. There are, of course, a number of assumptions built into any technical procedure and, frequently, these assumptions cannot be tested. In the *NIST Recommended Practice Guide*, the assumptions inherent in steps associated with lifetime prediction are clearly stated in each section, and implications that arise if the assumptions are violated are discussed at the end of the same section.

As Figure 1 shows, there are four steps required in lifetime prediction for brittle materials: evaluation of the initial strength distribution, quantification of susceptibility to environmentally-enhanced crack growth (dynamic fatigue tests), determination of the upper limit of the strength in the dynamic fatigue test, and determination of the confidence limits in the individual tests. These steps combine to give the lifetime prediction. The first three steps are independent and can be conducted in any order.

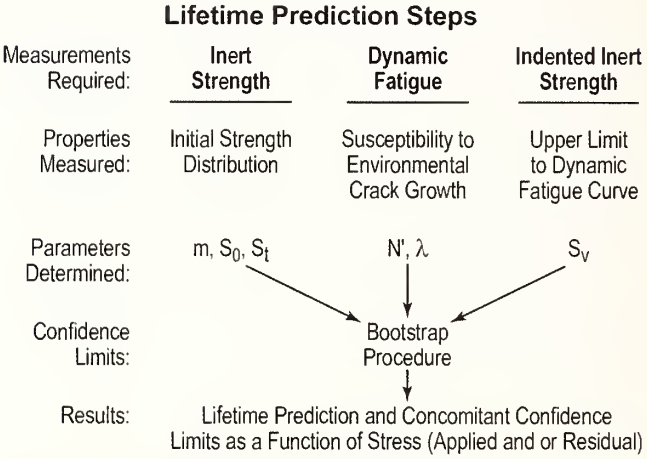

Figure 1: *Flowchart summarizing the steps in the lifetime prediction process.*

Initial Strength Distribution

In principle, the initial strength distribution can be determined in three ways: (1) a statistical characterization of the initial strength distribution; (2) an over-load proof-test to establish a minimum strength; or (3) direct nondestructive flaw detection from which strength can be calculated. In practice, non-destructive flaw detection has not yet reached the level for which quantitative strength or lifetime predictions can be made in brittle materials.

The statistical strength characterization approach is particularly useful to evaluate the suitability of particular materials, processing procedures, and surface treatments for a given application. However, because the approach is statistical, it cannot guarantee that components will have strengths greater than some minimum value; rather, it provides a failure (or survival) probability for a given load level. The idea behind the statistical strength distribution characterization is the following. Because

the most critical flaw in a component or test specimen leads to failure, it is not the distribution of flaws itself that is important, but rather the distribution of the extremes of the flaws. Strength distributions are typically described by the Weibull distribution, which is one of three extreme-value distributions. Tests are usually conducted on small coupons the processing history and surface treatment of which mimic those of the final component. Measurements are conducted at high loading rate and in an inert environment (*e.g.*, a dry gaseous nitrogen environment) to avoid environmental effects. After the Weibull strength distribution has been obtained and analyzed, a particular probability of failure, F, can then be associated with a corresponding initial strength.

In contrast, the over-load proof test establishes the upper limit on the most critical flaw in a component or, equivalently, the lower limit on the initial strength distribution. This technique can be expensive since real components are tested. However, a properly conducted proof test completely eliminates the problem of failure through statistical outliers that is unavoidable when the Statistical Strength Distribution technique is used. One simply applies an over-load stress to each component, typically two to three times the service stress. Any components with critical flaws larger than a predetermined size, or with strengths less than a predetermined minimum (namely the proof-test stress), will break; such components are automatically eliminated from the distribution. The requirements for a properly conducted proof test are stringent. Specifically, the proof test must be devised such that the stress at each location of a component exceeds the service stress in that same location by an amount at least as large as the recommended proof-test ratio. The proof test must be performed under controlled conditions of environment and proof-test load cycle; the most critical aspect is to have conditions as inert as possible and to unload from the proof stress as rapidly as possible.

Environmentally-Enhanced Flaw Growth

It is known that flaws in materials under stress can react with certain environments resulting in bond rupture and flaw growth at stresses well below the nominal bond strength of the material. Water is particularly effective at enhancing fracture in many brittle materials. In addition, water is almost ubiquitous in either liquid or vapor phase. Therefore, it is essential that the effects of water-enhanced fracture be incorporated into any lifetime prediction model. Because the process of environmentally-enhanced fracture is only partially understood, expressions relating crack growth velocity, V, to stress intensity factor, K_I, are typically phenomenological rather than truly theoretical. Although several crack-growth-rate expressions have been proposed, the one used in almost all lifetime predictions for brittle materials is the power law, $V \alpha K_I^N$, because this expression can be handled analytically. However, the life prediction formalism can be applied with other crack growth expressions if numerical techniques are used. The experimental approach used to obtain the parameters that control environmentally enhanced crack growth is called dynamic fatigue. In this test, the strengths of test bars are measured as a function of stressing rate *in the environment of interest.* The form of the dynamic fatigue curve depends upon the assumed relationship between K_I and V; for the power law, the curve log[Strength] *vs.* log[Stress Rate] is linear. To reduce scatter in the data, test bars with large, identical flaws (*i.e.*, indentations) are typically used.

Dynamic Fatigue Upper Limit

The upper limit to the dynamic fatigue strength is determined using the same procedure as that used to obtain the Weibull distribution: high loading rate and an inert atmosphere. However, instead of using the natural flaw population as the strength limiting defects, the same size of indentations that were used in the dynamic fatigue experiments is used.

Confidence Limit Determination

The results from tests 1–3 are combined to give a lifetime prediction. However, there is still no way to estimate how statistically significant the lifetime prediction is. To obtain the most information from the lifetime prediction model, it is necessary to estimate the confidence limits associated with the prediction. One approach to evaluate the confidence limits is to use the bootstrap technique. This is a statistical procedure that takes advantage of modern computing power and makes it relatively straightforward to determine confidence limits. The approach applies to any data set that is independent and identically distributed. The major assumption with the bootstrap technique is that the data used to evaluate the lifetime adequately represent the statistical scatter in the experiments. If this condition is met, the bootstrap technique permits the user to estimate the time to failure at whatever confidence level is desired.

The combined measurements and analyses outlined in the Guide provide both lifetime prediction and concomitant confidence determination for brittle structures under load.

The *NIST Recommended Practice Guide: Mechanical Reliability and Life Prediction for Brittle Materials* is NIST special publication SP 960-9, and it will be available free of charge. It will also be available on the NIST website.

For More Information on this Topic

Contact: G. White, E. Fuller, Jr., S. Freiman

G. White, E. Fuller, Jr., S. Freiman, *NIST Recommended Practice Guide: Mechanical Reliability and Life Prediction for Brittle Material,* NIST SP 960-9 (to be published).

Materials Structure Characterization

Materials science and engineering is the area of science concerned with understanding relationships between the composition, structure, and properties of materials and the application of this knowledge to the design and fabrication of products with a desired set of properties. Thus, measurement methods for the characterization of materials structure are a cornerstone of this field. MSEL supports a wide array of techniques and instrumentation for materials measurements. Facilities include optical and electron microscopy, optical and electron scattering and diffraction, and major x-ray facilities at the National Synchrotron Light Source (NSLS) at Brookhaven Laboratory, and at the Advanced Photon Source (APS) at Argonne National Laboratory.

Synchrotron radiation sources provide intense beams of x-rays enabling leading-edge research in a broad range of scientific disciplines. Materials characterization using x-rays from synchrotron sources forms a major part of the Materials Structure Characterization Program. This includes the development and operation of experimental stations at the NSLS and at the APS. At the NSLS, NIST operates a soft x-ray station in partnership with Dow and Brookhaven National Laboratory. At the APS, NIST is a partner with the University of Illinois at Urbana/Champaign, Oak Ridge National Laboratory, and UOP, in a collaboration called UNICAT. At both facilities, NIST scientists, and researchers from industry, universities, and government laboratories, perform state-of-the-art measurements on a wide range of advanced materials. Studies currently underway include: ceramic coatings; defect structures arising during deformation of metals, ceramics, and polymers; defect structures in semiconductors and single-crystal proteins; and atomic-scale and molecular-scale structures at surfaces and interfaces in polymeric, catalytic, and metal/semiconductor systems.

Ceramic powders are precursors for over 80% of ceramic manufacturing. As a result, a major focus in the Ceramics Division is the accurate and reliable measurement of the physical and chemical properties of ceramic powders, including sub-micrometer and nanometer sized powders. These measurements are critical to ensuring processes and products of high quality, minimal defects, and consequent economic benefits. Another area of concern to ceramic manufacturing is powder dispersion in a fluid vehicle for shape forming and other uses. The chemical and physical characteristics of powders dispersed in liquids are evaluated to understand the influence of surface charge, dissolution, precipitation, adsorption, and other physicochemical processes on the dispersion behavior. In addition to these activities, standard reference materials for use as primary calibration standards and national/international standards for particle size and size distribution, pore volume, and particle dispersion measurements are being developed in collaboration with industrial partners, measurement laboratories, and academic institutions in the U.S., Europe, and Asia.

The NIST effort in materials characterization has a strong emphasis on electron microscopy, which is capable of revealing microstructures within modern nanoscale materials and atomic-resolution imaging and compositional mapping of complex crystal phases with novel electronic properties. The MSEL microscopy facility consists of two high-resolution transmission electron microscopes (TEM) and a high-resolution, field-emission scanning electron microscope (FE-SEM) capable of resolving features down to 1.5 nm. Novel experimental techniques using these instruments have been developed to study multilayer and nanometer-scale materials.

Through this MSEL Program, measurement methods, data, and standard reference materials (SRMs) needed by the U.S. polymers industry, research laboratories, and other federal agencies are provided to characterize the rheological and mechanical properties of polymers and to improve polymer processibility. In response to critical industry needs for *in-situ* measurement methodologies, a substantial effort is underway to develop optical, dielectric, and ultrasonic probes for characterizing polymer processing. Improved methods for determining molecular mass distribution of polymers are developed because of the dramatic effect it has on processibility and properties. Mechanical properties and performance are significantly affected by the solid-state structure formed during processing. Importantly, unlike many other common engineering materials, polymers exhibit mechanical properties with time dependent viscoelastic behaviors. As a result, techniques are being developed that measure the solid-state structure and rheological behavior of polymeric materials. Recent program activities exploit advances in mass spectrometry using matrix assisted laser desorption ionization (MALDI) to develop a primary tool for the determination of the molecular masses of synthetic polymers, with particular emphasis on commercially important polyolefins. The polymer industry and standards organizations assist in the identification of current needs for SRMs, and based on these needs, research on characterization methods and measurements is conducted leading to the certification of SRMs.

Contact: David Black

Synchrotron Beam Line Operation and Development

The synchrotron radiation project is focused on the operation and continued development of unique experimental facilities at the Advanced Photon Source (APS) at Argonne National Laboratory and at the National Synchrotron Light Source (NSLS) at Brookhaven National Laboratory. The emphasis is on the development and application of microstructural characterization tools and techniques that allow researchers from industry, universities, and government laboratories to perform state-of-the-art measurements on technologically advanced materials.

David Black

It has been an excellent year for the Synchrotron Beamline Operation and Development Project. At the NSLS, the NIST/Dow Chemical materials science beam line (U7A) has become a lead experimental facility on the UV ring. NIST research at U7A was featured on the covers (Figure 1) of the July 23, 2002 issue of *Langmuir* and the May/June 2002 issue of *Synchrotron Radiation News*. In addition, the unique capabilities of U7A enabled researchers from NIST, BNL, and the University of Oslo to gain new insights into MgB_2: Unraveling the symmetry of the hole states near the Fermi level in the MgB_2 superconductor, *Phys Rev Lett*, **88** (2002).

Figure 1: *Covers of the July issue of* Langmuir *(See also the Highlight "Measuring monolayer templates for fabricating nanoparticle assemblies of number density gradients" in this Report.) and the May/June issue of* Synchrotron Radiation News. *(Reprinted with permission from* Langmuir, *July 23, 2002, 18, cover image. Copyright 2002, American Chemical Society.)*

The UNICAT collaboration at the APS supports activities in ultra small angle x-ray scattering (USAXS) as well as the emerging technique of USAXS imaging on the insertion device line 33-ID. NIST researchers are investigating nanoparticle dispersions to explore and calibrate agglomeration phenomena in a range of submicrometer and nanoparticle dispersions of interest in catalysis and powder metrology. The relationships between primary particle size and agglomerate morphology and crystallite size (for a possible nanocrystalline SRM) are being explored.

The new technique of USAXS imaging has been used to image structures in bovine cartilage. Figure 2a shows localized scattering from a USAXS image (1) near the bone (the bright feature at the bottom is bone) and Figure 2b shows a bright region (2) approximately 400 mm farther away. The structure in Figure 2b is not visible by any other imaging technique. Selected area USAXS scans from these regions provides quantitative data on the microstructures in these regions.

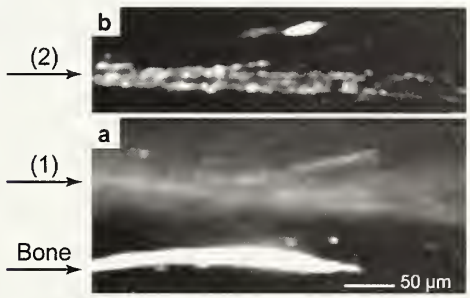

Figure 2: *USAXS images of bovine cartilage.*

On the hard x-ray ring at the NSLS, we operate beam line X23A2 and support the operation of X24A. X23A2 enjoyed continued high interest with more than 32% of operations time devoted to general users. A recent EXAFS study on X23A2 of thin $SrTiO_3$ films grown epitaxially on Si(001) substrates revealed the presence of a displacive ferroelectric phase transition in which the Ti atoms move from the center of the $SrTiO_3$ unit cell. Currently, it is believed that the strain imposed on the layers by the substrate plays a significant role in this transition. The discovery of this effect could facilitate the development of ferroelectric metal-oxide field-effect transistors.

At X24A, NIST researchers have investigated the chemical bonding in the transition-metal oxide rutile TiO_2. The site-specific x-ray photoelectron spectroscopy results reveal chemical hybridization of the cation and ligand orbitals on each site and demonstrates that this hybridization contributes significantly to the electronic structure. This analysis should serve as a benchmark for the interpretation of the more complex transition-metal oxides and the unique physical phenomenon that they exhibit.

Contributors and Collaborators

A.J. Allen, H.E. Burdette, D.A. Fischer, G.G. Long, J.C. Woicik, L.E. Levine, S. Sambasivan; J. Ilavsky (Purdue); P. Jemian, P. Zschack, H. Hong, J. Karapetrova (University of Illinois); A. Kuperman (Dow); Y. Platonov, J. Wood (Osmic Inc.)

Small-Angle Scattering Characterization of Materials

The properties and performance of many materials for technological applications can be controlled by tailoring their microstructures. To achieve this, quantitative microstructure characterization over the length scale from nanometers to micrometers is highly desirable and frequently essential. This project addresses this need by combining a range of x-ray and neutron small-angle scattering measurements with other measurements and novel analysis methods aimed at providing the microstructure (or nanostructure) link between processing and properties.

Andrew Allen and Gabrielle Long

A long-standing objective of this project has been predictive modeling of materials properties as a function of measured microstructure. This year, we used microstructure results from small-angle neutron scattering in a model for predicting properties of plasma-sprayed yttria-stabilized zirconia (YSZ) thermal barrier coatings (TBC's). TBC's were prepared from four different powder feedstocks, and were characterized by SANS, with the results for the porosity (blue), interlamellar pores (red), cracks (yellow) and globular pores (pale blue) shown in Figure 1. The microstructure model constructed from these data is shown in Figure 2.

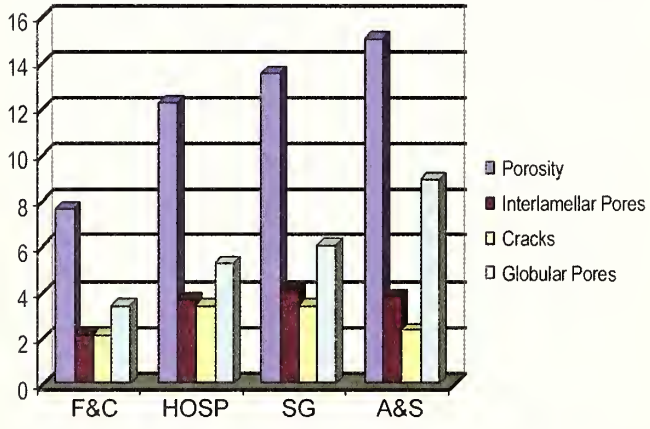

Figure 1: *SANS-determined component porosities for TBC's plasma-sprayed from: Fused and Crushed (F&C), Sol-Gel (SG), Agglomerated and Sintered (A&S), and Plasma-Densified (HOSP) powder feedstocks.*

Finite element model (FEM) analysis was applied to the model microstructure to predict, from first principles, the thermal conductivities (Figure 3) and elastic moduli (similar trend), both parallel (L) and perpendicular (T) to the spray direction. While the predicted thermal conductivities, *K*, are overestimated, the trend is correct for 3 of the 4 TBC's. Further work is underway to improve the predictions.

Another area is the discovery by means of scanning electron microscopy (SEM) and ultra-small-angle x-ray scattering (USAXS) of nanometer pores that, if tailored, may improve the reliability and lifetime of high-velocity oxygen fuel (HVOF) YSZ coatings, an alternative TBC form. Recent work demonstrated the potential for deposition of YSZ by HVOF. These coatings had been previously ignored because their low jet temperature fabrication precludes complete melting of YSZ particles. However, questions remain concerning coating reliability. SEM studies of HVOF YSZ deposits revealed nanometer voids. The void size distributions were derived from USAXS data using a maximum entropy routine. The mean opening dimension in the nanometer void population is 64.5 nm. Stabilizing these voids against sintering could improve reliability.

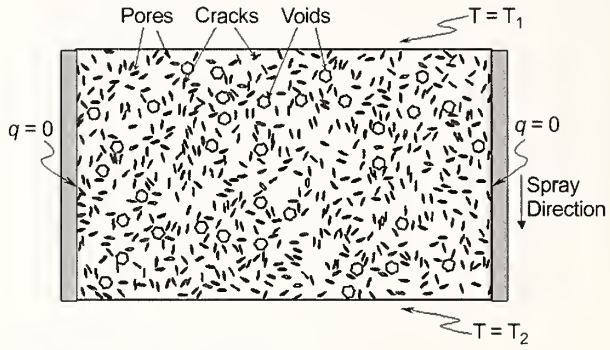

Figure 2: *Model Microstructure.*

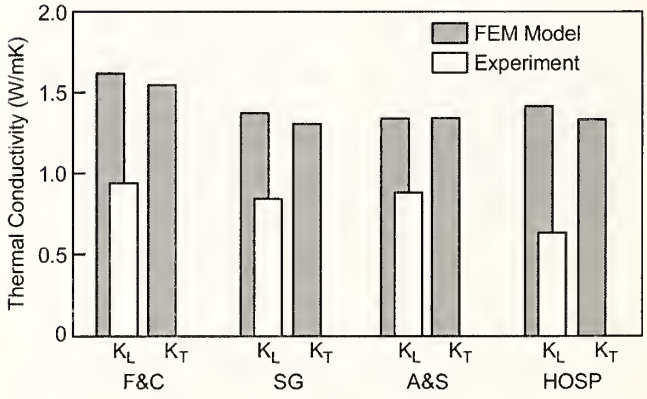

Figure 3: *Measured and predicted thermal conductivities.*

Contributors and Collaborators

T.A. Dobbins (Ceramics); P.R. Jemian (University of Illinois); J. Ilavsky (Purdue University); A. Kulkarni, S. Sampath, H. Herman (SUNY, Stony Brook); C.A. Johnson, J.A. Ruud (GE Corporate Research); L. Kabacoff (Office of Naval Research)

Nano-Structure of Grain Boundaries in Vitreous Bonded Ceramics

The structure and composition of grain boundaries in fine ceramic materials determines their physical properties. Grain boundary structure is particularly important in nano-materials for which the grain boundary to grain volume ratio is high. This program seeks to understand the structure of grain boundaries as boundary thickness approaches the nano-meter scale of resolution. Systematic differences were observed in boundary structure as a function of grain misorientation. Grain boundary wetting is predicted by a thermodynamic formalism developed for this project.

Sheldon Wiederhorn and Bernard J. Hockey

The structure of grain boundaries in vitreous bonded aluminum oxide was studied in bicrystals with varying misorientation of the adjacent grains. The grain boundary phase was a calcium alumino-silicate glass having an anorthite composition. Several types of boundaries were examined, including symmetric basal plane tilt boundaries and small and large angle twist boundaries on the basal plane. The structure of the boundary depended on both the misorientation of the two crystals forming the bicrystal and the orientation of the boundary between the bicrystals. Studies showed that bicrystal boundaries containing a basal plane on one side of the boundary were always decorated with Ca and Si. Furthermore, large angle tilt boundaries that contained a basal plane were always wetted with glass. As the orientation angle of the grain boundary increased, the grain boundary structure went through a transition, from a fully-wetted boundary, to a partially-wetted boundary, and then to a boundary that was completely dry. This last transition occurred at an angle of about 40° to the symmetric boundary plane.

In the coming year, we intend to determine the effect of an applied normal pressure on the boundary structure. The current investigation made boundaries under a modest applied pressure, 10 MPa, which produced boundaries that were identical to those predicted from a wetting theory that assumes no interaction between the two boundary surfaces. We expect the applied pressure to push the boundaries into closer proximity and to modify their structure.

In addition to modifying the structure of the boundary, we intend to measure their fracture resistance by the method of He and Hutchinson. In this technique, a crack is propagated into the boundary as a function of angle, and a critical angle for propagation along the boundary is determined. From this angle and the elastic constants and fracture toughness of the crystals on each side of the boundary, the toughness of the boundary can be determined. The boundary toughness will be measured as a function of boundary separation.

This type of information is useful for improving the strength and toughness of silicon nitride. We hope to obtain results that are generally useful to a wide range of ceramic materials.

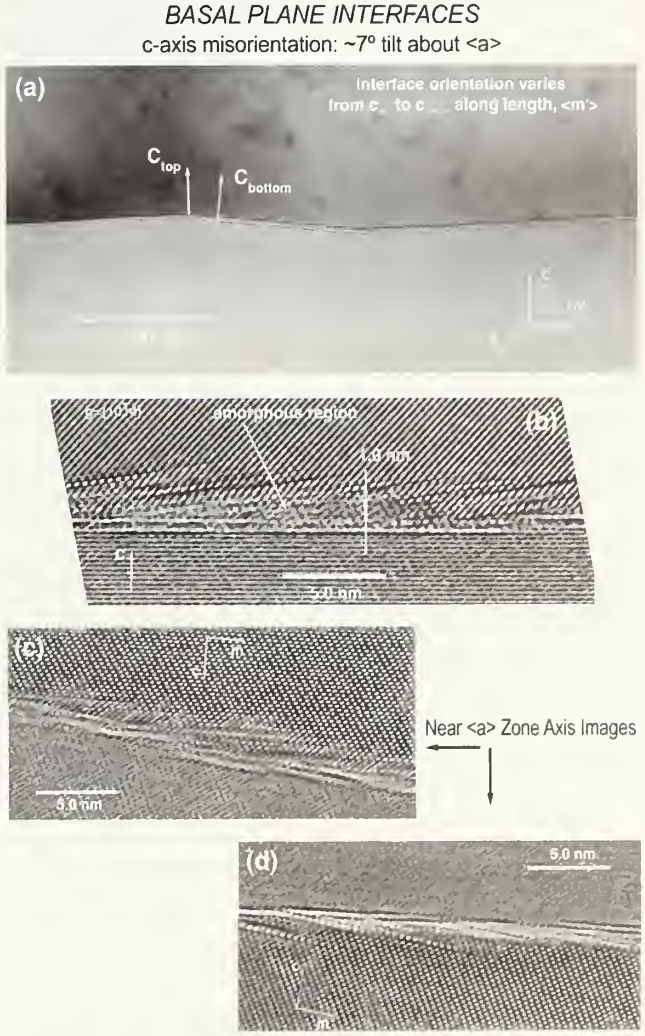

Figure 1: *Bicrystal grain boundary produced by growth roughly normal to the c-plane. The crystals are misoriented by 7° about the <a> axis. Boundaries all contain Ca and Si, but some, (c) and (d), are so narrow that it is difficult to see if these elements in the form of a glass. The facetted structure of the boundary in (a) is typical of the wetted Wulff shape of crystals with these orientations.*

Contributors and Collaborators

J. Blendell (Ceramics); R. French (E.I. DuPont DeNemours and Co.); J.-S. Lee, M.-K. Kang (Seoul National University, Korea)

Powder Diffraction Standards

The powder diffraction technique is well suited, and widely used, for quantitative phase analysis of crystalline samples. It allows the user to probe all crystallographic reflections of a given d space range with a single scan. However, existing methods require the assumption that there is no non-crystalline material within the sample. Substantial improvement in the accuracy of the powder diffraction method can be realized with improved standards that can address the issue of non-crystalline inclusions in the test mixtures.

James P. Cline

The measurement of phase abundances within mixtures is readily accomplished using the powder diffraction technique as the diffraction intensity from a given phase is proportional to its quantity within the sample. The method is used in a broad range of technical applications as the only stipulation is that the sample consists of a polycrystalline monolith, or, more commonly, a powder. While any one of a number of powder diffraction techniques can be used for data collection, the most common is the laboratory x-ray diffractometer of which there are 20,000 in operation worldwide. There are two primary methods for data analysis: the reference intensity ratio, RIR, method, compares measured diffraction intensities with those collected from standards. More recently, the Quantitative Rietveld Analysis, QRA, method was developed, in which diffraction patterns for each phase are calculated from their respective crystal structures and fit to the observed data through a least squares refinement. Since QRA makes use of the entire pattern in the analysis, and can account for systematic effects, it affords considerable improvement in accuracy over the RIR method.

Bragg diffraction offers no information on the amorphous fraction of materials as it contributes intensity only to the background. The importance of this limitation is realized when considering a finely divided solid: surface reactions and relaxation will invariably lead to a surface region which will not diffract in the same way as the bulk. A 10 nm to 20 nm layer may contain several percent amorphous material. With the advent of QRA, the issue of amorphous content has come to the fore. Background level measurements can, in principle, be used to infer amorphous content. However, at the low levels under consideration, the internal standard method is preferred as Bragg intensity can be determined more accurately than slight changes in background level. Comparison of the results from the diffraction experiment, with the initial mass ratio of the standard (of known amorphous content) to unknown, permits amorphous content determination. To provide a suitable standard for this procedure, we are seeking to re-certify the primary NIST quantitative analysis SRM, SRM 676, alumina, with respect to its amorphous content. From this, the remaining NIST SRMs certified for quantitative analysis will also be certified for amorphous content.

The experimental approach is based on an analysis of the phase abundance of mixtures of intrinsic, float-zone silicon and SRM 676. Success of the approach requires: the measurements are accurate, the silicon is perfect, all of the amorphous material associated with it is confined to the crystallite surface, and the amorphous layer thickness is invariant with respect to crystallite size. The mass fraction of silicon, determined via QRA, can then be plotted relative to the surface area, or amorphous content, of the silicon. These data can be extrapolated to yield a value for mass fraction of silicon that would possess "zero" amorphous content. Thus, the discrepancy between this mass fraction and that of the initial weighing would indicate the true amorphous content of the alumina.

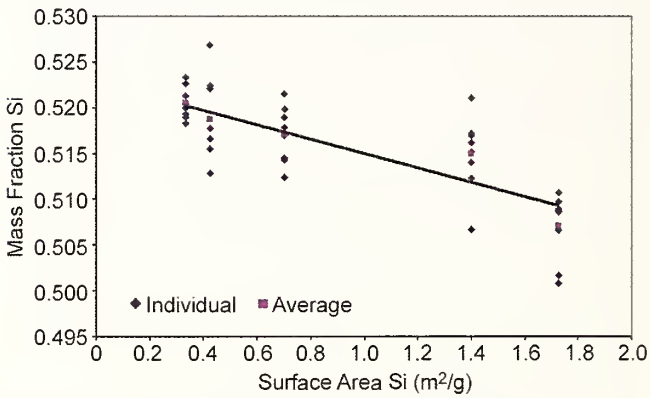

Figure 1: *Analysis of TOF data, yielding amorphous content of SRM 676.*

Time-of-Flight (TOF), neutron data, and high-energy, 67 keV, synchrotron data were collected. The results from the later data were not dependent on the use of the extinction model, which was considered a weak link in the analysis. These two methods yielded results that were within 7% of one another: 4.4% vs. 4.1%. Additional synchrotron data are being collected at lower energies. These experiments are the first that are capable of measuring low levels of amorphous content in an absolute manner. The convergence of the various methods renders the results credible.

Contributors and Collaborators

R.S. Winburn (Minot State University); R.B. Von Dreele (LANSCE); A. Huq, P.W. Stephens (State University of New York/Stony Brook)

Powder Measurements

Powder-based applications require measurement infrastructure and technical guidance for development of reliable, cost-effective materials and manufacturing processes. We provide standard reference materials (SRMs), standard methods, data and basic research relating to the physical and interfacial property measurements of fine particulates and dispersions. We focus on submicrometer and nanosize dimensions for applications in the microelectronics and advanced ceramics industries.

Vincent Hackley and Ajit Jillavenkatesa

Fine powders, comprised of particles having submicrometer dimensions, are used in a broad spectrum of commercial applications. They are used as building blocks for advanced structural materials, as drug carriers, catalysts, pigments, memory and photographic elements, abrasives, and in phosphor and thermal coatings. They are a critical component (or nuisance) in many environmental and industrial systems, from atmospheric soot to magneto-rheological fluids. We develop solutions for generic problems shared by a broad customer base, including industry, academia, standards development organizations, and research programs at NIST. Our objectives are to explore new techniques, to develop new methodologies, to provide critical data, and to produce industry standards for physical and interfacial property measurements of fine powders in the dispersed and consolidated state.

The first joint CRM-SRM, developed in collaboration with BAM in Germany, was completed. This first of its kind, co-produced, co-labeled meso-pore reference material will be used for the validation of Hg-intrusion instruments.

A highly successful 3 year international pre-standardization study with researchers in Japan and Germany was completed. The study laid the groundwork for drafting ISO standards for electrokinetic measurements and quantification of coarse particle content. Several papers and presentations, and three draft standards, resulted entirely or in part from this collaboration. This part of the project will continue under the auspices of the Versailles Project for Advanced Materials & Standards (VAMAS).

A NIST Recommended Practice Guide was published on *The Use of Nomenclature in Dispersion Science & Technology*. SP 960-3, the third volume in this series, was prepared as a desk-reference for researchers, process engineers, technicians and students. It addresses areas such as agglomeration, colloidal stability, interfacial & electrokinetic properties, and rheology.

Broad industry acceptance is seen from the large number of requests and positive feedback. Copies are available upon request. Inquire at: *dispersion@nist.gov*.

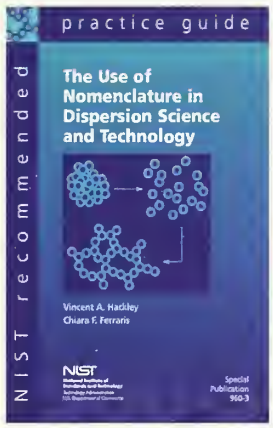

Certification of SRM 1003c using laser light scattering, electrozone sensing, and scanning electron microscopy has been completed. This material is certified for particle size distribution over the range of 20 μm to 50 μm. The development of a new smaller particle size distribution glass bead standard, SRM 1021, has been completed. This 1 μm to 20 μm material is also being certified using laser light scattering and electrozone sensing.

Qualification studies were conducted on a series of, TiO_2, ZrO2, Al_2O_3, and SiO_2 powders for development as an SRM in the 100 nm–500 nm size range. These studies involved measurements of preliminary size distribution, density and surface area. Based on these characteristics, particle shape distribution and x-ray absorption cross-section, the TiO_2 powder was chosen as the candidate material. A protocol for reproducible dispersion of the TiO_2 powders of interest was developed. Powder dispersion characteristics were studied by varying the dispersion mechanism and using additives.

Particle size distribution characterization of the TiO_2 powder system was conducted by x-ray disc centrifuge analyses, laser light scattering and SEM. Different techniques to enable suitable specimen preparation for electron microscopy analysis were examined in detail. Particle size analyses by laser light scattering focused on the influence of instrumental parameters, primarily the role of the optical constants (real and imaginary component of refractive indices). Based on the research conducted during this FY, a TiO_2 powder SRM with a size distribution spanning the 100 nm to 500 nm range is now ready for production.

Contributors and Collaborators

J. Kelly, L. Lum, D. Minor (Ceramics); C. Ferraris, D. Bentz, G. Mulholland (BFRL, NIST); M. Naito, H. Abe (JFCC, Japan); R. Wäsche, P. Klobes, (BAM, Germany); U. Paik, Y. Kim (Hanyang University, Korea); C. Kreller (Maryland-Baltimore Co.); C. Saltiel (Synergetic Technologies); D. Zampini (Degussa Construction Chemicals); V. Gupta, (W.R. Grace)

Materials for Micro- and Optoelectronics

U.S. microelectronics and related industries are in fierce international competition to design and produce smaller, lighter, faster, more functional, and more reliable electronics products more quickly and economically than ever before. At the same time, there has been a revolution in recent years in new materials used in all aspects of microelectronics fabrication.

Since 1994, the NIST Materials Science and Engineering Laboratory (MSEL) has worked closely with the U.S. semiconductor, component, packaging, and assembly industries. These efforts led to the development of an interdivisional MSEL program committed to addressing industry's most pressing materials measurement and standards issues central to the development and utilization of advanced materials and material processes. The vision that accompanies this program — to be a key resource within the Federal Government for materials metrology development for commercial microelectronics manufacturing — is targeted through the following objectives:

- Develop and deliver standard measurements and data;
- Develop and apply *in situ* measurements on materials and material assemblies having micrometer- and submicrometer-scale dimensions;
- Quantify and document the divergence of material properties from their bulk values as dimensions are reduced and interfaces contribute strongly to properties;
- Develop models of small, complex structures to substitute for, or provide guidance for, experimental measurement techniques; and
- Develop fundamental understanding of materials needed in future micro- and opto-electronics and magnetic data storage.

With these objectives in mind, the program presently consists of projects led by the Metallurgy, Polymers, Materials Reliability, and Ceramics Divisions that examine and inform industry on key materials-related issues. These projects are conducted in concert with partners from industrial consortia, individual companies, academia, and other government agencies. The program is strongly coupled with other microelectronics programs within government and industry, including the National Semiconductor Metrology Program (NSMP) at NIST. Materials metrology needs are also identified through industry groups and roadmaps including the International Technology Roadmap for Semiconductors (ITRS), International SEMATECH, the IPC-Embedded Passive Devices Taskgroup, the IPC Lead-free Solder Roadmap, the National Electronics Manufacturing Initiative (NEMI) Roadmap, the Optoelectronics Industry Development Association (OIDA) roadmaps, and the National [Magnetic Data] Storage Industry Consortium (NSIC).

Although there is increasing integration within various branches of microelectronics and optoelectronics, the field can be considered to consist of three main areas. The first, microelectronics, includes needs ranging from integrated circuit fabrication to component packaging to final assembly. MSEL programs address materials metrology needs in each of these areas, including, for example, lithographic polymers and electrodeposition of interconnects, electrical, mechanical, and physical property measurement of dielectrics (interlevel, packaging, and wireless applications), and packaging and assembly processes (lead-free solders, solder interconnect design, thermal stress analysis, and co-fired ceramics).

The second major area is optoelectronics, which includes work that often crosses over into electronic and wireless applications. Projects currently address residual stress measurement in optoelectronic films, and wide bandgap semiconductors. Cross-laboratory collaborations with EEEL figure prominently in this work.

The third area is magnetic data storage, where the market potential is already large and growing and the technical challenges extreme. NSIC plans to demonstrate a recording density of 40 times today's level by 2006. To reach these goals, new materials are needed that have smaller grain structures, can be produced as thin films, and can be deposited uniformly and economically. New lubricants are needed to prevent wear as the spacing between the disk and head becomes smaller than the mean free path of air molecules. MSEL is working with the magnetic recording industry to develop measurement tools, modeling software, and magnetic standards to help achieve these goals. MSEL works in close collaboration with the Electronics and Electrical Engineering Laboratory, the Physics Laboratory, the Information Technology Laboratory, and the Manufacturing Engineering Laboratory as partners in this effort.

Contact: Debra Kaiser

Optical and Structural Characterization of Optoelectronic Semiconductors

Photonics manufacturers need to better understand how composition, strain, inhomogeneity and defects affect the performance of optical emitters and detectors made from III-V compound semiconductors. In the Optical and Structural Characterization of Optoelectronic Semiconductors Project, we are measuring critical properties of thin film structures relevant to device performance by a variety of spectroscopic techniques. The project is currently focused on deep UV to near IR (250 nm to 850 nm) emitting materials: $Al_xGa_{1-x}As$, $Al_xGa_{1-x}N$ and $In_yGa_{1-y}N$.

Lawrence Robins and Grady White

Medium to wide bandgap III-V semiconductors enable display, lighting, and data storage technologies, based on their optical emission and their ability to detect at deep UV to near IR wavelengths. Progress in the development of GaN, $Al_xGa_{1-x}N$ and $In_yGa_{1-y}N$ devices (250 nm to 550 nm) has been hampered by problems with materials growth and structure, such as film/substrate lattice mismatch, high defect and impurity concentrations, and structural/compositional inhomogeneity. $Al_xGa_{1-x}As$ (650 nm to 850 nm) is a better developed technology, but the industry still needs improved accuracy in measurements of alloy composition and residual strain. We have, therefore, undertaken several initiatives to address these needs for improved metrology methods and accurate measurements.

1) A calibration curve was determined for the dependence of the photoluminescence (PL) emission energy on Al fraction (x) in $Al_xGa_{1-x}As$ films for $x < 0.37$, near room temperature, based on reflection high energy electron diffraction (RHEED) and wavelength dispersive spectroscopy (WDS) measurements of x.

2) Correlated Raman and PL measurements were performed on $Al_xGa_{1-x}As$ films as a function of applied biaxial stress to 350 MPa. Two primary Raman peaks, described as AlAs-like and GaAs-like, were observed in films with $x = 0.2$ and $x = 0.5$. The differing stress and composition dependencies of the Raman and PL peaks allow us to determine both the Al fraction and the magnitude of the stress. Measurements suggest that the stress coefficient of each Raman peak is approximately constant as a function of x, with the AlAs-like peak showing a larger stress coefficient than the GaAs-like peak.

3) The ordinary refractive index, $n_o(E)$, and absorption coefficient, $\alpha(E)$, were measured in the 200 nm to 2500 nm range for several $Al_xGa_{1-x}As$ films by spectroscopic transmittance, $T(E)$, and reflectance, $R(E)$, correlated with discrete-wavelength prism-coupled waveguide-mode measurements of n_o. EDS measurements of x enabled determination of the x dependence of $n_o(E)$ and $\alpha(E)$. Transmittance, $T(E)$, and reflectance, $R(E)$, spectra of a representative sample are plotted in Figure 1.

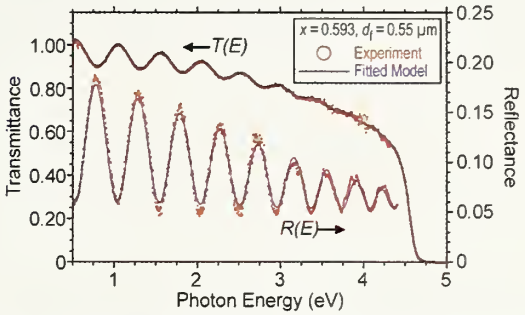

Figure 1: *Transmittance and reflectance measurements (red) and model (blue) for a $Al_xGa_{1-x}N$ sample.*

The index–film thickness product $n_o(E)d_f$ was determined from the spacing of the interference fringes in $T(E)$ and $R(E)$; similarly, $\alpha(E)d_f$ was determined at energies near the bandgap from the absorption cutoff of $T(E)$. To determine the individual factors n_o, α, and d_f, a two-Sellmeier-term model for $n_o(E)$ was adjusted to best match the n_o values from the discrete wavelength waveguide mode measurements, while simultaneously fitting the $T(E)$ and $R(E)$ data. The $n_o(E)$ and $\alpha(E)$ curves obtained from this multiple optimization procedure are shown in Figure 2.

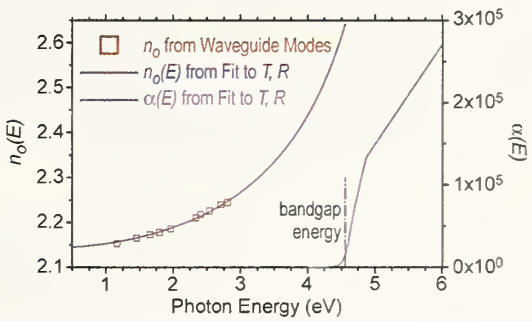

Figure 2: *Ordinary refractive index and absorption coefficient obtained in the optimization procedure.*

Contributors and Collaborators

C.E. Bouldin, A.J. Paul, M.D. Vaudin (Ceramics); J.T. Armstrong, R.B. Marinenko (Surface and Microanalysis); K.A. Bertness, N.A. Sanford (Optoelectronics); A.V. Davydov, A.J. Shapiro (Metallurgy); J.G. Pellegrino (Physical and Chemical Properties); A.V. Dmitriev, D.V. Tsvetkov (TDI); S. Keller, U.K. Mishra, S.P. DenBaars (UCSB)

Nanotribology

The head-disk interface has become an important scientific and technological issue in the data storage industry. To reach 155 Gb/cm^2 areal density and fast data transfer, the spacing between the head and the disk is shrinking to 3.5 nm for speeds approaching 40 m/s. Occasional contacts will test the strength and robustness of the protective carbon and lubricant coatings, each of which is only one nanometer thick. Measuring and evaluating material properties and their response to impact under these conditions has become a significant technological need.

Stephen Hsu, Richard Gates, Patrick Pei, Pu-Sen Wang, Jerry Chuang, and Dan Fischer

Ceramics Division researchers continue to work with the National Storage Industry Consortium (NSIC) as members of the Tribology Working Group. We have achieved significant progress in four project areas: 1) the development of a high-speed impact test to simulate head-disk collisions under ramp-load and unload operating conditions; 2) the creation of a finite element model for calculating stress concentrations and deformation as a result of such impacts; 3) the development of a master calibration sample for film thickness measurements of complex hydrocarbon molecules on hard disks in the one nanometer ± 0.2 nm range; 4) the development of an electron spin resonance technique to measure the unpaired electrons in carbon overcoats with MMC Corporation.

These projects, taken together, represent our efforts in addressing two crucial technological issues facing the magnetic hard disk industry: how should the disk be protected from occasional high-speed head-disk contacts when the head is flying faster and lower; how should we define surface reactivity and bonding in new carbon overcoats while ensuring durability.

NSIC has set the ambitious goal of reaching 155 Gb/cm^2 areal density by 2006 with a concurrent increase in data transfer rate approaching 100 Gbit/s. This translates to a 10-fold increase in capacity in four years.

To increase the areal density, the flight height and the carbon overcoat thickness must be reduced to 3.5 nm and 1 nm respectively. Since the protection of the disk depends on the combination of the lubricant and the carbon overcoat, thinner overcoats may reduce the durability. NSIC is working on improved overcoats and lubricants.

Head disk interface operation has shifted from constant-start-and-stop mode to a ramp-load-and-unload mode. The head is parked on the ramp outside the disk. For read and write operations, the head flies in and retrieves/writes data and then retreats to the ramp to park. This design minimizes head disk contacts. However, because of the reduced flight height, waviness of the disk, or rotational wobble, occasional contacts between the head and disk do occur and sometimes catastrophically. This kind of random contact takes place under high speed flying conditions and is difficult to measure.

A ridge is artificially created on a disk and a ruby ball is used to collide with the ridge under high speed conditions (see technical highlight). The impact force and the deformation are measured. Preliminary test results show the ranking of lubricants and overcoats agree with field experience. This quick test enables screening of different coating/lubricant combinations for their effectiveness in protecting the disk. A finite element model has also been successfully developed to predict the stress concentrations and deformation for a hard disk. The interaction of various mechanical properties of different layers can be simulated.

Another aspect of improved protection is the lubricant. The spacing allows only a monolayer of molecules to protect the surface. Hydrocarbon molecules hold promise to improve the bonding strength and self-repairing properties of the lubricant film. Current lubricant (perfluoropolyether) has limited solubility of functional molecules. We have demonstrated that a multi-component molecular assembly can be achieved by using hydrocarbon molecules. However the performance depends on film thickness. There is no known acceptable method to accurately measure the film thickness of a complex hydrocarbon film on an atomically rough surface at 1 nm scale. A master calibration sample was successfully developed using a circular barrier to contain a solution with a known amount of solute on an actual hard disk. The solution is frozen in liquid nitrogen and slowly evaporated under controlled conditions. Uniformity of the film is checked by FTIR. Samples of average film thickness were then measured by various methods and the correlation constants were obtained. This enables the use of hydrocarbon molecules for hard disk applications.

The bonding characteristics of lubricant molecules with overcoats are important in shear resistance. An electron spin resonance technique was developed to measure unpaired electrons of overcoats quantitatively. Working with MMC Corporation, a series of hard disk carbon overcoats on a glass substrate was measured. This technique is expected to provide a tool to control surface reactivity/energy.

Contributors and Collaborators

M. Bai; MMC Corp, UC Davis, NSIC (IBM, Seagate, Readrite, Maxtor), Pennzoil-Quaker State

Phase Equilibria and Properties of Dielectric Ceramics

Ceramic compounds with exploitable dielectric properties are widely used in technical applications such as actuators, transducers, and resonators or filters for wireless communications. The commercial competitiveness of next-generation devices depends on new ceramics with improved properties and/or reduced processing costs. Experimental phase equilibria determination, integrated with systematic chemistry-structure-property studies (experimental, theoretical, and modeling) contribute toward the fundamental understanding and rational design of these technologically important materials.

Terrell A. Vanderah, Benjamin P. Burton, Eric J. Cockayne, and Igor Levin

Ternary oxides in the Bi_2O_3-ZnO-Nb_2O_5 system exhibit high-dielectric constants (ε), relatively low dielectric losses, and compositionally tunable temperature coefficients of capacitance (τ_c). Such properties combined with sintering temperatures of less than 950°C render these materials attractive candidates for capacitor and high-frequency filter applications in multilayer structures co-fired with silver electrodes. The system features two structurally distinct ternary compounds, $Bi_{1.5}Zn_{0.92}Nb_{1.5}O_{6.92}$ (ε = 145, τ_c = –400 MK^{-1}) and $Bi_2Zn_{2/3}Nb_{4/3}O_7$ (ε = 80, τ_c = +200 MK^{-1}), which exhibit very dissimilar dielectric properties and form temperature-stable, commercially important mixtures. However, the absence of structural information for both phases has precluded understanding of the unusual dielectric properties; in particular, $Bi_{1.5}Zn_{0.92}Nb_{1.5}O_{6.92}$ ceramics exhibit dielectric relaxation, attributed to a dipolar glass-like mechanism, while no such behavior is observed for $Bi_2Zn_{2/3}Nb_{4/3}O_7$. Recent studies combined electron, x-ray, and neutron powder diffraction techniques to elucidate the crystal structures of these compounds which feature pyrochlore and zirconolite-like structures, respectively. The results reveal that displacive disorder in $Bi_{1.5}Zn_{0.92}Nb_{1.5}O_{6.92}$ is responsible for the high dielectric constant and the relaxation phenomenon.

Subsolidus phase relations have been determined for the BaO:TiO_2:Ta_2O_5 system and the BaO:Ta_2O_5 subsystem, which are pertinent to the processing of Ta_2O_5-based ceramics for cellular base station resonators and filters. $BaTiO_3$ dissolves a considerable amount of Ta^{5+} by forming Ti^{4+} vacancies. The formation of $Ba_3Ti_4Ta_4O_{21}$, a member of the hexagonal $A_3M_8O_{21}$–type ternary oxides, was confirmed as well as its solid solution. Several new compounds have been found, including four members of the orthorhombic "rutile-slab" homologous series, $BaTi_nTa_4O_{11+2n}$, with n-values 3,5,7,9. Three ternary phases with close-packed [Ba,O] layer structures related to that of *6L* $Ba_4Ti_{13}O_{30}$ were found: *13L* $Ba_{18}Ti_{53}Ta_2O_{129}$, *7L* $Ba_{10}Ti_{27}Ta_2O_{69}$, and *8L* $Ba_6Ti_{14}Ta_2O_{39}$. The crystal structures of the *13L* and *7L* phases were determined by single-crystal x-ray diffraction. Phases with tetragonal tungsten bronze related structures occur over large compositional ranges, both within the ternary and along the BaO-Ta_2O_5 binary.

$PbZr_{1-x}Ti_xO_3$ (PZT) is an important piezoelectric material that has applications in transducers. A first-principles-based effective Hamiltonian was developed for Zr-rich PZT. This model is the first that reproduces the correct sequence of phase transitions in this system: orthorhombic to rhombohedral to cubic, as the temperature increases.

Other important transducer materials include relaxor ferroelectrics. An effective Hamiltonian was developed for the relaxor ferroelectric $PbSc_{1/2}Nb_{1/2}O_3$ (PSN), based on first-principles calculations. This model allows one to simulate the structure and dielectric properties of PSN as a function of cation ordering, temperature, and applied fields, in systems representing as many as 300,000 atoms. Molecular dynamics methods allow the polarization dynamics and frequency dependence of the dielectric permittivity to be studied. The local electric field at the Pb sites due to the charged Sc and Nb ions has been calculated (see Figure 1) and incorporated into the model. The results establish a clear link between chemical disorder and dielectric response, and they indicate "nanoscale texture," i.e., the size and geometrical arrangement of domains play a fundamental role in the observed macroscopic properties.

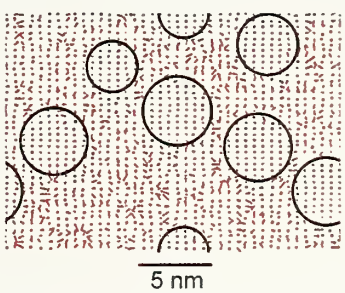

Figure 1: *Local electric fields in a model for the relaxor ferroelectric PSN. Experiments suggest that relaxor ferroelectrics contain chemically-ordered regions in a disordered matrix and that such inhomogeneities may be responsible for the relaxor behavior. Computations show that chemically-ordered regions in PSN (circles) have much lower local fields than the disordered matrix.*

Contributors and Collaborators

R.S. Roth, W. Wong-Ng, J.E. Maslar (CSTL); R. Geyer (EEEL); S. Bell (TRAK Ceramics, Inc.); C.A. Randall (Penn State); J.C. Nino (Penn State); K. Leung (Sandia); L. Bellaiche (University of Arkansas); U. Waghmare (JNCASR, Bangalore, India); S. Prosandeev (Rostov State University, Russia); V. Zelezny and J. Petzelt (Czech Academy of Sciences)

Phase Diagrams in High Temperature Superconductors

Phase diagrams serve as "road maps" for processing high T_c superconductors. Of current interest are the $Ba_2RCu_3O_{6+x}$ (R = Sm, Gd and Er) superconductors. The critical single-phase regions of $Ba_{2+x}(Nd_{1+x-y}R_y)Cu_3O_{6+z}$ for R = Gd, Y and Yb were determined such that both flux-pinning and melting can be tailored and optimized. The construction of subsolidus phase diagrams of these systems, and the role of phase equilibria and kinetics in the formation of the $Ba_2YCu_3O_{6+x}$ phase, are deemed important for the rapid advancement of second generation coated conductor technology.

Winnie Wong-Ng and Lawrence Cook

NIST phase equilibrium research has continued to provide critical information pertinent to the development of practical superconductors. DOE has supported high T_c research through a program of intensive R&D focused on wire and cable for high-impact commercial applications. This effort includes three principal groups of superconductors: (1) 1st generation Bi-Pb-Sr-Ca-Cu-O (BSCCO)-based wire/tape produced by the Ag-powder-in-tube (PIT) technique; (2) 2nd generation $Ba_2RCu_3O_7$-type (Y-213 and R-213, R = lanthanide) coated-conductors produced by rolling-assisted biaxially-textured substrate/ion beam assisted deposition (RABiTS/IBAD); (3) the recently discovered MgB_2 material.

By mixing the smaller lanthanides (Gd, Y, Yb) with the larger Nd in the $Ba_{2-x}(Nd_{1+x-y}R_y)Cu_3O_{6+z}$ (Nd-213) superconductor, both the flux-pinning and the melting properties can be tailored and optimized. A size trend in the single phase solid solution prepared in air was observed. Due to the closer match in size of $Nd^{3+}$with Gd^{3+} than Nd^{3+} with Y^{3+}, and Nd^{3+} with Yb^{3+}, the solid solution region is largest for the Gd-substituted system and smallest for the Yb-substituted system. We have successfully characterized selected solid solution members by x-ray, neutron, and electron diffraction, and by differential thermal analysis (DTA). There is considerable improvement of $J_c(H)$ for samples with partial Y-substitution at higher field at 77 K, compared with that of $Ba_2NdCu_3O_{6+z}$ and $Ba_2YCu_3O_{6+z}$. This improvement is likely due to the increased flux pinning as a result of doping of Nd^{3+} in the Ba^{2+} site.

The "BaF_2 *ex situ*" process and the liquid-phase-epitaxy process are promising methods for producing long-length high quality Y-213 superconductor. Therefore investigation of the phase relationships in the system BaF_2-BaO-Y_2O_3-CuO_x-H_2O is another area of concentration. Using specially constructed controlled-atmosphere instrumentation and a strategic approach, we succeeded in determining the presence of low temperature liquids in this air-sensitive multicomponent reciprocal Ba-Y-Cu//O,F system, which can be modeled in compositional space as a trigonal prism. This prism can be viewed as consisting of three tetrahedra (BaO-Y_2O_3-CuO_x-BaF_2, BaF_2-YF_3-CuF_2-CuO_x, and BaF_2-Y_2O_3-CuO_x-YF_3). We have also initiated a more detailed study of melt equilibria in the BaF_2-BaO-Y_2O_3-CuO_x system. The role of $Ba(OH)_2$ in this system, as related to low-temperature melting, was identified as warranting further investigation. All this information is important for both the "BaF_2" process and liquid phase epitaxy process.

To control film properties, it is important to understand the details of Y-213 phase evolution from amorphous "BaF_2" films. To collect data at a faster rate over a broader range, we have used a position-sensitive detector on the high-temperature x-ray diffractometer. Three sets of films with different thickness (provided by R. Feenstra of the Oak Ridge National Laboratory) have been studied. We found that the growth of the Y-213 phase is controlled by the reaction at the interface of the Y-213/precursor, not by diffusion. Sufficient water vapor pressure is critical for Y-213 formation. The detailed phase evolution sequence, kinetics of phase formation, and the texture of these films as a function of processing parameters, will continue to be pursued.

A smaller effort was spent on the study of the melting equlibria of the Pb-doped and Pb-free Bi-2223 superconductors. In collaboration with FSU, the Pb-free 2223 phase was found to be in equilibrium with eight phases in the Bi-Sr-Ca-Cu-O system. Investigation continues to obtain a complete set of subsolidus 4-phase volumes, which is necessary for the determination of the primary phase field. We have measured the enthalpy of formation of MgB_2, at 298 K by solution calorimetry. The vapor pressure of MgB_2 up to 1100°C was also successfully measured using a thermogravimetric effusion method.

As data accumulate, we anticipate increased use of thermodynamic methods for data smoothing and extrapolation, with the ultimate goal of producing a comprehensive phase equilibria model for each of the three major high T_c systems. By providing the phase equlibria data as the basis for optimal processing, high T_c technology will be advanced through reductions in cost and improvements in performance.

Contributors and Collaborators

I. Levin, M. Vaudin, J.P. Cline (Ceramics); Q. Huang, B. Toby (Reactor); L. Swartzendruber (Metallurgy); A. Kearsley (Mathematical and Computational Sciences); R. Klein (Chemistry); T. Holesinger (LANL); R. Feenstra (ORNL); M. Rupich (AMSC); J. Storer (3M); J. Kaduk (BP-Amoco); R. Meng (University Houston); M. Suenaga (BNL); and PVPSS Sastry (FSU).

Combinatorial Methods

The Combinatorial Methods Program develops novel high-throughput measurement techniques and combinatorial experimental strategies specifically geared towards materials research. These tools enable the industrial and research communities to rapidly acquire and analyze physical and chemical data, thereby accelerating the pace of materials discovery and knowledge generation. By providing measurement infrastructure, standards, and protocols, and expanding existing capabilities relevant to combinatorial approaches, the Combinatorial Methods Program lowers barriers to the widespread industrial implementation of this new R&D paradigm.

The Combinatorial Methods Program has adopted a two-pronged strategy for meeting these goals. The first of these is an active research and development program designed to better tailor combinatorial methods for the materials sciences and extend the state of the art in combinatorial techniques. Measurement tools and techniques are developed to prepare and characterize combinatorial materials libraries, often by utilizing miniaturization, parallel experimentation, and a high degree of automation. A key concern in this effort is the validation of these new approaches with respect to traditional "one at a time" experimental strategies. Accordingly, demonstrations of the applicability of combinatorial methods to materials research problems provide the scientific credibility needed to engender wider acceptance of these techniques in the industrial and academic sectors. In addition, the successful adoption of the combinatorial approach involves a highly developed "workflow" scheme. All aspects of combinatorial research, from sample "library" design and library preparation to high-throughput assay and analysis, must be integrated through an informatics framework which enables iterative refinement of measurements and experimental aims. Combinatorial Methods Program research projects give illustrations of how these processes are implemented effectively in a research setting.

NIST-wide research collaborations, facilitated by the Combinatorial Methods Program, have produced a wide range of new proficiencies in combinatorial techniques which are detailed in a brochure, "Combinatorial Methods at NIST" (*NISTIR 6730*), and online at *www.nist.gov/combi*. Within MSEL, novel methods for combinatorial library preparation are designed to encompass variations of diverse physical and chemical properties, such as composition, film thickness, processing temperature, surface energy, chemical functionality, UV-exposure, and topographic patterning of organic and inorganic materials ranging from polymers to nanocomposites to ceramics. In addition, new instrumentation and techniques enable the high-throughput measurements of adhesion, mechanical properties, and failure mechanisms, among others. The combinatorial effort extends to multiphase, electronic, and magnetic materials, including biomaterials assays. On-line data analysis tools, process control methodology, and data archival methods are also being developed as part of the Program's informatics effort.

The second aspect of the Combinatorial Methods Program is an outreach effort designed to facilitate technology transfer with institutions interested in acquiring combinatorial capabilities. The centerpiece of this effort is the NIST Combinatorial Methods Center (NCMC), an industry-university-government consortium organized by MSEL that became operational on January 23, 2002 via a kick-off meeting in San Diego. Although it is still in the growth stage, the impact of NCMC activities is readily apparent as 11 industrial partners and the Air Force Research Lab have already joined the NCMC membership program. The NCMC facilitates direct interaction between NIST staff and these industrial partners, and provides a conduit by which Combinatorial Methods Program research products, best practices and protocols, instrument schematics and specifications, and other combinatorial-related information can be effectively disseminated. This outreach is mediated in large part by a series of tri-annual workshops for NCMC members. The first NCMC meeting, "Library Design and Calibration," was held on April 26, 2002 at NIST, and it provided information essential to starting a combinatorial research effort. The second meeting (October 2002) will concentrate on combinatorial approaches to adhesion and mechanical properties. Further information on NCMC can be found on the website at *www.nist.gov/combi*.

Contact: Peter Schenck

Combinatorial Tools for Oxide Thin Films

Combinatorial methods are increasingly used by industry for the discovery and optimization of inorganic materials for use in nanoscale films in electronic, optical and magnetic applications. We have developed novel approaches for thin film library fabrication and high throughput characterization of thickness and optical properties applicable to ceramic, metal and ceramic/metal composites. These techniques have been demonstrated for model $BaTiO_3$-$SrTiO_3$ film libraries for next generation wireless, memory and logic devices, and Au-NiO libraries for use as transparent electrodes in optoelectronic devices.

Peter K. Schenck and Debra L. Kaiser

We have developed two combinatorial tools that can be applied to a broad range of inorganic materials: a pulsed laser deposition (PLD) system for thin film library fabrication, and a rapid throughput, spatially-resolved spectroscopic reflectometry technique for mapping film thickness and refractive index. To date, $BaTiO_3$-$SrTiO_3$, Au-Ni, and Au-NiO film libraries have been deposited and characterized using these tools.

PLD is a versatile rapid-prototyping tool for thin films. Congruent vaporization leads to stoichiometric material transfer, permitting complex target compositions. It is also a high-energy process that allows lower substrate temperatures and higher deposition rates. In this research, a conventional single-target PLD system was retrofitted to a dual-beam, dual-target configuration designed for the fabrication of graded composition films. A positionable horizontal mask is installed to allow variation of an additional process parameter such as temperature or gas pressure during deposition. Substrate temperatures up to 800°C can be achieved. *In situ* diagnostics including high-speed imaging and a dual deposition rate monitor are used to fine-tune the process in real time. A 500 nm thick film library spanning the full composition range between the two target compositions is deposited in less than one hour.

Thickness and optical property assays are performed on the film libraries using a semi-automated spectroscopic reflectometry apparatus designed and fabricated in our laboratory. This instrument is equipped with a bifurcated fiber optic probe to illuminate the sample and to obtain the reflected light, and a miniature fiber-optic-coupled spectrometer to collect the entire spectrum simultaneously at each measurement position. The reflectivity of the film-substrate system relative to the bare substrate is calculated and fitted to a model from which thickness, refractive index and absorption coefficient can be derived. A procedure, based on this apparatus, was developed to predict the composition map in a film using the measured thickness map or deposition pattern from films deposited from the individual targets. Correlation of the pattern obtained by summation of the two individual target patterns with the pattern from a film deposited using both targets under otherwise identical conditions was excellent. Assuming negligible diffusion of the deposited species, it was then possible to predict the composition map from the individual target deposition patterns.

To study thinner films, and films on transparent substrates, the spectroscopic reflectometer was modified to extend the wavelength coverage to 200 nm and to allow for transmission measurements. A deuterium lamp and UV spectrometer were added to the apparatus. A test of the shorter wavelength and transmission mode capability is demonstrated in Figure 1. There is excellent agreement in the data in the region of spectral overlap. Kinematic sampling heads allow rapid change between reflection and transmission modes. A dual bifurcated probe has been added to allow two sources to illuminate the film and both spectrometers to analyze the reflected light.

Determination of the optical properties of the deposited film is limited by the accuracy to which the properties of the bare substrate are known. Since the latter are very dependent on the treatment of the substrate, a spectroscopic ellipsometer is being added to characterize the substrates prior to film deposition.

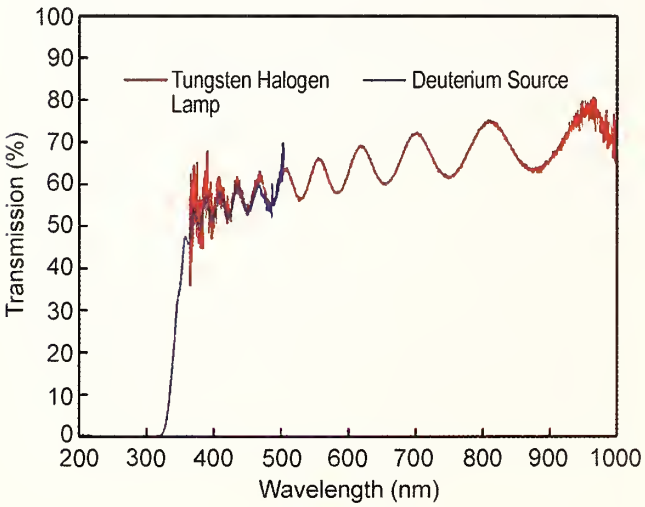

Figure 1: *Test of the UV-Visible Transmission Spectrometer on a single-composition $BaTiO_3$-$SrTiO_3$ film.*

Contributors and Collaborators

M. Vaudin, J. Kim, J. Blendell (Ceramics Division); E. Stokes (General Electric)

Materials Property Measurements

This program responds both to MSEL customer requests and to the DOC 2005 Strategic Goal of "providing the information and framework to enable the economy to operate efficiently and equitably." For example, manufacturers and their suppliers need to agree on how material properties should be measured. Equally important, engineering design depends on accurate property data for the materials that are used.

The MSEL Materials Property Measurement Program works toward solutions to measurement problems, on scales ranging from the macro to the nano, in four of the Laboratory's Divisions (Ceramics, Materials Reliability, Metallurgy, and Polymers). The scope of its activities goes from the development and innovative use of state-of-the-art measurement systems, to leadership in the development of standardized test procedures and traceability protocols, to the development and certification of Standard Reference Materials (SRMs). A wide range of materials is being studied, including polymers, ceramics, metals, and thin films (whose physical and mechanical properties differ widely from the handbook values for their bulk properties).

Projects are directed to innovative new measurement techniques. These include:

- Measurement of the elastic, electric, magnetic, and thermal properties of thin films and nanostructures (Materials Reliability Division);
- Alternative strength test methods for ceramics, including cylindrical flexure strength and diametral compression (Ceramics Division); and
- Coupling micromechanical test methods with failure behavior of full-scale polymer composites through the use of microstructure-based object-oriented finite element analysis (Polymer Division in collaboration with the Automotive Composites Consortium).

The MSEL Materials Property Measurement Program is also contributing to the development of test method standards through committee leadership roles in standards development organizations such as ASTM and ISO. In many cases, industry also depends on measurements that can be traced to NIST Standard Reference Materials (SRMs). This program generates the following SRMs for several quite different types of measurements.

- Charpy impact machine verification (Materials Reliability Division);
- Hardness standardization of metallic materials (Metallurgy Division);
- Hardness standardization and fracture toughness of ceramic materials (Ceramics Division); and
- Supporting the Materials Property Measurements Program is a modeling and simulation effort to connect microstructure with properties. The Object-Oriented Finite-Element (OOF) software developed at NIST is being used widely in diverse communities for material microstructural design and property analysis at the microstructural level.

In addition to the activities above, the Materials Reliability, Metallurgy, Ceramics, and Polymers Divisions provide assistance to various government agencies on homeland security and infrastructural issues. Projects include assessing the performance of structural steels as part of the NIST World Trade Center Investigation, advising the Bureau of Reclamation (BOR) on metallurgical issues involving a refurbishment of Folsom Dam, advising the Department of the Interior on the structural integrity of the U.S.S. Arizona Memorial, advising the U.S. Customs Service on materials specifications for ceramics, and advising the Architect of the Capitol on repair procedures for cracks in the outer skin of the Capitol Dome.

Contact: Douglas Smith

Failure Modes in Biomechanical Layer Structures

Biomechanical prostheses such as dental crowns, total hip replacements, heart valves and spinal disk replacements are becoming more commonplace in an ever-aging population. The lifetimes of such prostheses are limited by materials properties. Accordingly, it is imperative that we understand the modes of failure in these systems. This program, with extramural partners (New York University, University of Maryland) and international guest scientists, seeks to determine fundamental ground rules for designing biomechanical systems for improved lifetime performance by identifying and analyzing clinically relevant damage modes.

Brian Lawn

Cracking and other damage modes in ceramic layers on soft substrates are of broad general interest because of the potential for lifetime-limiting premature failures. This is especially true of biomechanical prostheses—dental crowns, hip replacements, heart valves, spinal disk replacements—where ceramic components are introduced to enhance wear resistance, strength, and chemical durability, and in the case of crowns, aesthetics are exposed to cyclic concentrated loads under stringent *in vivo* environmental conditions. A proper understanding of the materials aspects of any such ceramic-based prosthetic device becomes a quality-of-life issue. In many such applications, the ceramic is just one component in combination with polymer and/or metal support sublayers, so a systems approach is essential.

In this program we characterize contact-induced damage modes in model layer systems—bilayers, trilayers (and even multilayers)— that simulate the basic loading features of biomechanical structures, and, at the same time, allow direct *in situ* observations of the damage evolution during loading and unloading. The most revealing are layer structures made from transparent components, *e.g.* ceramic coating layers on clear polymer substrates or glass coatings on metal substrates. Critical conditions for damage initiation can then be directly monitored and quantified.

Using this approach, we have been able to identify damage modes believed to be responsible for the failure of clinical prostheses, especially dental crowns. Analytical relations expressing the critical applied loads (*e.g.* biting force, body weight on hip replacements) in terms of ceramic layer thicknesses and material properties (strength, toughness, modulus, hardness) have been determined. These relations can be used to determine optimal interlayer dimensions and material properties for any given layer system. Design criteria for this optimization are being laid down.

This work has been funded by the National Institute of Dental and Craniofacial Research. Materials scientists, engineers and clinicians are involved. The first five-year stage of this program has been completed. A second five-year stage is now beginning. Several dental materials companies participate in this program.

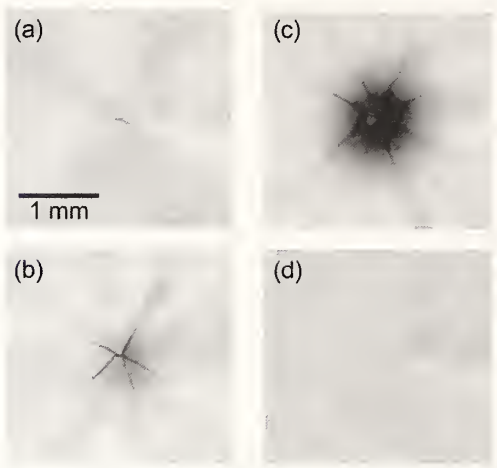

Figure 1: In situ *observations of crack evolution during loading (a–c) and unloading (d) of alumina ceramic plate on transparent polymer substrate (undersurface, viewed from below contact).*

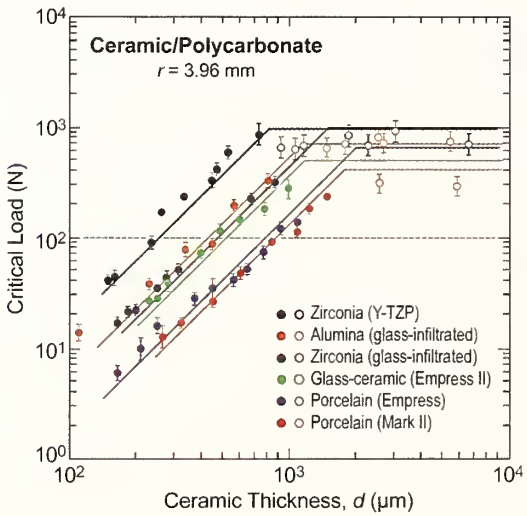

Figure 2: *Data showing critical load to produce damage in ceramic/polymer bilayers. These data are useful in ranking materials for optimal layer combinations.*

Contributors and Collaborators

D. Rekow, V. Thompson (New York University); I. Lloyd, Y. Deng (University of Maryland); A. Pajares, P. Miranda (University of Extremadura); D.K. Kim (KAIST); Ivoclar–Vivadent, Norton–Desmarquest, Vita Zahnfabrik, Amedica Corp., Ceramco, Therics

Mechanical Property Measurements

This project focuses on the development and standardization of strength and hardness test methods and the acquisition of elastic, plastic and adhesion data for thin films. Innovative test methods are refined and standardized to meet the needs of a broad sector of the ceramic community including structural, electronic, and biological applications. Our goal is to refine or create practical, high-quality test methods for use in design, materials development and/or materials specification.

Said Jahanmir and George Quinn

The first wave of mechanical property test standards have dramatically improved and rationalized testing procedures for advanced ceramics and thin films in the United States. Indeed, worldwide harmonization and standardization are also well underway. There are limitations to some of the standards, however, and the ceramics community would like to see alternatives. For example, many small ceramic components are fabricated in rod shapes and it is impractical or inefficient to prepare rectangular beam specimens or very long tension specimens. The dental ceramics community would prefer strength tests based on the pill-shaped diametral compression strength test as opposed to direct tension or flexural strength tests. Hence, alternative specimen geometries that meet the needs of the engineering materials communities are desired.

A key step in the preparation/grinding of strength test specimens is the preparation procedure. Diamond grinding creates subsurface damage that affects strength. The Ceramic Machining Consortium program concluded this year, and valuable lessons learned from the program were incorporated into several American Society for Testing and Materials (ASTM) standards. The specimen preparation procedure in the ASTM strength test standard C 1161 for flexural strength of rectangular beam specimens was extensively revised. The standard machining procedure is intended to minimize the influence of machining. A new standard developed at NIST, C 1495, was adopted by ASTM for assessing the effect of machining by grinding on strength testing of rectangular bars. ASTM standard C 1322 for fractographic analysis of fracture origins was also extensively revised and now includes many new illustrations and advice for detecting machining damage.

A thorough fractographic examination of machining damage was conducted on a reaction-sintered silicon nitride. As a result of this study, machining damage cracks, that previously had been difficult to detect and characterize, are now easily identified. Hundreds of bars and rods that had been ground under a variety of conditions were examined and several important trends were detected. By far, the dominant factor controlling size and severity of machining damage was the grinding wheel grit size. This is not an unexpected finding, but the full quantification of the effect is new.

We are actively involved in national and international efforts to develop standard test methods for Instrumented Indentation Testing (IIT) of thin films, and to compare the results of IIT tests on films to those obtained by other methods such as Surface Acoustic Wave measurements made at NIST Boulder (Donna Hurley, Materials Reliability Division, MSEL) and the Bundesanstalt für Materialforschung und-prüfung (BAM). A major effort in this area is underway within the Versailles Project on Advanced Materials and Standards (VAMAS) Technical Working Area 22 (TWA 22), currently chaired by NIST. A large international round robin IIT test of thin film specimens was organized and carried out with substantial NIST involvement to compare the results from different machines and different analysis methods. A second project is underway in TWA 22 to compare the results of several adhesion tests (scratch, bend and indentation) on several thin film systems, and a third project is just beginning in the area of elastic property measurements for thin films. In addition, NIST and BAM in Germany have a joint program in progress to develop standard or certified reference film systems for mechanical test methods.

To evaluate double-torsion and dynamic fatigue in flexure test methods, crack growth in sapphire was investigated in dry and water-saturated environments. The specimens were oriented for prospective fracture either along the m-plane or along the r-plane of the crystal. Variation of the flexural strength of dry specimens was insignificant with respect to loading rate. Flexure specimens with m-plane orientation fractured on the m-plane at 20°C, but they fractured on the r-plane at 800°C. Flexure specimens with r-plane orientation fractured 9° off the r-plane at both temperatures. Crack growth was measured on the double-torsion specimens both by direct observation and by load relaxation. Crack growth on double-torsion specimens with m-plane orientation required at 800°C only about 70% of the stress-intensity factor needed at 20°C. Approximately 1.5 times greater stress-intensity factor was required to initiate crack growth in double-torsion specimens with r-plane orientation, but the crack growth was erratic, tending to fracture slightly askew of the r-plane and then jumping suddenly along the r-plane.

Contributors and Collaborators

D. Smith, L. Ives, R. Krause (Ceramics Division); B. Mikijelj (Ceradyne); R. Chand (Chand-Kare); J. Salem (NASA-Glenn); J. Swab (U.S. Army Research Laboratory); W. Mandler (Enceratec Corporation); R. Cutler (Ceramatec); M. Jenkins (University of Washington); N. Jennett (NPL, U.K.); U. Beck (BAM, Germany); T. Ohmura (NRIM, Japan)

Microstructural Design

The properties, performance, and reliability of a ceramic material depends not only on intrinsic material properties, but also on the microstructure that evolves during processing and use. To establish generic relationships between processing, microstructure, and material properties, we are developing analytical, statistical, and computational tools to elucidate and characterize these correlations, so one can accurately predict in-service material behavior and, ultimately identify processing routes for tailoring material microstructures to enhance material properties and performance.

Edwin R. Fuller, Jr. and David M. Saylor

Fundamental understanding of the correlations between processing, microstructure, and material properties is the core of materials science. To help elucidate this understanding, we are developing analytical, statistical and computational tools to characterize and quantify ceramic microstructures. An ultimate goal is the application of this knowledge to form accurate predictive models of microstructural evolution and behavior for advanced ceramic materials. The measurement and characterization tools are microscopy techniques, including optical, scanning electron, and orientation imaging, with analytical and statistical analyses. The microstructural data thus provided enables a quantitative specification of ceramic microstructures. This quantitative description is incorporated into microstructure models that are the basis for finite-element simulations for predicting microstructural evolution and material properties. The methodology thereby incorporates real microstructures into predictive models, thus providing more representative results. Furthermore, aspects of the microstructure that are relevant to a property of interest may be readily identified so that ways to tailor it to enhance performance may be developed.

As part of a cooperative research project with Carnegie Mellon University, we have developed a new stereological technique to measure distributions of grain-boundary configurations (crystal misorientation and grain-boundary plane) in polycrystalline materials from a single experimental observation plane. It is widely recognized that the types of grain boundaries in materials, and the manner in which they are connected, affect a wide range of properties and, ultimately, materials performance and reliability. However, the natural complexity of the grain-boundary network has prevented a statistically-significant characterization of its distribution. Accordingly, the information needed to produce (or even specify) desirable microstructures is lacking. The new measurement technique makes it possible to specify the statistical distribution of grain-boundary configurations in a polycrystalline material with relative ease. It has been verified by application to both virtual and real polycrystals. We plan to utilize this technique to measure and quantify the evolution of grain-boundary distributions in ceramic materials during processing.

Computer models have become vital tools for predicting performance and reliability of materials. By conducting virtual experiments, these models provide us with facile means for examining material response to a wide variety of experimental conditions. However, to form accurate predictive models, we must have starting configurations that are representative of real microstructures. Thus, jointly with Alcoa Technical Center and Carnegie Mellon University, we have developed computational tools that incorporate quantitative descriptions of microstructure into stochastic models, yielding simulated microstructures that are statistically identical to those of the real material. We currently can include spatial variations in grain size, shape, and orientation, as well as grain-boundary statistics, into the three-dimensional simulated microstructures. These model microstructures will serve as a basis for finite-element simulations to predict material properties, as well as microstructural evolution. Furthermore, these algorithms can be used to create hypothetical microstructures in an attempt to identify optimal configurations for a particular application.

Physical properties, such as thermal conductivity, elastic moduli and residual stresses, are crucial to component design and reliability. As physical and mechanical properties are often difficult to measure directly, an alternate stratagem is to develop numerical schemes for determining these properties directly from the complex material microstructure. Such a computational tool, called OOF, has been developed at NIST. OOF, which stands for Object Oriented Finite element analysis, allows materials scientists to simulate the physical properties of complex microstructures from an image of that microstructure. Both elastic and thermoelastic versions of OOF are available on the NIST CTCMS website. The next version, currently under development in collaboration with ITL, will incorporate multi-fields and their interactions. In collaboration with GE Corporate R&D Center, we have validated that OOF predicts effective thermal conductivity for plasma-sprayed thermal barrier coatings (TBC's). Other applications include elastic behavior of TBC's, residual stresses, thermal expansion and microcrack damage evolution in polycrystalline ceramics and building stones, and domain switching in ferroelastic materials.

Contributors and Collaborators

S.A. Langer (Mathematical & Computational Sciences Division, ITL); A.C.E. Reid, W.C. Carter (Massachusetts Institute of Technology); G.S. Rohrer, A.D. Rollett (Carnegie Mellon University); J. Fridy, H. Weiland (Alcoa Technical Center); J. Ruud, N.S. Hari, A. Mogro-Campero (GE Corporation R&D Center)

Data Evaluation and Delivery

Accurate materials data are increasingly critical to the rapid design and manufacture of the cost-effective, reliable products that characterize 21st century life. The MSEL Data Evaluation and Delivery Program is working to facilitate the building of interoperable materials structure, phase, and property databases needed by the scientific and industrial communities, and to develop strategies for visualizing multi-dimensional datasets needed for materials selection in product design.

To this end, the FY2002 Projects in the MSEL Data Evaluation and Delivery Program were focused on:

- Improving materials data transfer between databases through development of a standard materials mark-up language (MatML);
- Developing a major compilation of elastic moduli data for polycrystalline oxide ceramics;
- Providing protocols for data evaluation to ensure that databases are populated with accurate data;
- Expanding the Ceramics WebBook which provides links to other sources of ceramic data and manufacturer's information, as well as selected data sets evaluated by NIST, including structural ceramics and high temperature superconductor databases, glossaries, and tools for analysis of ceramic materials;
- Completing the first release of a new Windows-based PC product for the Inorganic Crystal Structure Database in cooperation with Fachinformationszentrum (FIZ) Germany
- Producing phase diagrams through the NIST/American Ceramic Society, Phase Equilibria Program;
- Developing approaches to viewing multidimensional mechanical property and phase diagram data for metals, through a series of simple — but useful — interactive calculations;
- Establishing a prototype site for linking NIST materials data with external datasets such as those developed and maintained by ASM International; and
- Developing a comprehensive database of critically evaluated properties of lead-free solders including multi-dimensional data from three national consortia, the National Center for Manufacturing Sciences (NCMS) Lead-Free Solder Project, the NCMS Fatigue Resistant Lead-Free Solder Project, and the National Electronics Manufacturing Initiative (NEMI) Lead-Free Assembly Project.

Contact: Charles Sturrock

Ceramic Phase Equilibria Database

The goal of this project is to develop and maintain a state-of-the-art database of critically-evaluated ceramic phase equilibria data for industrial and academic customers. It is a collaborative effort between the Ceramics Division and the American Ceramics Society.

Terrell A. Vanderah and Peter K. Schenck

Phase diagrams are used throughout the ceramics industry to understand and control the complex phenomena which underlie advanced industrial production and materials performance. To serve the need for reliable phase diagram data, the Phase Equilibria Data Center along with the American Ceramic Society (ACerS) jointly published a series of critically evaluated collections of phase diagrams. The series originally was published under the title "Phase Diagrams for Ceramists," (1964–1992). It is now published under the more general title "Phase Equilibria Diagrams" to emphasize that the data are useful to the broader materials community.

The "Phase Equilibria Diagrams" series provides current, evaluated data on the phase equilibria of ceramics and related materials, and also provides bibliographic, graphical and analytical services so that researchers have access to reliable up-to-date data for designing, using, applying, analyzing, and selecting those materials. The published portion of the database includes approximately 16,000 entries with nearly 26,000 phase diagrams contained in nineteen books, and a CD-ROM. Over 53,000 units have been sold worldwide. Approximately 1000 new entries are collected from the primary literature each year.

Currently underway is a complete modernization of the 1980's HP-based system to a relational database using PC's. The new system is expected to come on line in 2003 and will be capable of electronic publishing in a variety of formats, including a Web-based version. Much of this year's efforts have involved assisting and working with on-site ACerS staff to design and build the new system, which must incorporate all of the scientific data relationships embodied in the original database. In addition, the NIST-ACerS team has completed the required modernization tasks including upgrading of the digitization software, originally written by NIST staff, and input of 2,000 commentaries and 6,955 diagrams from older volumes of the series that did not exist as electronic files.

The topical volume *"Electronic Ceramics: Oxides of Ti, Nb, and Ta"*, edited by R.S. Roth, is nearing completion and will go to press approximately December 2002 (approximately 800 entries and 1080 diagrams). An example of a phase diagram from this volume is shown in Figure 1. Most of the systems in this monograph will be of major interest to the fields of dielectric, ferroelectric, and piezoelectric ceramics. Following this volume preparation, there will be the publication in early 2003 of a newly updated *"Cumulative Index,"* which will provide comprehensive coverage of published data sorted by chemical system and author. Also in preparation is *"Volume XIV — Oxides"* (spring 2004) which will contain a wide variety of metal, non-metal, and semi-metal oxide systems — more than 900 entries with 1300 diagrams are already available for inclusion. The possibility of a future volume on ceramics for energy applications is currently being explored.

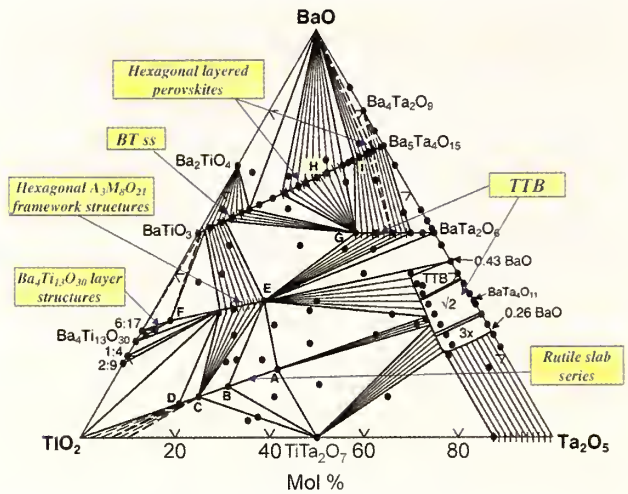

Figure 1: *Recently completed NIST phase diagram for the system BaO:TiO_2:Ta_2O_5, to be included in the upcoming database publication,* "Electronic Ceramics: Oxides of Ti, Nb, and Ta" (available in early 2003, *Am. Ceram. Soc.*).

Contributors and Collaborators

M.A. Harne, R.S. Roth, H. Ondik, H.F. McMurdie; C. Cedeno, J. You, N. Swanson, E. Farabaugh, M. Mecklenborg (The American Ceramic Society)

Crystallographic Databases for Non-Organic Materials

The materials community uses crystallographic data models on a daily basis to visualize, explain, and predict the behavior of chemicals and materials. Access to reliable information on the structure of crystalline materials helps researchers concentrate on experimental work in directions that optimize the discovery process. This project develops, maintains, and disseminates evaluated full-structural crystallographic data in modern computerized formats, along with scientific software tools to exploit the content of these databases.

Vicky Lynn Karen and Alec Belsky*

To meet the needs of the industrial, scientific and technical communities, this project covers three areas: a) building and maintaining state-of-the-art databases containing the structures of non-organic substances, including ceramics, metals and inorganic materials; b) developing software tools for the calculation and standardization of derived data items as well as modules for the intelligent access of these data; and c) providing access to these databases through modern user interfaces and networking capabilities. Access to crystal structure data can be key to solving research and applications problems involving materials in the chemical (catalytic materials), petroleum (zeolites), and the electronics (epitaxial growth and thin films) industries. These data are of interest to analysts in materials design, properties prediction, and compound identification. Better quality data and modern products should help users gain an increased understanding of materials properties and help companies to lower costs and increase research efficiency.

The Inorganic Crystal Structure Database (ICSD) is produced cooperatively by the Fachinformationszentrum Karlsruhe and NIST. The ICSD is a comprehensive collection of crystal structure data of inorganic compounds containing more than 60,000 entries and covering the literature from 1915 to the present. To be included in the database, the structure has to be fully characterized, the atomic coordinates determined and the composition fully specified. In addition to the published data, many items are added through expert evaluation or are generated by computer programs, such as the reduced cell, the Wyckoff sequence, and the mineral group. This year, various subsets of the data were prepared and examined in detail by crystallographic experts, and numerous corrections were made using scientific and database management system criteria. This expert evaluation is an on-going data center activity.

The first release of a new Windows-based PC product for the Inorganic Crystal Structure Database was completed in FY02. Throughout this year, several iterative cycles of review, test, and revision (both internal and external to NIST) were completed for the software and database content. The new PC product and Demo CDROM was presented to the worldwide crystallographic community at the XIX Congress and General Assembly of the International Union of Crystallography, August 2002. The new software product is tabular in design and allows searches in five general categories: Chemistry, Crystal Data, Reduced Cell, Symmetry and Reference Data. The software includes enhanced features for the characterization of materials based on lattice search and chemistry search modules, and it provides three-dimensional visualization and powder pattern simulation for inorganic structures.

In the Chemistry search, we have designed what we refer to as an "exclusive OR." When a first attempt to characterize a material fails, a researcher can usually define the components that went into a synthesis. This type of search allows the user to input several starting materials and automatically search on all possible components rather than trying to input them by hand. Once a search has been made, the user can generate a three-dimensional view of the structure, calculate powder patterns, or export the information into other applications. The Crystal Data Screen allows searches by structure type and authors. A lattice-based search has been added to allow the user to input an experimentally determined cell, calculate the reduced cell, and then search the ICSD. This is possible because the archival database has been augmented to include the standard, reduced cell. All symmetry properties are searchable including space group, Wyckoff position, and Pearson symbol. In the Reference screen, the mineral name, mineral group and various keywords such as temperature, pressure, or type of experiment can be searched; all text fields are searchable including title of publication, authors' names, and additional remarks.

The ICSD can be accessed in a hierarchical mode or in a Boolean mode using AND, OR, NOT logic and multiple result sets can be generated. The different result sets can be combined and individual entries selected by the user to customize the results for a specific problem. Finally, there is extensive flexibility in exporting the results into user-defined and standard formats for compatibility with outside applications.

Contributors and Collaborators

*NIST Measurement Services Division, Technology Services; Fachinformationszentrum Karlsruhe, Germany; D. Watson (Cambridge Crystallographic Data Centre, UK); S. Young (NIST Measurement Services Division, Technology Services); C. Sturrock (Ceramics Division)

Materials Property Data and Data Delivery

Advances in materials science and engineering, from the production of new material phases, the refinement of measurement capabilities, and the modeling of material behavior, create increasing demands for data that are evaluated and readily available in a directly functional format. Projects focused on the development of evaluation methodology, comprehensive databases, and advanced information delivery techniques for materials property data are responding to those needs.

Ronald G. Munro and Edwin F. Begley

The domestic market for advanced structural ceramics was estimated in the year 2000 to be on the order of $800 million with more than 100 companies involved in the production of ceramics. The major markets for this substantial material production included cutting tools, engines, heat exchangers for higher energy efficiency, biomedical implants and devices, the aerospace industry, and defense applications. The availability of reliable property data has been cited as one of the essential components of the technology base that enables advanced materials to be integrated into this important marketplace. The Ceramics Division has taken a lead in providing this critical information to the ceramics community by means of its efforts in data evaluation.

Reliable data are a cornerstone for engineering designs using advanced materials and for the development of new materials. Essential to the efforts to provide reliable data are compilations of property values that are sufficiently extensive and comprehensive so that significant data evaluation analyses may be successfully applied to them. Such compilations serve two important sectors of technology. For scientific studies, they serve as relatively generic collections of data providing the basis for statistical and theoretical analyses of general property relations. For engineering applications, they serve as sources of specific property values to be used in product design and manufacturing. In the latter applications, computer-aided design and manufacturing techniques, that are used to simulate a product's behavior under the desired operating specifications often require data spanning a suitable range of thermal conditions.

Central to this effort is data evaluation. This evolving discipline is providing the essential means to ensure not only the quality of the property values, but also the mutual integrity of the property relations, i.e., data values of related properties should be mutually compatible. In this effort, it must be recognized that properties of ceramics often depend significantly on chemical constituency (the presence of sintering aids or dopants), physical characteristics (density, porosity, and microstructure), and environmental factors (temperature, pressure, and atmosphere). Furthermore, there are a number of measured quantities, sometimes referred to as engineering properties, whose values depend on specific details of the measurement procedure. These considerations are an integral part of data evaluation, and recognizing their consequences is an essential step in the effort to identify mutual dependencies of material properties, to discover the manner in which underlying variables affect measured values, and to resolve apparent discrepancies among independent property reports.

Significant advances were made in FY02 in all aspects of the efforts to establish and distribute evaluated data: the development of data evaluation methods, advances in a materials markup language (MatML), and data compilation.

A major effort was focused on a substantial compilation of elastic moduli data for polycrystalline oxide ceramics, in which the particular emphasis was on the dependence of the moduli on porosity and temperature. For a comprehensive discussion of this development, see the Technical Highlight, Elastic Moduli Data for Polycrystalline Oxide Ceramics, in this report.

Compilations of evaluated data currently are maintained in three collections, all of which are available *via* the Ceramics Divisions website (*http://www.ceramics.nist.gov*) under the topic, Ceramics WebBook. Two of the collections, the Structural Ceramics Database (SCD) and the High Temperature Superconductors Database (HTS), are large, general reference compilations that are searchable by property and material keywords, as well as by author's name and publication source. A major update to the SCD was described in this report series in FY01. The third collection, known as the Property Data Summaries (PDS), provides data sets focused on specific topics. In FY02, the results of a comprehensive study on the material properties of polycrystalline titanium diboride was added to the PDS collection.

Attention also has been given to the growing need to implement collections of evaluated data on the web in a manner amenable to distributed computing and automated processing. The principal effort addressing this issue has been the development of a materials markup language, MatML. For a comprehensive discussion of this topic, see the Technical Highlight in this report series in FY01.

Contributors and Collaborators

Data efforts: S. Freiman, S. Dapkunas, C. Sturrock, M. Cellarosi, J. Harris (Ceramics); *Materials markup language:* J.G. Kaufman (Kaufman Assoc.); F. Cverna (ASM Int'l); D. Fleming (Automation Creations, Inc.); C. Grethlein (AMPTIAC); D. Mies (MSC Software); M. Mitchell (NASA); C. Nunez (Centor Software); S. McCormick (ESM Software); M. Sullentrup (Boeing Co.)

Advanced Manufacturing Methods

An increasingly competitive manufacturing environment drives the search for new materials and processing techniques to make them. In most cases, materials processing steps determine the microstructure and performance of the material while manufacturing costs determine price. Industry needs measurement methods, standards, and data that will help monitor, control, and improve processing methods. These tools are also needed to help understand materials processing and to develop new processing methods and materials with enhanced properties. This is as true for highly developed, well-established industries as it is for rapidly growing or emerging industries. It is also true for all types of materials, processes, and products. The industrial competitiveness of the United States depends on U.S. manufacturers' ability to use the measurement tools to develop and advance their manufacturing methods. In many cases, the needed tools are generic and their impact would be greatly enhanced if they became industry wide standards. Therefore, MSEL is working to develop measurement methods and standards to enable industry to achieve these goals. This work is often being conducted in close collaboration with industry through consortia and standards organizations. The close working relationship developed with industry through these organizations not only ensures the relevance of the research projects, but also promotes an efficient and timely transfer of research information to industry for implementation. Since different materials and industries frequently have similar measurements needs, and most industrial products have multiple materials components, this program covers the processing of ceramics, metals, and polymers.

Research in the Ceramics Division focuses on development of test methods for the assessment of contact damage and wear, development of test methods and predictive models for evaluation of mechanical properties at elevated temperatures, and development of models for prediction of coating properties and performance. One project focuses on low temperature co-fired ceramics (LTCC), a manufacturing method being developed largely for portable wireless modules because it promises to allow for a reduction in the size and cost of modules used in high-frequency applications while improving performance. Because dimensional tolerances are critical in this process, accurate measurements and predictive models of dimensional changes during sintering are necessary for the commercialization of LTCC modules. Measurement methods and predictive models for the overall shrinkage and the local variations in sintering near vias and interconnects are being developed.

Projects in the Metallurgy Division cover several processing and measurement methods. The performance of metallic components in products is strongly dependent on processing conditions that determine microstructural features, such as grain size and shape, texture, the distribution of crystalline phases, macro- and microsegregation, and defect structure and distribution. Expertise is applied from a wide range of disciplines, including thermodynamics, electrochemistry, fluid mechanics, diffusion, x-ray, and thermal analysis, to develop measurement methods and understand the influence of processing steps for industries as diverse as automotive, aerospace, coatings, and microelectronics. Rapidly growing and emerging industries such as biotechnology and nanotechnology are dependent upon the development of new advanced manufacturing methods that can produce metallic components with the desired characteristics and performance. Current projects focus on measurements and predictive models needed by industry to design improved processing methods, provide better process control, develop improved alloy and coating properties, and reduce costs. Important processing problems being addressed include melting and solidification of welds, solidification of single crystals, powder production and consolidation, and coating production by thermal spray and electrodeposition.

Polymeric materials have become ubiquitous in the modern economy because of their ease of processing. However, these materials can exhibit complex and sometimes catastrophic responses to the forces imposed during manufacturing, thereby limiting processing rates and the ability to predict ultimate properties. The focus of the Polymers Division is directed towards microscale processing, modeling of processing instabilities, and on-line process monitoring of polymeric materials. Our unique extrusion visualization facility combines in-line microscopy and light scattering for the study of polymer blends, extrusion instabilities, and the action of additives. Current applications focus on understanding and controlling the "sharkskin instability" in polymer extrusion and observation of the dielectric properties of polymer nanocomposites. Fluorescence techniques are developed to measure critical process parameters such as polymer temperature and orientation that were hitherto inaccessible. These measurements are carried out in close collaboration with interested industrial partners.

Contact: Said Jahanmir

Processing of Low Temperature Co-Fired Ceramics

Low temperature co-fired ceramics (LTCC) are rapidly becoming the technology of choice for RF components and modules for portable wireless applications. LTCC technology has demonstrated that it can enable the high density integrated packages meeting the requirements for portable wireless. Commercialization of these modules requires the accurate prediction of dimensional changes during sintering in order to design passive integrated components (resistors, capacitors and inductors) in the LTCC module.

John E. Blendell and Jay S. Wallace

Low temperature co-fired ceramics (LTCC) are finding increasing use in portable wireless applications due to their high dielectric constant, low loss and high Q. These features allow a reduction in the size of modules for high-frequency applications. In addition, LTCC can include integrated passive components, they are environmentally robust, and they can be rapidly produced. These factors lead to a significant cost advantage for LTCC modules. Because dimensional tolerances are critical for high-frequency applications, accurate predictive models of dimensional changes during sintering are necessary for the commercialization of LTCC modules.

Modeling the evolution of the microstructure, and the dimensional changes that take place during sintering, is being carried out using a combination of phase field methods and object-oriented finite element analysis. This allows accurate modeling of sintering processes with arbitrary boundary conditions. The finite element models are being used to solve for the stress state of the powder compact. These stress profiles will be used in the phase field model to predict mass flow and microstructural evolution during firing. Preliminary two-particle models have been constructed to study the shrinkage in a glass phase. These models will be extended to multiple particle models to allow the interactions that can cause rearrangement of the particles to take place.

An important aspect of this research is the verification of the models developed. We have constructed an optical hot stage microscope for direct examination of the surface of the LTCC tapes during sintering. The movement of markers placed on the surface has shown that there is anisotropic shrinkage, Figure 1. Not all markers move towards a common center, but rather there is local rotation of the markers, indicating local variations in shrinkage.

Optical transmission through the unsintered tapes was measured, Figure 2. The measurements show density variations on the 100 μm scale, consistent with the sintering results. The transmission measurements are being extended into the near IR region using an IR diode laser to improve the resolution of the density variation data.

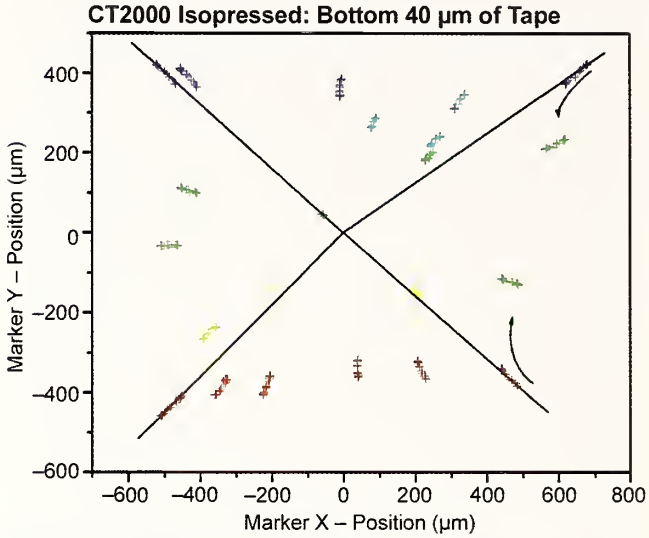

Figure 1: *Hot stage optical microscope measurement of surface marker movement showing anisotropic shrinkage.*

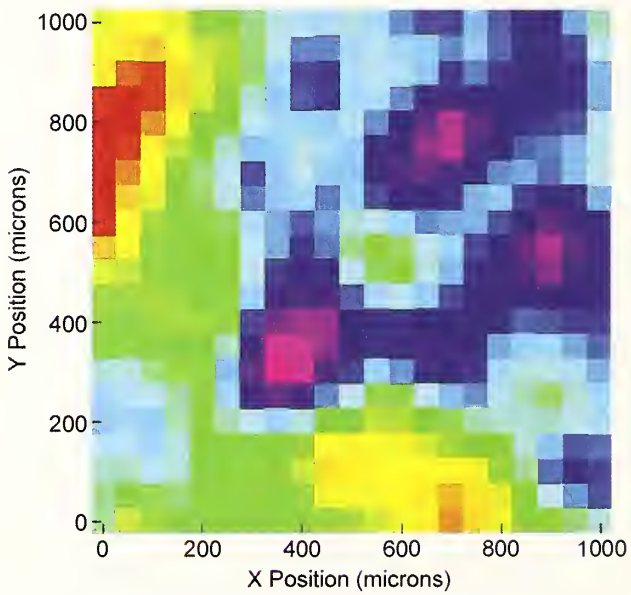

Figure 2: *Optical transmission of unsintered tape showing variations due to particle packing variations.*

Contributors and Collaborators

P. Schenck, B. Hockey (Ceramics Division); J. Warren (Metallurgy Division); M. Locatelli (University of Washington, Seattle, WA)

Contact Damage

Simple and reliable test methods are necessary to characterize structural ceramics intended to replace metals in heavy vehicle applications. In collaboration with our Contact Reliability Working Group—comprising corporate, national laboratory and university members—we are refining test methods and developing standards to characterize rolling contact fatigue in silicon nitride.

Said Jahanmir and William Luecke

Reliability and cost effectiveness are critical issues for implementing ceramics in diesel engines. Ceramic components in engines serve under demanding conditions characterized by high contact loads, elevated temperatures, and corrosive environments. To ensure reliable service life, standard test methods are needed to evaluate the performance of candidate ceramics. In collaboration with diesel engine companies in the U.S., as well as participants from Germany and Japan under the auspices of the International Energy Agency (IEA), we are evaluating and refining test methods for characterizing the contact fatigue behavior of ceramics under rolling and sliding conditions that simulate cam roller followers, valves and valve seats. An integral part of this project is evaluating the effect of machining damage on contact reliability as well as possible interactions between machining damage and contact damage that may lead to premature failure. In addition, we are investigating the relationship between ceramic microstructure and performance reliability.

Current test methods for evaluating the rolling contact fatigue (RCF) performance of silicon nitride are inadequate because improved grades of silicon nitride either do not fail, or they fail by wear instead of RCF. This makes it impossible to evaluate their performance. We have attempted to refine an existing method, the three-ball-on-rod test, so that it once again produces failure by rolling contact fatigue. In the usual application of the test method, the contact load is applied via three specially prepared alloy steel balls to the silicon nitride test rod, which spins at 3600 rpm. With modern bearing-grade silicon nitride, it is the alloy steel balls that fail and terminate the test, usually with minimal wear of the silicon nitride test rod. Although it has been argued that during the test the ball wears and deforms, reducing the contact stress on the rod, we have established that most of the rod wear occurs after the ball fails, presumably from spall debris. Replacing the alloy steel balls with silicon nitride balls resulted in rod spalls for some test rods, but other rods suffered severe wear, even at contact loads below those employed by the alloy steel ball tests.

In a parallel research project, we are characterizing the contact damage resistance of a number of silicon nitrides in an effort to correlate the properties measured in this simple indentation test with the damage formed during rolling contact. We are using single-cycle indentation using WC spheres to characterize the critical loads for quasi-plastic deformation as well as for formation of ring cracks. Despite the fact that their Vickers and Knoop hardness vary by less than 10%, the 11 silicon nitrides exhibit significantly different response to contact damage, measured by the size of the residual impression, d_{max}, left by high-load spherical indentation. (See Figure 1).

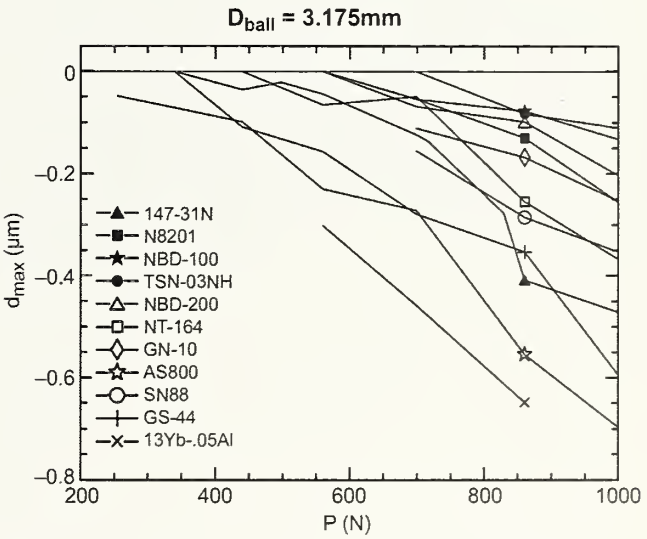

Figure 1: *Residual impression depth as a function of load for several silicon nitrides.*

Contributors and Collaborators

B. Mikijelj (Ceradyne); M. Andrews (Caterpillar); T. Yonushonis (Cummins); P. Wilbur (Colorado State University); R. Chand (Chand Associates); W. Kanematsu (AIST, Chubu, Japan); M. Woydt (BAM, Berlin, Germany); M. Ferber (ORNL); S. Diamond (US-DOE)

Ceramics Division Databases and Standards

NIST SRMs are available for purchase from the NIST Standard Reference Materials Program, accessible from the NIST home page, www.nist.gov.

NIST Standard Reference Database 84 — FIZ/NIST Inorganic Crystal Structure Database (August 2002); first release of a new Windows-based PC product for the Inorganic Crystal Structure Database, (NIST authors: V.L. Karen and A. Belsky). Available for purchase at *http://www.nist.gov/srd/nist84.htm.*

NIST Standard Reference Database 30: Structural Ceramics Database. Expanded to over 30,000 numeric values. (NIST authors: R.G. Munro and E.F. Begley). Available online at *http://www.ceramics.nist.gov/srd/scd/scdquery.htm.*

NIST Property Data Summary for Titanium Diboride. (NIST author: R.G. Munro). Available online at *http://www.ceramics.nist.gov/srd/summary/scdtib2.htm.*

NISTIR **6853**, "Elastic Moduli Data for Polycrystalline Oxide Ceramics," (NIST author: R.G. Munro). National Institute of Standards and Technology, (2002). Currently available in printed copy.

ASTM C 1161, (2002), "Standard Test Method for Flexural Strength of Advanced Ceramics at Ambient Temperature," (NIST contributor: G. Quinn).

ASTM C 1322, (2002), "Standard Practice for Fractography and Characterization of Fracture Origins in Advanced Ceramics," (NIST contributor: G. Quinn).

ASTM F 2094, (2001), "Standard Specification for Silicon Nitride Bearing Balls," (NIST contributor: G. Quinn).

ASTM C 1211, (2002), "Standard Test Method for Flexural Strength of Advanced Ceramics at Ambient Temperature," (NIST contributor: G. Quinn).

ISO Standard 17565, (2001), "Fine Ceramics (Advanced Ceramics, Advanced Technical Ceramics) — Test Method for Flexural Strength of Monolithic Ceramics at Elevated Temperature," (NIST contributor: G. Quinn).

ISO 18756, (2002), "Fine Ceramics (Advanced Ceramics, Advanced Technical Ceramics) — Determination of Fracture Toughness of Monolithic Ceramics at Room Temperature by the Surface Crack in Flexure (SCF) Method," (NIST contributor: G. Quinn).

Standard Reference Material 8010, "Sand for Sieve Analysis," (NIST leader: J. Kelly).

Standard Reference Material 1003c, "Particle Size Standard 20 μm to 50 μm," (NIST leader: J. Kelly).

Standard Reference Material 1897, "Specific Surface Area Standard," (NIST leader: D. Minor).

Standard Reference Material 1918, "Mercury Porosimeter Intrusion Standard," (NIST leader: D. Minor).

Ceramics Division FY02 Annual Report Publication List

Abe H., Naito M., Wäsche R., Hackley V., Hotta Y., "Influence of Particle Size and Solid Loading on the Determination of the Isoelectric Point (IEP) of Ceramic Powders by Different Methods." *Key Eng. Mater.*, **206-213**, pp. 3–6, (2002).

Allen, A.J., Long, G.G., Boukari, H., Ilavskya, J., Kulkarni, A., Sampath, S., Herman, H., Goland, A.N., "Microstructural characterization studies to relate the properties of thermal-spray coatings to feedstock and spray conditions." *Surface & Coatings Technology,* **146**, pp. 544–552, Sep.–Oct. 2001.

Ankudinov, A.L., Bouldin, C.E., Rehr, J.J., Sims, J., Hung, H., "Parallel calculation of electron multiple scattering using Lanczos algorithms." *Physical Review B*, **65**, pp. 104–107, (2002).

Armstrong, N., Kalceff, W., Cline, J.P., and Bonevich, J., "A Bayesian/Maximum Entropy method for the certification of a nanocrystallite-size NIST Standard Reference Material." *Proceedings of Size Strain III*, Trento, Italy, December 2–5, 2001.

Armstrong, N., Kalceff, W., Cline, J.P., Bonevich, J., "Bayesian inference of nanoparticle-broadened x-ray line profiles." *Special Edition: Proceedings of Accuracy in Powder Diffraction III*, April 2001.

Bar–On, I., Quinn, G. D., Salem, J., and Jenkins, M.J., "Fracture Toughness Standard Test Method C 1421-99 for Advanced Ceramics." *Fatigue and Fracture Mechanics*, Vol. 32, pp. 315–335, ASTM STP 1406, ed. R. Chona, American Society for Testing and Materials, West Conshohoken, PA, 2001.

Begley, E.F., and Sturrock, C.P., "The Background and Development of MatML, a Markup Language for Materials Property Data." Proceedings of the 18th International CODATA Conference, CODATA, Paris, France, (2002).

Belsky, A.J., Hellenbrandt, M., Karen, V.L., Lucksch, P., "New developments in the Inorganic Crystal Structure Database (ICSD): accessibility in support of materials research and design." Acta Crystallographica Section B, *Structural Science*, **B58**, pp. 364–369, 2002.

Bendersky, L.A., Levin, I., Roth, R.S., and Shapiro, A., "$Ca_4Nb_2O_9$-$CaTiO_3$ Phase Equilibria and Microstructures." *J. Solid State Chem.*, **160**, pp. 257–271, (2001).

Bhat, R.R., Fischer, D.A., and Genzer, J., "Fabricating planar nanoparticle assemblies with number density gradients." *Langmuir*, **18**, pp. 5640–5643, (2002).

Black, D., Polvani, R., and Quinn, G.D., "Using X-ray Topography to Study Fracture of Single-Crystal Ceramics." Fractography of Glasses and Ceramics, IV, *Ceramic Transactions,* Vol. 122, pp. 267–282. Ed. J. Varner and G. Quinn, American Ceramic Society, Westerville, OH, 2001.

Blendell, J. and Handwerker, C.A., "Grain Growth in Ceramics." *Encyclopedia of Materials: Science & Technology*, Elsevier, 2001.

Blendell, J.E., Locatelli, M.R., Wallace, J.S., Hockey, B.J., "Modeling of Anisotropic Shrinkage During Sintering of Low Temperature Cofired Ceramic Tapes." IMAPS Advanced Technology Workshop on Ceramic Applications for Microwave and Photonic Packaging, Providence, RI, May 2–3, 2002.

Bouldin, C., Sims, J., Hung, H., Rehr, J.J., and Ankudinov, A.L., "Rapid calculation of x-ray absorption near edge structure using parallel computing." *J. of X-ray Spectrometry*, **30** [6], pp. 431–434, (2001).

Burton, B.P., and Cockayne, E., "Prediction of the $Na_{1/2}Bi_{1/2}O_3$ Ground State." *Fundamental Physics of Ferroelectrics 2001*, pp. 82–90, (AIP Conference Proceedings Series 582). Ed. Krakauer, H., American Institute of Physics, Woodbury, NY, 2001.

Burton, B.P., and Cockayne, E., "Unexpected Ground State Structures in Relaxor Ferroelectrics." *Ferroelectrics*, **270**, pp. 173–178, (2002).

Burton, B.P., Dupin, N., Fries, S.G., Grimvall, G., Fernandez Guillermet, A., Miodownik, P., Oates, W.A., and Vinograd, V., "Using Ab Initio Calculations in the CALPHAD Environment." *Z. Metallkd*, **92**, pp. 514–525, (2001).

Choi, J.H, Kim, D.K., Hockey, Wiederhorn, S.M., B.J., Blendell, J., Handwerker, C.A., "The Equilibrium Shape of Internal Cavities in Ruby and the Effect of Surface Energy Anistropy on the Equilibrium Shape." *J. Amer. Ceram. Soc.*, **85** [7], pp. 1841–44, (2002).

Cheary, R.W., Coelho, A.A., and Cline, J.P., "Fundamental Parameters Line Profile Fitting in Laboratory Diffractometers." *Special Edition: Proceedings of Accuracy in Powder Diffraction III*, April 2001.

Cockayne, E., "Comparative Dielectric Response in $CaTiO_3$ and $CaAl_{1/2}Nb_{1/2}O_3$ from First Principles." *J. Appl. Phys.*, **90**, pp. 1459–1468, (2001).

Cockayne, E., Burton, B.P., and Bellaiche, L., "Temperature-Dependent Behavior of $PbSc_{1/2}Nb_{1/2}O_3$ from First Principles." *Fundamental Physics of Ferroelectrics 2001,* pp. 192–201, (AIP Conference Proceedings 582). Ed. Krakauer, H., American Institute of Physics, Woodbury, NY, 2001.

Cook, L.P., Wong-Ng, W., and Suh, J., "DTA/TGA study of eutectic melting in the system BaF_2-BaO-Y_2O_3-CuO_x-H_2O." MRS Proceeding, **659**, Balachandran, et al., eds., *High-Temperature Superconductors-Crystal Chemistry, Processing and Properties, II,* 4.8, (2001).

Dieng, L.M., Ignatov, Y., Tyson, T.A., Croft, M., Dogan, F., Kim, C.-Y., Woicik, J.C., and Grow, J., "Observation of changes in the atomic and electronic structure of single-crystal Yba2Cu3O6.6 accompanying bromination." *Physical Review B,* **66**, 014508, (2002).

Dillingham, J., Wong-Ng, W., Levin, I., "Phase Equilibria of the SrO-Yb_2O_3-CuO_x System." *Int. J. Inorg. Mater.*, **3**, p. 569, (2001).

Fang, H.W., and Hsu, S.M., "Micro-cutting Mechanism Study of Surface Texture Controlled UHMWPE wear particle generation." J.V. Sengers, Proceedings of the Biomaterials Society annual meeting, May 2002.

Fang, H.W., Hsu, S.M., and Sengers, J.V., "Effects of Surface Feature Dimensions on Particle Dimensions and Aspect Ratio for a Surface Texture Controlled UHMWPE Particle Generation Process." Transactions of the 28th Society for Biomaterials, May 2002.

Farber, L., Levin, I., Borisevich, A., Gray, I.E., Roth, R.S., Davies, P.K., "Structural Study of $Li_{1+x-y}Nb_{1-x-3y}Ti_{x+4y}O_3$ Solid Solutions." *J. Solid State Chem.*, **166**, (2002).

Ferraris, C., Hackley, V.A., Avilés, A.I. and Buchanan, C.E., "Analysis of the ASTM Round-Robin Test on Particle Size Distribution of Portland Cement: Phase I." *NISTIR* **6883**, National Institute of Standards & Technology, Technology Administration, USDOC, Gaithersburg, MD, (2002).

Fischer, D.A., Sambasivan, S., Kuperman, A., Platonov, Y., and Wood, J.L., "Focusing Multilayer Mirror Detection System for Carbon K Edge Soft X-ray Absorption Spectroscopy." *Review of Scientific Instruments*, **73**, pp. 1469–1475, (2002).

Fischer, D.A., Sambasivan, S., Kuperman, A., Platonov, Y., and Wood, J.L., "Catalytic Carbon K edge X-ray Absorption Spectroscopy: Multilayer Mirror Detection System." *Science Highlight*, 2001 National Synchrotron Light Source Annual Report 2-117 to 2-120.

Fischer, D.A., Sambasivan, S., Kuperman, A., Platonov, Y., and Wood, J.L., "Multilayer mirror fluorescence detection system for photon-in photon-out *in-situ* carbon K-edge NEXAFS." *Synchrotron Radiation News*, special photon-in photon-out issue, **15**, pp. 16–20, (2002).

Freiman, S.W., and Quinn, G.D., "How Property Test Standards Help Bring New Materials to the Market." *ASTM Standardization News*, Oct. 2001, pp. 26–31.

Freiman, S.W., and Quinn, G.D., "How Standards Help Bring New Materials to Market." *Facets*, p1 +5 *International Union of Materials Research Societies*, **1**, [3], July 2002.

Gamble, L.J., Ravel, B., Fischer, D.A., and Castner, D.G., "Surface Structure and Orientation of PTFE Films Determined by Experimental and FEFF8-Calculated NEXAFS Spectra." *Langmuir*, **18**, pp. 2183–2189, (2002).

Hackley, V.A., "Polyelectrolyte Adsorption in Bioceramic Systems: Hydroxyapatite as a Substrate Material." Polymers in Particulate Systems: Properties and Applications, *Surfactant Science Series*, Vol. 104, pp. 295–323. Ed. V.A. Hackley, P. Somasundaran and J.A. Lewis, Marcel Dekker, New York, 2001.

Hackley, V.A. and Ferraris, C.F., "Use of Nomenclature in Dispersion Science and Technology." *NIST Recommended Practice Guide 960-3*, DoC Technology Administration, National Institute of Standards and Technology, Gaithersburg, MD, 2001.

Hackley, V.A., Patton, J., Lum, L.H., Wäsche, R., Abe, H., Naito, M., Hotta, Y. and Pendse, H., "Analysis of the Isoelectric Point in Moderately Concentrated Alumina Suspensions by Electroacoustic and Streaming Potential Methods." *J. Dispersion Sci. Tech.*, **23**, [5], pp. 601–617, (2002).

Hackley, V.A., Somasundaran, P. and Lewis, J.A., Eds., "Polymers in Particulate Systems: Properties and Applications." *Surfactant Science Series*, Vol. 104, Marcel Dekker, New York, 2001.

Hastie, J.W., Bonnell, D.W., and Schenck, P.K., "Application of a new thermochemical measurement method for nuclear materials at temperatures beyond 300 K." *J. Nuclear Materials*, **294**, pp. 175–178, (2002).

Hastie, J.W., Bonnell, D.W., and Schenck, P.K., "Laser-Assisted Vaporization Mass Spectrometry: Application to Thermochemistry at Very High Temperature." *NISTIR* **6793**, September 2001.

Haugan, T., Wong-Ng, W., Cook, L.P., Geyer, R.G., Brown, H.J., Swartzendruber, L., and Kaduk, J., "Development of Low Cost $(Sr,Ca)_3Al_2O_6$ Dielectrics for $Bi_2Sr_2CaCu_2O_{8+d}$ Applications." *IEEE Transactions on Applied Superconductivity*, Part III, **11**, (No. 1), p. 3305, (2001).

Haugan, T.J., Fowler, M.E., Tolliver, J.C., Barnes, P.N., Wong-Ng, W., and Cook, L.P., "Flux pinning and properties of solid-solution $(Y,Nd)_{1+x}Ba_{2-x}Cu_3O_{7-z}$ superconductors." Ed. A. Goyal, et. al., Transaction Volume, High Temperature Superconductor Processing, Electronics Division Focus Session at the 2002 ACerS annual meeting, St. Louis, MO, April 29 to May 1, 2002.

Hockey, B.J., Kang, M.K., Wiederhorn, S.M., and Blendell, J., "Low Angle Grain Boundary Dewetting in Sapphire." *Microscopy and Microanalysis*, **7**, Supplement 2, Proceedings: Microscopy and Microanalysis, 2001, Long Beach, CA, Aug. 5–9, 2001.

Hryniewicz, P., Szeri, A.Z., and Jahanmir, S., "Application of Lubrication Theory to Fluid Flow in Grinding. Part I: Flow Between Smooth Surfaces." *Journal of Tribology*, **123**, pp. 94–100, (2001).

Hryniewicz, P., Szeri, A.Z., and Jahanmir, S., "Application of Lubrication Theory to Fluid Flow in Grinding. Part II: Influence of Wheel and Workpiece Roughness." *Journal of Tribology*, **123**, pp. 101–108, (2001).

Hsu, S.M., McGuiggan, P.M., Zhang, J., Wang, Y., Yin, F., Yeh, Y.P., and Gates, R.S., "Scaling Issues in the Measurement of Monolayer Films." NATO/ASI Proceedings on the Fundamentals of Tribology and Bridging the Gap between Macro- and Micro/ Nanoscales, *Nato Science Series: Mathematics, Physics and Chemistry*, Vol. 10, Kluwer, Amsterdam, 2001.

Hsu, S.M., "What is the Role of Wear Testing and Joint Simulator Studies in Discriminating among materials and Designs?" American Academy of Orthopedic Surgeons, *Implant Wear 2000 Book*, 2001.

Hsu, S.M., and Shen, M.C., "Wear Maps." Chapter 9 of the *Modern Tribology Handbook*, Volume I, Edited by Bharat Bhushan, CRC Press, NY, 2001.

Hsu, S.M., and Gates, R.S., "Boundary Lubrication and Boundary Lubricating Film." Chapter 11 of the *Modern Tribology Handbook*, Volume I, Edited by Bharat Bhushan, CRC Press, NY, 2001.

Hsu, S.M., "Molecular Basis of Lubrication." Keynote paper, Proceedings of the Asian F&L Conference, Asian F&L Publisher, Manila, Phillippines, January 2002.

Hsu, S.M., Gates, R.S., and Deckman, D., "Ceramics Lubrication." Invited paper, Proceedings of CIMTEC 2002, (10th International Ceramics Congress), July 15–18, Florence, Italy.

Ilavsky, J., Stalick, J.K., Wallace J. "Thermal spray yttria-stabilized zirconia phase changes during annealing." *Journal of Thermal Spray Technology*, **10**, (3), pp. 497–501, September 2001.

Jahanmir, S., and Jacobs, J., "Update 2001: Standard Experiments in Engineering Materials, Science, and Technology." Proceedings of National Educators Workshop, October 14–17, 2001, Gaithersburg, Maryland.

Jeffrey, G.A. and Karen, V.L., "Crystallography." *The AIP Physics Desk Reference*. Ed. E. Richard Cohen, David R. Lide, and George L. Trigg, Chapter 9, pp. 306–348, Springer-Verlag, New York, 2002.

Jenkins, M., Quinn, G.D., Salem, J.A., and Bar-On, I., "Development, Verification and Implementation of a National Full-Consensus Fracture Toughness Test Method Standard for Advanced Ceramics." *Fracture Resistance Testing of Monolithic and Composite Brittle Materials*, ASTM STP 1409, pp. 49–75. Ed. J.A. Salem, M.G. Jenkins, and G.D. Quinn, ASTM, West Conshohocken, PA, 2002.

Jillavenkatesa, A., Kelly, J.F., and Dapkunas, S.J., "Some Issues in Particle Size and Size Distribution Characterization of Powders." *Am. Pharm. Rev.*, **5**, [2], pp. 98–105, (2002).

Karen, V.L. and Belsky, "NIST Standard Reference Database 84." FIZ/NIST Inorganic Crystal Structure Database, (August 2002).

Kaufman, J.G., Begley, E.F., and Sturrock, C.P., "MatML — A Data Interchange Markup Language for Material Scientists and Engineers." Proceedings of the 2002 ASM International Conference, ASM International, Materials Park, OH, (2002).

Kelly, J.F. and Jahanmir, S., "Study of Moisture and Binder Content of Spray Dried Alumina Granules." DOE Internal Pub., 2002.

Krause, Jr., R.F., Wiederhorn, S.M., and Kueber, J.J., "Misalignment-Induced Bending in Pin-Loaded Tensile-Creep Specimens." *J. Am. Ceram. Soc.*, **84**, [1], pp. 145–52, (2001).

Krause, Jr., R.F., Wiederhorn, S.M., and Li, C., "Tensile Creep Behavior of a Gas-Pressure Sintered Silicon Nitride Containing Silicon Carbide." *J. Am. Ceram. Soc.*, **84**, [10], pp. 2394–400, (2001).

Levin, I., Robins, L.H., Vaudin, M.D., Tuchman, J.A., Lakin, E., Sherman, M.J., Ramer, J., "Spontaneous compositional modulation in the AlGaN layers of a thick AlGaN/GaN multilayer structure." *Journal of Applied Physics*, **89**, [1], pp. 188–193, (2001).

Levin, I., Chan, Y.Y., Maslar, J.E., Vanderah, T.A., and Bell, S.M., "Phase Transitions and Microwave Dielectric Properties in the Perovskite-Like $CaAl_{0.5}Nb_{0.5}O_3$–$CaTiO_3$ System." *J. Appl. Phys.*, **90**, (2), pp. 904–914, (2001).

Levin, I., Vanderah, T.A., Coutts, R., and Bell, S.M., "Phase Equilibria and Dielectric Properties in Perovskite-Like $(1\text{-}x)LaCa_{0.5}Zr_{0.5}O_3$–$ATiO_3$ (A = Ca, Sr) Ceramics." *J. Mater. Res.*, **17**, [7], pp. 1729–1734, (2002).

Levin, I., Amos, T.J., Nino, J.C., Vanderah, T.A., Randall, C.A., Lanagan, M.E., and Reaney, I.M., "Crystal Structure of Compound $Bi_2Zn_{2/3}Nb_{4/3}O_3$," *J. Mater. Res.*, **17**, [6], pp. 1406–1411, (2002).

Levin, I., Chan, J.Y., Scott, J.H., Farber, L., Vanderah, T.A., and Maslar, J.E., "Complex Polymorphic Behavior and Dielectric Properties of Perovskite-Related $Sr(Sr_{1/3}Nb_{2/3})O_3$." *J. Solid State Chem.*, **166**, pp. 24–41, (2002).

Long, G.G., Allen, A.J., Black, D.R. , Burdette, H.E., Fischer, D.A., Spal, R.D., and Woicik, J.C., "National Institute of Standards and Technology Synchrotron Radiation Facilities for Materials Science." *J. Res. Nat. Inst. Stand. Technol.*, **106** (2001), pp. 1141–1154, (2002).

Luecke, W.E., Armstrong, T.R., "Creep of lanthanum gallate." *J. Mater. Res.*, **17**, (3), pp. 532–541, (2002).

Luecke, W.E., "Results of an international round-robin for tensile creep rupture of silicon nitride." *J. Am. Ceram. Soc.*, **85**, (2), pp. 408–414, (2002).

Matsui, M., Jahanmir, S., Mustaghaci, H., Naito, M., Uematsu, K., Waesche, R., and Morrell, R., "Improved Ceramics Through New Measurements, Processing and Standards." Proceedings of PAC RIM IV, American Ceramic Society, 2002.

McGuiggan, P.M., Zhang, J., Hsu, S.M., "Comparison of friction measurements using the atomic force microscope and the surface forces apparatus: the issue of scale." *Tribology Letters*, **10**, (4), pp. 217–223, 2001.

Mighell, A.D., "Lattice Symmetry and Identification —The Fundamental Role of Reduced Cells in Materials Characterization." *J. Res. Natl. Stand. Technol.*, **106**, pp. 983–995, (2001).

Mighell, A.D., Wong-Ng, W., *Special Issue: Crystallography at NBS/NIST.*" Ed. A.D. Mighell & W. Wong-Ng, *J. Res. Natl. Stand.*, **106**, pp. 889–1071, (2001).

Mihalkovic, M., Al-Lehyani, I., Cockayne, E., Henley, C.L., Moghadam, N., Moriarty, J.A., Wang, Y., and Widom, M., "Total-energy Based Structure Prediction for Decagonal Al-Ni-Co." *Physical Review B*, **65**, article 104205, (6 pages), (2002).

Munro, R.G., "NIST Materials Properties Databases for Advanced Ceramics." *J. Res. Natl. Inst. Stand. Technol.*, **106**, pp. 1045–1050, (2001).

Munro, R.G., "Elastic Moduli Data for Polycrystalline Oxide Ceramics." *NISTIR* **6853**, National Institute of Standards and Technology, (2002).

Newell, D.B., Pratt, J.R., Kramar, J.A., Smith, D.T., Feeney, L.A., and Williams, E., "Si Traceability of Force at the Nanonewton Level." *Proc. Natl. Conf. of Stds. Labs. Intl.*, 2001 Workshop and Symp., Washington, D.C., 2001.

Paik, U., Kim, J.P., Lee, T.W., Jung, Y.S., Park, J.G., and Hackley, V.A., "The Effect of Si Dissolution on the Stability of Silica Particles and its Influence on Chemical Mechanical Polishing for Interlayer Dielectrics." *J. Korean Phys. Soc.*, **39**, pp. S201–S204, (2002).

Pratt, J.R., Newell, D.B., Williams, E.R., Smith, D.T., and Krama, J.A., "Towards a Traceable Nanoscale Force Standard." Proceedings of the EUSPEN 2nd International Conference, Turin Italy, 2001, Vol. 1, pp. 470–473.

Quinn, G., "Fracture Toughness Testing of Ceramics." Chapter 4-9-7d, *Encyclopedia of Materials: Science and Technology*, Elsevier, September 2001.

Quinn, G., "Special Mechanical Testing Methods for Ceramics." Chapter 4-9-7n, *Encyclopedia of Materials Science and Technology*, Elsevier, September 2001.

Quinn, G.D., Xu, K., Gettings, R., Salem, J.A., and Swab, J., "Standard Reference Material 2100: Ceramic Fracture Toughness." *Fatigue and Fracture Mechanics*, Vol. 32, pp. 336–350, ASTM STP 1406. Ed. R. Chona, American Society for Testing and Materials, West Conshohoken, PA, 2001.

Quinn, G.D., and Swab, J.J., "Comparisons of Calculated and Measured Flaw Sizes." Fractography of Glasses and Ceramics IV, *Ceramic Transactions*, Vol. 122, pp. 175–192. Ed. J. Varner and G. Quinn, American Ceramic Society, Westerville, OH, 2001.

Quinn, G.D., Ives, L.K., Jahanmir, S., and Koshy, P., "Fractographic Analysis of Machining Cracks in Silicon Nitride Rods and Bars." Fractography of Glasses and Ceramics IV, *Ceramic Transactions*, Vol 122, pp. 343–365. Ed. J. Varner and G. Quinn, American Ceramic Society, Westerville, OH, 2001.

Quinn, G.D., "The Fracture Toughness Round Robins in VAMAS: What We Have Learned." *Fracture Resistance Testing of Monolithic and Composite Brittle Materials*, pp. 107–126, ASTM STP 1409. Ed. J.A. Salem, G.D. Quinn, and M.G. Jenkins, ASTM, West Conshohocken, PA, 2002.

Quinn, G.D., Xu, K., Gettings, R.J., Salem, J.A., and Swab, J.J., "Does Anyone Know the Real Fracture Toughness? SRM 2100: The World's First Ceramic Fracture Toughness Reference Material." *Fracture Resistance Testing of Monolithic and Composite Brittle Materials*, pp. 76–93, ASTM STP 1409. Ed. J.A. Salem, G.D. Quinn, and M.G. Jenkins, ASTM, West Conshohocken, PA, 2002.

Quinn, G.D., and Salem, J.A., "Effect of Lateral Cracks Upon Fracture Toughness Determined by the Surface Crack in Flexure Method." *J. Am. Ceram. Soc.*, **85**, [4], pp. 873–80, (2002).

Quinn, G.D., "Refinements to the Surface Crack in Flexure Method for Fracture Toughness of Ceramics." *Key Engineering Materials*, Vol. 206–213, pp. 633–636, Proceedings of the 7th European Ceramic Society Conference, Brugge, Trans Tech, Switzerland, 2002.

Radovic. M., Barsoum, M.W., El-Raghy, T., et al. "Effect of temperature, strain rate and grain size on the mechanical response of Ti_3SiC_2 in tension." Acta Mater **50**, (6), pp. 1297–1306.

Ravikiran, A., and Jahanmir, S., "Effect of Contact Pressure and Load on Wear of Alumina." *Wear*, **250**, pp. 980–984, (2001).

Robins, L.H., Armstrong, J.T., Vaudin, M.D., Bouldin, C.E., Woicik, J., Paul, A.J., Thurber, W.R., Miyano, K.E., Parker, C.A., Roberts, J.C., Bedair, S.M., Piner, E.L., Reed, M.J., El-Masry, N.A., Donovan, S.M., and Peraton, S.J., "Optical and structural studies of compositional inhomogeneity in strain-relaxed indium gallium nitride films." 2000 IEEE International Symposium on Compound Semiconductors Institute of Electrical and Electronics Engineers, Inc., pp. 507–512, 2000.

Saigal, A., and Fuller, Jr., E.R., "Analysis of Stresses in Aluminum-Silicon Alloys." Computational Materials Science, **21**, [1], pp. 149–158, (2001).

Schwarz, J., Liu, R., Newell, D.B., Steiner, R., Williams, E.R., Smith, D.T., Erdemir, A., and Woodford, J., "Hysteresis and Related Error Mechanisms in the NIST Watt Balance Experiment." *J. of Research of the NIST*, **106**, [4], p. 627, (2001).

Sims, J.S., George, W.L., Sattefield, S.G., Hung, H.K., Hagedorn, J.G., Ketcham, P.M., Griffin, T.J., Hagstrom, S.A., Franiatte, J.C., Bryant, G.W., Jaskolski, W., Martys, N.S., Bouldin, C.E., Simmons, V., Nicolas, O.P., Warren, J.A., et al., "Accelerating Scientific Discovery Through Computation and Visulization II." *J. Res. Natl. Inst. Stand. Tech.*, **107**, pp. 233–245, (2002).

Skirl, S., Krause, Jr., R.F., Wiederhorn, S.M., and Roedel, J., "Processing and Mechanical Properties of Al_2O_3 /Ni_3Al Composites with Interpenetrating Network Microstructure." *J. Am. Ceram. Soc.*, **84**, [9], pp. 2034–40, (2001).

Smith, D.T., Woody, S., and Pratt, J.R., "Compact Force Sensors for Low-Force Mechanical Probe Calibration." *Proc. Int. Meas. Confed.*, Joint International Conference on Force, Mass, Torque, Hardness and Civil Engineering Metrology in the Age of Globalization, Celle, Germany, Sept. 24–26, 2002.

Spal, R.D., Riley, G.N., Christopherson, C.J., "Supercurrent dissipation and strain-induced damage in Bi, Supercurrent Pb(2)$Sr_2Ca_2CU_3O10$/Ag tape." *Appl. Phys. Lett.*, **80**, (9), pp. 1412–1414, Feb 25, 2002.

Spal, R.D., "Singular current density in the planar superconductor/normal metal/superconductor junction." *J. Appl. Phys.*, **91**, (5), pp. 3090–3094, (2002).

Sturrock, C.P., Begley, E.F., and Kaufman, J.G., "MatML-Materials Markup Language Workshop Report." *NISTIR* **6785**, National Institute of Standards and Technology, (2001).

Sturrock, C.P., and Begley, E.F., "MatML: A New Language for Automating the Exchange of Materials Property Data Over the World Wide Web." *Advanced Materials and Process Technology Newsletter*, Vol. 6, No. 2, AMPTIAC, Rome, NY, (2002).

Vanderah, D.J., Arsenault, J., La, H., Silin, V., Meuse, C.W., and Gates, R.S., "Helical, Disordered, and What that Means: Structural Characterization of a New series of Methyl 1-Thiaoligo(ethylene Oxide) Self-Assembled Monolayers." Materials Research Society Spring Meeting Proceedings.

Vaudin, M.D., and Kaiser, D.L., "Workshop on texture in electronic applications." *J. of Research of the NIST*, **106**, [3], pp. 605, (2001).

Vaudin, M.D., "Crystallographic Texture in Ceramics and Metals." *J. of Research of the NIST*, **106**, [6], pp. 1063–1070, (2001).

Vaudin, M.D., Fox, G.R., Kowach, G., "Accuracy and Reproducibility of X-ray Texture Measurements on Thin Films." *MRS Proceedings*, San Francisco, CA, Spring 2002 Meeting.

Vedula, V.R., Glass, S.J., Saylor, D.M., Rohrer, G.S., Carter, W.S., Langer, S.A., and Fuller, Jr., R.R., "Residual Stress Predictions in Polycrystalline Alumina." *J. Am. Ceram. Soc.*, **84**, [12], pp. 2947–54, (2001).

Wallace, J.S., Huh, J.-M., Blendell, J.E., Handwerker, C.A., "Grain Growth and Twin formation in 0.74 PMN–0.26 PT." *J. Amer. Ceram. Soc.*, **85**, [6], pp. 1581–4, (2002).

Wäsche, R., Naito, M., and Hackley, V.A., "Experimental Study on Zeta Potential and Streaming Potential of Advanced Ceramic Powders." *Powder Tech.*, **213**, [2,3], pp. 275–281, (2002).

White, G.S., Blendell, J.E., and Fuller, Jr., E.R., "Domain Stability in PZT Thin Films." *Integrated Ferroelectric*, **38**, [1–4], pp. 69–78, (2001).

White, G.S., Fuller, Jr., E.R., and Freiman, S.W., "Mechanical Reliability and Life Prediction for Brittle Materials." Chapter 28 in *Handbook of Materials Selection*, pp. 809–828, Myer Kutz, Ed. (John Wiley & Sons, Inc., New York, NY, 2002).

Woicik, J.C., Nelson, E.J., Heskett, D., Warner, J., Berman, L.E., Karlin, B.A., Vartanyants, I.A., Hasan, M.Z., Kendelewicz, T., Shen, Z.X., Pianetta, P., "X-ray standing-wave investigations of valence electronic structure." *Physical Review B*, **64**, (12): art. no. 125115, Sept. 15, 2001.

Wong-Ng, W., Kaduk, J.A., Greenwood, W., and Dillingham, J.A., "Powder X-ray Reference Patterns of $Sr_2RGaCu_2O_7$ (R = Pr, Nd, Sm, Eu, Gd, Dy, Ho, Er, Tm, Yb and Y)." *J. Res. Natl. Inst. Stand. Technol.*, **106**, (4), p. 691, (2001).

Wong-Ng, W., Huang, Q., Levin, I., Kaduk, J.A., Dillingham, J., Haugan, T., Suh, J., and Cook, L.P., "Crystal Chemistry and Phase Equilibria of Selected SrO-R_2O_3-CuO_x and Related Systems, R= Lanthanides and yttrium." *Int. J. Inorg. Mater.*, **3**, p. 1283, (2001).

Wong-Ng, W., Kaduk, J.A., Dillingham, J. "Crystallographic studies and x-ray reference patterns of $Ba_5R_8Zn_4O_{21}$ by Rietveld Refinements." *Powder Diffraction*, **16**, (3), p. 131, (2001).

Wong-Ng, W., McMurdie, H.F., Hubbard, C.R., and Mighell, A.D., "JCPDS-ICDD Research Associateship (Cooperative Program with NBS/NIST)." *J. Res. Natl. Stand. Technol.*, **106**, pp. 1013–1028, (2001).

Wong-Ng, W., Cook, L.P., Suh, J., Levin, I., Vaudin, M., Feenstra, R., and Cline, J.P., "Phase Relationships and Phase Formation in the System BaF_2-BaO-Y_2O_3-CuO_x-H_2O." *MRS Proceedings*, **659**, Materials for High-Temperature Superconductor Technologies, M.P. Paranthaman, et al., eds, Materials Research Society, Warrendale, PA, pp. 337, (2002).

Wu, S., Patterson, B.R., Ferber, M.K., and Fuller, Jr., E.R., "Influence of Crack Path on Crack Resistance of Brittle Matrix Composites." *Ceramic Engineering & Science Proceedings*, Vol. 22, [3], pp. 269–276, Composites & Advanced Ceramic Materials, Mrityunjay Singh and Todd Jessen, eds. (The American Ceramic Society, Westerville, OH, 2001).

Xu, H.H., Quinn, J.B., Smith, D.T., Antonucci, J.M., Schumacher, G.E., and Eichmiller, F.C., "Dental Resin Composites Containing Silica-Fused Whiskers: Effects of Whisker-to-Silica Ratio on Fracture Toughness and Indentation Properties." *Biomaterials*, **23**, pp. 735–742, (2002).

Yang, H., AlBrithen, H., Smith, A.R., Borchers, J.A., Cappelletti, R.L., Vaudin, M.D., "Structural and magnetic properties of eta-phase manganese nitride films grown by molecular-beam epitaxy." *Applied Physics Letters*, **78**, [24], pp. 3860–3862, (2001).

Zhang, X.H., Gates, R.S., Anders, S., and Hsu, S.M., "An Accelerated Wear Test Method to Evaluate Lubricant Thin Films on Magnetic Hard Disks." *Tribology Letters*, **11**, (1), pp. 15–21, 2001.

Zimmerman, M.H., Baskin, D.M., Faber, K.T., Fuller, E.R., Allen, A.J., Keane, D.T., "Fracture of a textured anisotropic ceramic." *Acta Materialia*, **49**, (16), pp. 3231–3242, (2001).

Ceramics Division

Chief

Gabrielle Long, *Acting*
Phone: 301–975–6119
E-mail: gabrielle.long@nist.gov

Deputy Chief

Vacant

Group Leaders

Ceramic Manufacturing
Said Jahanmir
Phone: 301–975–3671
E-mail: said.jahanmir@nist.gov

Phase Equilibria
Terrell Vanderah
Phone: 301–975–5785
E-mail: terrell.vanderah@nist.gov

Film Characterization and Properties
Douglas Smith, *Acting*
Phone: 301–975–5768
E-mail: douglas.smith@nist.gov

Materials Microstructural Characterization
David Black, *Acting*
Phone: 301–975–5976
E-mail: david.black@nist.gov

Surface Properties
Stephen Hsu
Phone: 301–975–6120
E-mail: stephen.hsu@nist.gov

Data Technologies
Charles Sturrock
Phone: 301–975–6027
E-mail: charles sturrock@nist.gov

Research Staff

Allen, Andrew
E-mail: andrew.allen@nist.gov
Small angle x-ray scattering
Ceramic microstructure analysis

Begley, Edwin
E-mail: edwin.begley@nist.gov
Materials informatics
Database management methods
Engineering database structures

Black, David
E-mail: david.black@nist.gov
Defect microstructures
Polycrystalline diffraction imaging
X-ray imaging

Blendell, John
E-mail: john.blendell@nist.gov
Ceramic processing and clean-room processing
Sintering and diffusion controlled processes

Bouldin, Charles
E-mail: charles.bouldin@nist.gov
X-ray absorption spectroscopy
Diffraction anomalous fine structure
GeSi heterojunction bipolar transistors

Burdette, Harold
E-mail: harold.burdette@nist.gov
X-ray optics
X-ray diffraction imaging
Instrumentation

Burton, Benjamin
E-mail: benjamin.burton@nist.gov
Calculated phase diagrams
Dielectric ceramics

Cellarosi, Mario
E-mail: mario.cellarosi@nist.gov
Glass standards
Forensic data

Chuang, Tze-Jer
E-mail: tze-jer.chuang@nist.gov
Finite-element modeling
Lifetime predictions
Nanocontact mechanics

Cline, James
E-mail: james.cline@nist.gov
Standard reference materials
High-temperature x-ray diffraction
Microstructural effects in x-ray diffraction
Rietveld refinement of x-ray diffraction data

Cockayne, Eric
E-mail: eric.cockayne@nist.gov
First-principles methods
Phase equilibria and properties of dielectrics

Cook, Lawrence
E-mail: lawrence.cook@nist.gov
High-temperature chemistry
Phase equilibria

Dapkunas, Stanley
E-mail: stanley.dapkunas@nist.gov
Databases
Ceramic coatings

Dobbins, Tabbetha
E-mail: tabbetha.dobbins@nist.gov
Small angle x-ray scattering
Small angle neutron scattering
Ceramic microstructrure analysis

Fischer, Daniel
E-mail: daniel.fischer@nist.gov
Soft x-ray absorption fine structure
X-ray scattering
Surface science

Freiman, Stephen
E-mail: stephen.freiman@nist.gov
Electronic ceramics
Mechanical properties

Fuller, Edwin
E-mail: edwin.fuller@nist.gov
Microstructural modeling and simulation
Influence of microstructure on fracture
Toughening mechanisms

Gates, Richard
E-mail: richard.gates@nist.gov
Tribo-chemistry of ceramics
Chemical analysis of ceramics
Nanometer film thickness

Hackley, Vincent
vince.hackley@nist.gov
Powder characterization
Interfacial properties of suspensions
Visco-elastic properties of suspensions

Harne, Mary
mary.harne@nist.gov
Phase equilibria data
Computerized data

Harris, Joyce
E-mail: joyce.harris@nist.gov
Data acquisition
Digitization and data entry

Hockey, Bernard
E-mail: bernard.hockey@nist.gov
Electron microscopy
High-temperature creep

Hsu, Stephen
E-mail: stephen.hsu@nist.gov
Nanotribology
Nanolubrication
Magneetic hard disk interface
MEMs stiction

Ives, Lewis
E-mail: lewis.ives@nist.gov
Wear of materials
Transmission electron microscopy
Machining of ceramics

Jahanmir, Said
E-mail: said.jahanmir@nist.gov
Wear mechanisms
Mechanics of contacts
Effects of machining on mechanical properties

Kaiser, Debra
E-mail: debra.kaiser@nist.gov
Ferroelectric oxide thin films
Physical properties and structures of high-temperature superconductors
Combinatorial material analysis

Karen, Vicky
E-mail: vicky.karen@nist.gov
Crystallographic databases and materials informatics
Lattice theory
Structural analysis

Kelly, James
E-mail: james.kelly@nist.gov
Quantitative scanning electron microscopy
Image analysis
Microstructure analysis
Powder standards

Krause, Ralph
E-mail: ralph.krause@nist.gov
Creep in flexure and tension
Fracture mechanics

Locatelli, Mark
E-mail: mark.locatelli@nist.gov
Microstructural Simulation Modeling
Ceramic Coating
Low temperature co-fired ceramics

Long, Gabrielle
E-mail: gabrielle.long@nist.gov
Small-angle x-ray and neutron scattering
Ceramic microstructure evolution as a function of processing
X-ray optics

Luecke, William
E-mail: william.luecke@nist.gov
Creep/creep rupture
Rolling contact fatigue
Ceramic membranes

Lum, Lin-Sien
E-mail: lin-sien.lum@nist.gov
Powder characterization
Instrumental analysis

Minor, Dennis
E-mail: dennis.minor@nist.gov
Porosity standards
Powder characterization
Standard Reference Materials

Munro, Ronald
E-mail: ronald.munro@nist.gov
Materials properties of advanced ceramics
Data evaluation and validation
Analysis of data relations

Paul, Albert
E-mail: albert.paul@nist.gov
Laser physics
Residual stress measurement

Pei, Patrick
E-mail: patrick.pei@nist.gov
Spectroscopic and thermal characterization
Magnetic Disk lubrication

Quinn, George
E-mail: george.quinn@nist.gov
Mechanical property test standards
Standard reference materials
Fractography

Robins, Lawrence
E-mail: lawrence.robins@nist.gov
Defect identification and distribution
Cathodoluminescence imaging and spectroscopy
Photoluminescence spectroscopy
Raman spectroscopy

Saylor, David
E-mail: david.saylor@nist.gov
Microstructural characterization
Microstructural imaging
Grain boundary analysis

Schenck, Peter
E-mail: peter.schenck@nist.gov
Emission and laser spectroscopy
Thin-film deposition
Computer graphics and image analysis
Combinatorial materials analysis

Smith, Douglas
E-mail: douglas.smith@nist.gov
Surface forces
Adhesion and friction
Instrumented Indentation

Spal, Richard
E-mail: richard.spal@nist.gov
X-ray optics
Diffraction physics
X-ray scattering

Sturrock, Charles
E-mail: charles.sturrock@nist.gov
Materials informatics
Data evaluation and validation
Predictive data mining

Vanderah, Terrell
E-mail: terrell.vanderah@nist.gov
Solid-state chemistry
Phase equilibria of microwave dielectrics

Vaudin, Mark
E-mail: mark.vaudin@nist.gov
Electron microscopy
Microscopy and diffraction studies of interfaces
Computer modeling of grain-boundary phenomena
Dielectric films

Wallace, Jay
E-mail: jay.wallace@nist.gov
Nano mechanics
Sintering
Microstructural development
Powder processing

Wang, Pu Sen
E-mail: pu-wang@nist.gov
Solid-state nuclear magnetic resonance
Spectroscopic characterization

White, Grady
E-mail: grady.white@nist.gov
Mechanical properties
Nondestructive evaluation
Stress measurements

Woicik, Joseph
E-mail: joseph.woicik@nist.gov
UV photoemission
X-ray standing waves
Surface and interface science

Wong-Ng, Winnie
E-mail: winnie.wong-ng@nist.gov
X-ray crystallography and reference patterns
Phase equilibria/crystal chemistry of high-Tc superconductors

Ying, Charles
E-mail: charles.ying@nist.gov
Atomic force microscope
Nanofriction
Adhesion

Guest Scientists and Graduate Students

Armstrong, Nicholas
University of Technology
Sydney Australia

Bai, Mingwur
Tohoku University

Bartsch, Marian
Institute for Materials Research
German Aerospace Center

Boukari, Hacene
University of Maryland

Bumrongjaroen, Walairat
Federal Highway Administration

Cedeno, Christina
American Ceramic Society

Coutts, Rachel
University of Maryland

Dillingham, Jermey
University of Maryland

Early, James
Consultant

Evans, Howard
Smithsonian Institution

Fang, Hsu-Wei
University of Maryland

Farabaugh, Edward
American Ceramic Society

Feldman, Albert
Consultant

Fu, Zugen
State University of New York at Stony Brook

Haller, Wolfgang
Consultant

Hastie, John
Consultant

Ilavsky, Jan
University of Maryland

Jemian, Peter
University of Illinois at Urbana/Champaign

Jillavenkatesa, Ajitkumar
Alfred University

Kim, Yin Yong
Seoul National University

Kim, Jang Yul
Hanyang University

Kulkarni, Anand
State University of New York

Levin, Igor
Catholic University

Lindsey, Tammy
Appalachian State University

McMurdie, Howard
Joint Center for Powder Diffraction Studies

Mighell, Alan
Consultant

Nuffer, Juergen
University of Technology, Darmstadt

Ondik, Helen
Consultant

Ozmen, Yilmaz
Pamukkale University, Turkey

Peiris, Suhithi
Naval Research Laboratory

Piermarini, Gasper
University of Maryland

Prosandeev, Serguei
Rostov State University

Ritter, Joseph
Consultant

Roberts, Ellis
Consultant

Roth, Robert
Viper Group

Sambasivan, Sharadha
Brookhaven National Laboratory

Swanson, Nils
American Ceramic Society

Texter, John
National Science Foundation

Wolfenstine, Jeffrey
U S. Army Research Laboratory

Yeager, Glenn
Trak Ceramics, Inc.

Ying, Tony
U.S. Mint of the Treasury Department

Organizational Charts

Materials Science and Engineering Laboratory

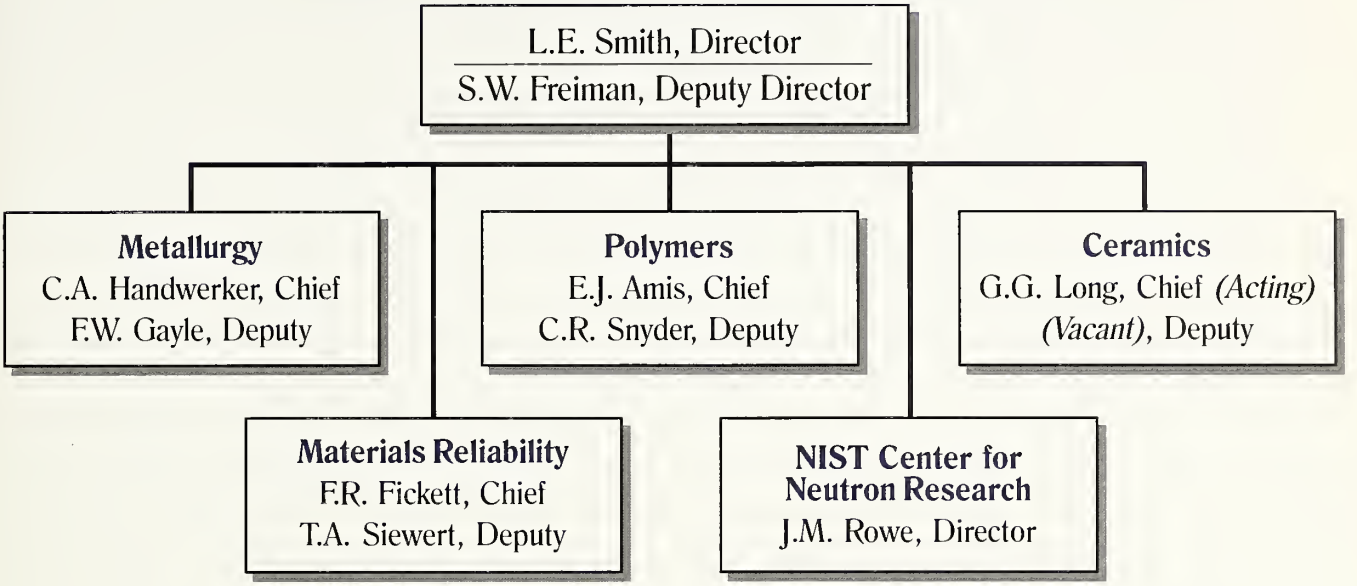

National Institute of Standards and Technology

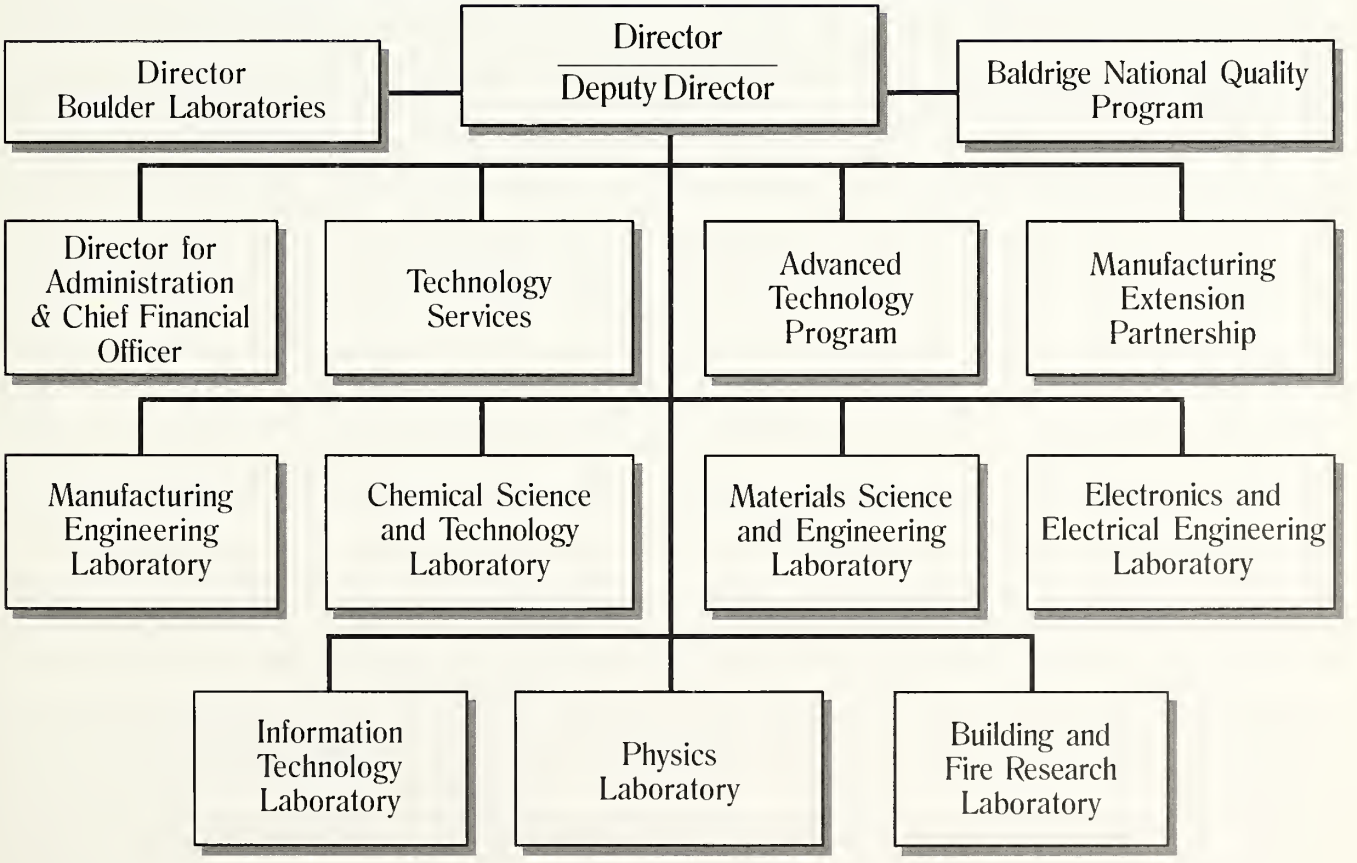

MSEL